TRANSCRIPTIONAL AND TRANSLATIONAL REGULATION OF CARDIAC PROGENITORS IN THE MOUSE AND ZEBRAFISH

APPROVED BY SUPERVISORY COMMITTEE

_____
Scott Cameron, M.D, Ph.D.

_____
Hiromi Yanagisawa, M.D., Ph.D.

_____
Michelle Tallquist, Ph.D

_____
Deepak Srivastava, M.D.

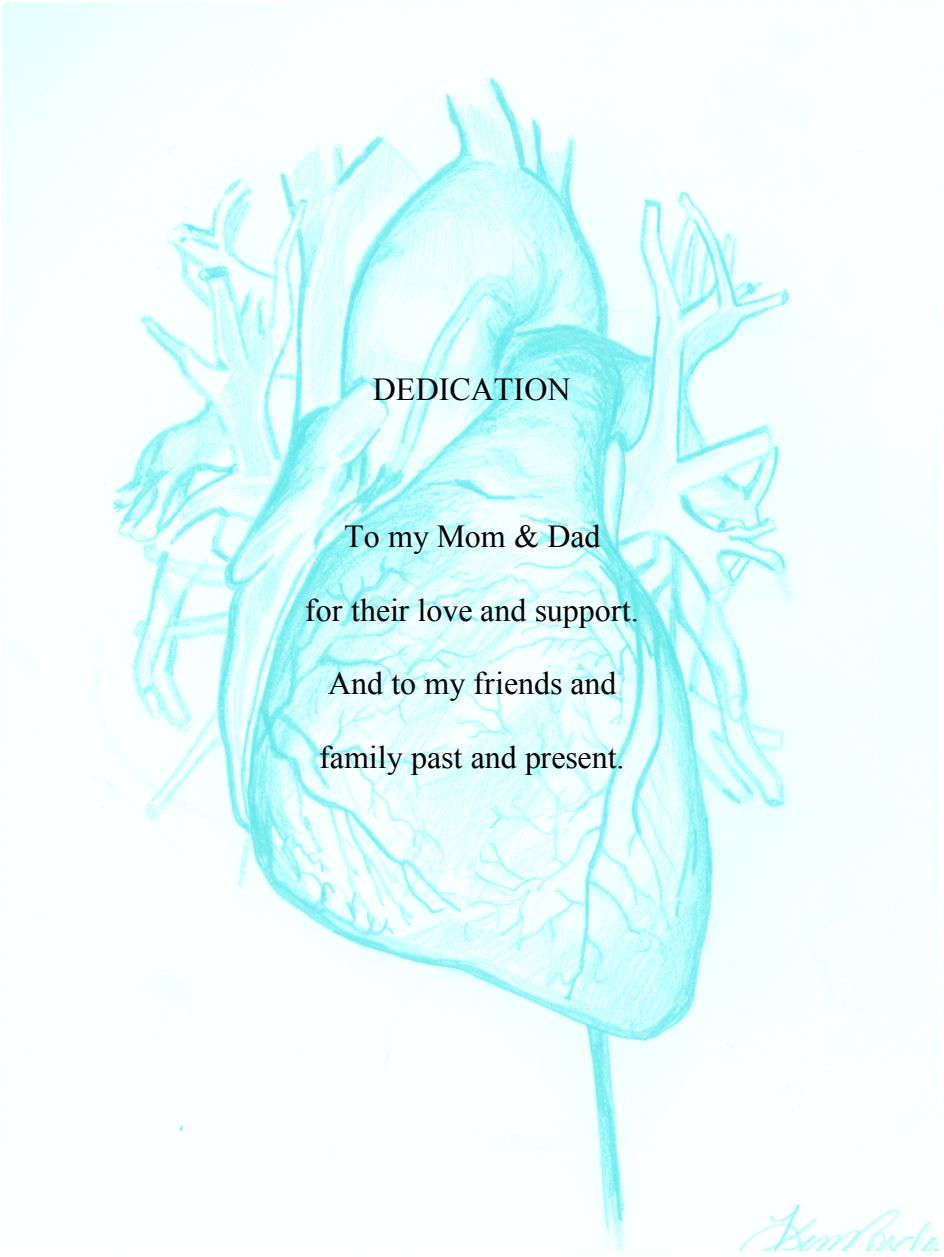

DEDICATION

To my Mom & Dad

for their love and support.

And to my friends and

family past and present.

TRANSCRIPTIONAL AND TRANSLATIONAL REGULATION OF CARDIAC PROGENITORS IN THE MOUSE AND ZEBRAFISH

by

KIMBERLY RENÉ CORDES

DISSERTATION

Presented to the Faculty of the Graduate School of Biomedical Sciences

The University of Texas Southwestern Medical Center at Dallas

In Partial Fulfillment of the Requirements

For the Degree of

DOCTOR OF PHILOSOPHY

The University of Texas Southwestern Medical Center at Dallas

Dallas, Texas

August, 2008

ACKNOWLEDGEMENTS

It is a pleasure to thank the many people who made this thesis possible.

It is difficult to overstate my gratitude to my Ph.D. supervisor, Dr. Deepak Srivastava. With his enthusiasm, his inspiration and his continuing support, he helped make academic science exciting and fun. Throughout this body of work, he provided encouragement, sound advice, good teaching, good company, and lots of good ideas. I would have been lost without him. I am extremely fortunate to have gotten to work closely with him.

I am indebted to my many current and past colleagues in the Srivastava lab for providing a stimulating and fun environment in which to learn and grow. I am especially grateful to those I have worked closely with: Kathryn Ivey, Alecia Muth, Sarah Morton, Neil Sheehy, and Joshua Ransom. I could not have moved forward with my thesis without your guidance and helpful discussions.

I am grateful to Dr. Bob Mahley, Dr. Doug Nixon and Mimi Zeiger at UCSF for teaching me presentation skills, which has become an invaluable tool as a young scientist.

I would like to thank my thesis committee members Scott Cameron, Hiromi Yanagisawa, and Michelle Tallquist for encouragement, advice, and support.

I am grateful to my past mentors, Dr. Peter Igarashi and Dr. Fangming Lin at UT Southwestern for their guidance, confidence, and developed friendship.

I wish to thank my best friends, Marika Olmstead, Andrea Erickson, Barbie Curtis, Jill Young, Erica Dingman, Kathy Ivey, Denise Srivastava, Morgan von Drehle, and Tres Riordan for helping me get through the difficult times, and for all the emotional support,

camaraderie, entertainment, and caring they provided. I am lucky to have such good friends.

I wish to thank my brother, Greg M. Cordes, and his family, for their love and support.

Lastly, and most importantly, I wish to thank my parents, Marilyn J. Cordes and Ronald M. Cordes. They raised me, supported me, motivated me, taught me, and above all, loved me. To them I dedicate this thesis.

TRANSCRIPTIONAL AND TRANSLATIONAL REGULATION OF CARDIAC PROGENITORS IN THE MOUSE AND ZEBRAFISH

Kimberly René Cordes, Ph.D.

The University of Texas Southwestern Medical Center at Dallas, 2008

Supervising Professor: Deepak Srivastava, M.D.

In vertebrates, the heart is the first organ to function and cardiac progenitors are among the first cell lineages to be established. Transcriptional networks control the specification of cardiac progenitors, however, it is not fully understood how some transcription factors function in particular cardiac progenitor populations. The basic helix-loop-helix, bHLH, transcription factor, Hand2 has been discovered over a decade ago, and has a severe loss-of-function cardiac phenotype *in vivo,* yet its function is still not completely known. It is expressed in the early cardiac progenitors of the neural crest cells and second heart field lineages. The first part of my thesis touches on the beginnings to understand the role of Hand2 in the cardiac neural crest progenitors.

Generally, expression levels in vertebrates reflect the combined transcription of both alleles of the gene being transcribed. Although there are notable exceptions (i.e., X chromosome genes), the presence of only one functional copy or more than two copies of a gene can have detrimental effects on the development of the organism. Many of the

genetic examples of congenital heart disease, which affects 1% of live births, are a result of a haploinsufficient gene dose. Like Hand2, which acts in a dosage-sensitive manner to regulate ventricular formation, the precise dose of proteins can be very important in regulating cardiac development. One way to fine-tune the activity of genes is through the newly identified class of small RNAs, microRNAs (miRNAs), which translationally repress the production of proteins by binding to target sites on messenger RNA (mRNA).

miRNAs provide a sophisticated way to adjust protein levels in a spatiotemporal manner. One miRNA may control several mRNAs, including transcription factors, which are the 'master switches' that regulate gene expression. And cooperatively, cell type-specific transcription factors can regulate the tissue-specificity of miRNA expression. Together with transcription factors, miRNAs function in cell fate determination, cell differentiation, proliferation and disease progression. Similar to transcription factors, which activate or repress a set of genes in a particular cell type, miRNAs create an environment, tailored for each cell type, allowing translation of some genes to occur, while repressing others. To date, less than a handful of miRNAs have been identified that function during heart development. The latter half of my thesis represents efforts to identify cardiac progenitor miRNAs and understand their function during development. I found that miRNA function is important in the cardiac mesodermal progenitors. In addition, I present a family of miRNAs, miR-143 and miR-145, that is specific to cardiac and smooth muscle progenitors, and I discuss their function in regulating their respective environments during cardiovascular development and disease.

TABLE OF CONTENTS

DEDICATION.....ii

ACKNOWLEDGEMENTS.....iv

ABSTRACT.....vii

TABLE OF CONTENTS.....ix

PUBLICATIONS.....xii

LIST OF FIGURES.....xiii

LIST OF ABBREVIATIONS.....xiv

CHAPTER ONE: **INTRODUCTION**.....1

Cardiac morphogenesis.....1

The First and Second Heart Fields.....3

The Neural Crest Cells.....5

The Outflow Tract.....7

The Cardiac Valves.....8

Transcriptional Regulation of Cardiac and Smooth Muscle Development....10

Nkx2.5.....10

Serum Response Factor.....11

Myocardin.....12

Translational Control of Cardiogenesis.....13

miRNA Biogenesis, Organization, and Target Recognition.....15

miRNA Function during Cardiogenesis.....18

Organization and Regulation of miR-1 and miR-133.....19

Function of miR-1 during Cardiogenesis.....20

REFERENCES.....24

CHAPTER TWO: HAND2 **IS REQUIRED IN THE NEURAL CREST FOR PROPER CRANIOFACIAL AND CARDIAC DEVELOPMENT**.....29

Introduction.....29

Results.....30

Craniofacial and Cardiovascular Phenotypes of Hand2 Conditional Mice.....30

Discussion.....31

Materials and Methods.....32

Mating and genotyping mice.....32

Histological Analysis.....33

Figures.....33

References.....**36**

CHAPTER THREE: **LOSS OF miRNA BIOGENESIS IN THE NEURAL CREST DISRUPTS CRANIOFACIAL AND CARDIOVASCULAR MORPHOGENESIS** 37
Abstract.....**37**
Introduction.....**38**
Results.....**40**
Loss of Dicer in the neural crest leads to craniofacial and cardiovascular defects.....40
Loss of Dicer does not affect neural crest cell migration.....41
Loss of Dicer affects the proper patterning of the first pharyngeal arch.....41
miRNAs Enriched in the neural crest cells.....42
miR-452 Rescues Dlx2 Expression.....43
Discussion.....**44**
Materials and Methods.....**46**
Mating and genotyping mice.....46
Histological analysis.....46
Optical Projection Tomography.....47
mRNA in situ hybridization.....47
Flow sorting and miRNA microarray.....47
Pharyngeal arch culture and transfection.....48
Quantitative RT-PCR.....48
Figures.....**49**
References.....**54**

CHAPTER FOUR: **REGULATION AND FUNCTION OF miR-143 AND miR-145 IN CARDIAC AND SMOOTH MUSCLE DEVELOPMENT**.....**56**
Abstract.....**56**
Introduction.....**57**
Results.....**59**
Conditional Dicer Inactivation in Cardiac Progenitors.....59
Identification of miRNAs Enriched in Cardiac Progenitors.....60
Expression and Regulation of miR-143 and miR-145 in Cardiac and Smooth Muscle.....61
miR-143 and miR-145 Function in Zebrafish.....63
miR-143 and miR-145 Regulates SRF-Dependent Pathways.....66
miR-145 Regulates Smooth Muscle Conversion.....69
miR-143 and miR-145 Are Down-regulated during Vascular Injury.....69
Discussion.....**70**
Materials and Methods.....**72**
Generation of Dicer Conditional Null Mice.....72
Transgenic Mice and Flow Cytometry.....73
miRNA Microarray and miRNA In Situ Hybridization.....73
Electromobility Shift Assay (EMSA).....73
Zebrafish lines.....74
Microinjection.....74

Confocal analysis.....74
Fish in situ hybridization.....74
miR-143 and miR-145 Target Analyses.....74
Quantitative real-time RT-PCR.....75
Cyclosporine A treatment.....76
Tissue Culture.....76
mRNA In-situ Hybridization, Immunohistochemistry and Western Blot Analysis.....76
Mouse Vascular Injury Model.....77
Figures.....**78**
References.....**91**

CHAPTER FIVE: **DISCUSSION AND FUTURE DIRECTIONS**.....**93**
Summary.....**93**
Unveiling the Function of Hand2 in the Cardiac Neural Crest.....**94**
miRNA Function in the Craniofacial and Cardiac Neural Crest.....**96**
Implications of miR-143/145 in Vascular Disease.....**97**
Conclusion.....**98**
References.....**100**

VITAE.....**THE END**

PUBLICATIONS

Lin F, Hiesberger T, **Cordes K,** Sinclair AM, Goldstein LS, Somlo S, Igarashi P**.** (2003) Kidney-specific inactivation of the KIF3A subunit of kinesin-II inhibits renal ciliogenesis and produces polycystic kidney disease. *PNAS*, 100(9), 5286-91.

Lin F, **Cordes K**, Li L, Hood L, Couser WG, Shankland SJ, Igarashi P. (2003) Hematopoietic stem cells contribute to the regeneration of renal tubules after renal ischemia-reperfusion injury in mice. *J Am Soc Nephrol,* 14(5),1188-99.

Haddad M, Lin F, Dwarakanath V, **Cordes K**, Baum M. (2004) Developmental changes in proximal tubule tight junction proteins. *Pediatric Research,* 57(3): 453-7.

Morton S, Scherz P, **Cordes K**, Ivey K, Stainier D, Srivastava D. (*in review*) microRNA regulation of organ patterning. Submitted to *PNAS.*

Cordes K, Srivastava D (*in press*) microRNA Regulation in Cardiac Development and Disease. In *Heart Development* (Rosenthal N, Harvey R, eds) 2nd Ed., Academic Press.

Cordes, K.*, Sheehy, N.*, Srivastava, D. microRNA requirement in the neural crest for proper craniofacial, thymus and heart development. *In preparation.*
*Authors contributed equally

Cordes, K., Morton, S., Ivey, K., Muth, A., White, M., Srivastava, D. miR-143 and miR-145 regulate endocardial and smooth muscle proliferation and differentiation. *In preparation.*

LIST OF FIGURES

CHAPTER ONE

Figure 1. Mammalian cardiac morphogenesis....2
Figure 2. Zebrafish cardiac morphogenesis....3
Figure 3. Schematic of *Hand2*-null mice....4
Figure 4. Four types of truncus arteriosus....7
Figure 5. miRNA biogenesis....16

CHAPTER TWO

Figure 1. Targeting and genotyping strategy for *Hand2* conditional mice....33
Figure 2. Morphology of *Hand2* conditional mutant hearts....34

CHAPTER THREE

Figure 1. Craniofacial and cardiac defects in *Dicer$^{loxP/loxP}$; Wnt1-cre* mutants...49
Figure 2. Loss of miRNA function in the neural crest affects pharyngeal arch patterning not migration....51
Figure 3. Neural crest-enriched miRNAs....52
Figure 4. miR-452 rescues *Dlx2* expression in PA1....53

CHAPTER FOUR

Figure 1. miRNA biogenesis is required in cardiac progenitors....78
Figure 2. miR-143/145 are highly conserved and are cardiac- and smooth-muscle-specific....79
Figure 3. SRF and Nkx2.5 directly regulate cardiac expression of miR-143 and miR-145 81
Figure 4. miR-143 and miR-145 are required for cardiac development in zebrafish and function by regulating endocardial differentiation....82
Figure 5. miR-143 and miR-145 target SRF-dependent pathways....85
Figure 6. miR-145 is necessary for Myocardin-dependent smooth muscle conversion and smooth muscle gene expression....87
Figure 7. miR-143 and miR-145 are downregulated in vascular injury and miR-145 targets the Ca^{2+}-dependent subunit *CamkII-delta*....88
Supplementary Figure 1. Schematic and genotyping strategy for *Dicer* conditional mutants....90

LIST OF ABBREVIATIONS

AA	aortic arch arteries
bHLH	basic helix loop helix
cDNA	complementary DNA
CHD	congenital heart disease
CnA	calcineurin a subunit
CsA	cyclosporine A
DA	dorsal aorta
DGCR8	DiGeorge critical region 8
DGS	DiGeorge syndrome
Dlx	distal-less transcription factor
DMEM	Dulbecco's Modified Eagle's Medium
DNA	deoxyribonucleic acid
EB	embryoid body
EF-1	elongation factor 1
Elk-1	ETS-like kinase
EMT	epithelial-to-mesenchymal transformation
ES	embryonic stem cell
ET-1	endothelin-1
FACs	fluorescent activated cell sorting
FBS	fetal bovine serum
FHF	first heart field
GAPDH	glyceraldehydes-3-phosphate dehydrogenase
HAND1	hand and neural crest-derivatives expressed 1
HAND2	hand and neural crest-derivatives expressed 2
hpf	hours post fertilization
Isl1	Islet-1
Klf4	kruppel-like factor 4

MADs box	MCM, Agamous, Deficiens, and SRF box
MEF2	myocyte enhancer factor 2
miRNA	microRNA
mRNA	messenger RNA
MRTF	Myocardin Related Transcription Factor
Myocd	Myocardin
MyoD	myoblast determination protein
NCC	neural crest cells
Nfat	nuclear factor of activated T-cells
Nkx2.5	NK2 related transcription factor
nt	nucleotide
OFT	outflow Tract
PA	pharyngeal arch
PBS	phosphate buffer saline
PCR	polymerase chain reaction
PDGF	platelet derived growth factor
PM	pharyngeal mesoderm
PTA	persistent truncus arteriosus
RGC-32	response gene to complement- 32
RNA	ribonucleic acid
RT-PCR	reverse transcriptase-polymerase chain reaction
RV	right ventricle
SHF	second heart field
SM22	smooth muscle 22 kD protein
SMC	smooth muscle cell
SRF	serum response factor
TA	truncus arteriosus
Tg	transgenic
TGF	transforming growth factor
UTR	untranslated region
Vegf	vascular endothelial growth factor

VSD	ventricular septal defect
WT	wild-type
YFP	yellow fluorescent protein

CHAPTER ONE

INTRODUCTION

CARDIAC MORPHOGENESIS

Congenital heart disease (CHD) is the leading non-infectious cause of mortality in the first year of birth, and affects 1–2% of all live births (5). Most forms of congenital heart disease result from aberrations in cardiac morphogenesis, such as defects in cardiac septation, valve formation, and proper patterning of the great vessels (5). Although genetic approaches have began to identify the underlying genes responsible for some forms of human CHD, the mechanisms of how these genes function remain unknown. A more precise understanding of the molecular framework that guides the formation of the heart will help decipher the causes of CHD, and help lead to therapeutic interventions.

In vertebrates, the heart is the first organ to develop in the embryo, and proper function of the cardiovascular system is essential for embryonic survival (6). A schematic of cardiac morphogenesis is depicted in Fig. 1. Early in gestation (day 15 in humans or day 7.5 in mouse), precardiac mesoderm forms a bilateral crescent that contains the progenitors that will give rise to the developing heart. The bilateral cardiac mesoderm migrates and fuses at the ventral midline to form a linear heart tube, which begins to beat and pump blood at this stage (day 21 in human or embryonic day 8.5, E8.5, in mouse). Failure of the bilateral cardiac mesoderm to fuse at the midline results in cardiac bifida (7). The tubular heart then undergoes a process known as rightward looping and is remodeled into ventricular and atrial chambers. In higher vertebrates, septal division of the chambers, formation of the valves, and aortic arch patterning occurs and establishes the four-chambered heart (4).

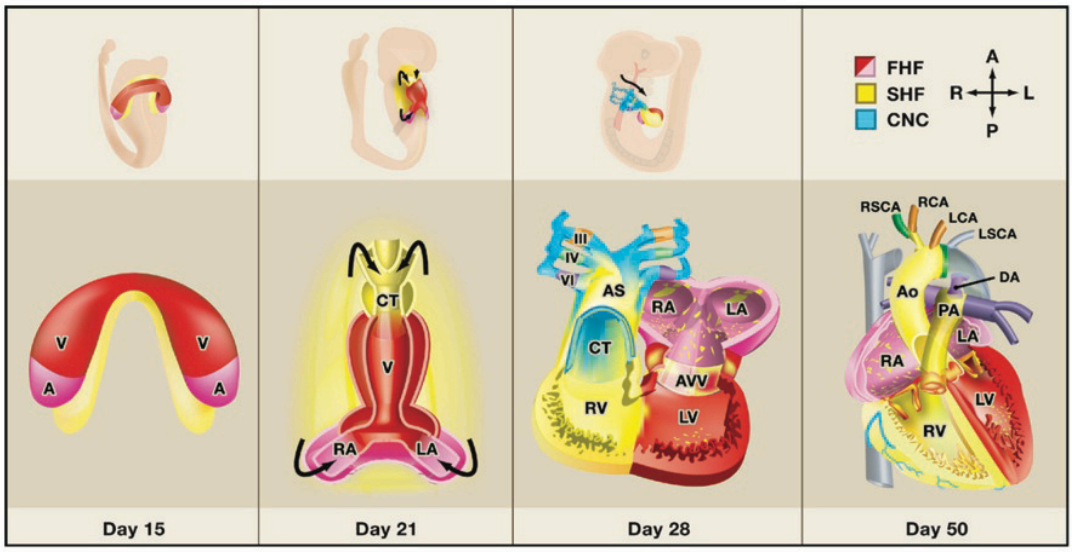

Figure 1. Mammalian cardiac morphogenesis. Oblique and frontal views of cardiac precursors during human cardiac development are shown. The first- (red/pink) and second-heart (yellow) fields contribute cells in a spatio-temporal manner during heart development, and contributes to cells of the atrium and left ventricle or outflow tract and right ventricle, respectively. The cardiac neural crest cells (blue) invade the pharyngeal arches at day 28 (mouse E10.5) and contribute to septation and remodeling of the outflow tract. V, ventricle; LV, left ventricle; LA, left atrium; RA, right atrium; AS, aortic sac; AVV, atrioventricular canal; Ao, aorta; PA, pulmonary artery; RSCA, right subclavian artery; LSCA, left subclavian artery; RCA, right carotid artery; LCA, left carotid artery; DA, ductus arteriosus. (4), image by K.R. Cordes)

The development and molecular patterning of the heart is highly evolutionary conserved between human, mouse, and zebrafish, making both the mouse and zebrafish ideal model organisms to study cardiac development and disease. As seen in Fig. 2, the development of the zebrafish heart mimics early cardiogenesis in the mouse, whereby the cardiac progenitor cells go through similar processes that are sequential but overlapping: specification of the precardiac mesoderm (~7 somites, s), determination of the bilaterally symmetric heart fields (~8 s), patterning of the heart field (~21 s, or 19.5 hours post fertilization, hpf), formation of the heart tube (~26 s or 22 hpf) and finally cardiomyocyte differentiation and rightward looping (~36–44 hpf) (3, 8).

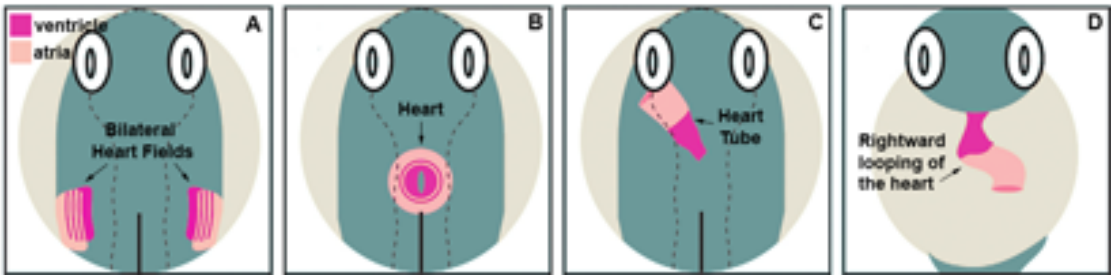

Figure 2. Zebrafish Cardiac Morphogenesis. Schematic representing the territories containing atrial cardiac progenitors (light pink) and ventricular cardiac progenitors (dark pink) in the bilateral cardiac regions, 7 somites (A), cardiac zone, 21 somites (B), linear heart tube, 30 hpf (C), and the mature cardiac chambers, 48 hpf (D; (modified from (3)).

The First and Second Heart Fields

The vertebrate heart forms from two distinct populations of cardiac progenitors, the first heart field and second heart field (FHF and SHF, respectively) that originate from a common progenitor population that segregates prior to the cardiac crescent stage (9). The ventricle (RV), outflow tract (OFT) and parts of the atria are derived from the SHF, while the FHF contributes cells to the left ventricle and atria (10, 11).

The FHF derives from cells in the lateral plate mesoderm that forms the crescent shape at approximately mouse E7.5 (Fig. 1). At E8.5, the FHF fuses at the midline to form the linear heart tube, which contains an inner endocardial layer and an outer myocardial layer of cells, and later becomes the left ventricle (4). At the linear heart tube stage, the FHF serves as a scaffold upon which cells from the SHF migrate and contribute cells to the cardiac chambers (9). FHF progenitors can be distinguished by the expression of specific transcription factors and signaling molecules, such as Tbx-5, Hand1, Bmp-Receptor I (BmpRI), and Bmp10 (12-14), whereas the SHF progenitors express factors such as Islet-1 and Hand2, discussed below (11, 15).

The LIM-homeodomain protein Islet-1 is required for the development of the SHF and its derivatives (11). The *Isl1* gene is expressed broadly during development,

with expression in the pharyngeal mesoderm and endoderm, and ventral neural tube (16, 11). Inactivation of *Isl1* in mice results in profound cardiac defects, such as failure to loop, and absence of RV and OFT derivatives (11).

Another transcription factor that is required for the development of the SHF is the basic helix-loop-helix, bHLH, protein heart and neural crest derivative-2, Hand2 (also known as dHAND). It is expressed in both the FHF and SHF progenitors at the cardiac crescent stage and its expression becomes restricted to the RV and OFT of the heart by E9.0 in mice. Hand2 is required for the expansion of the RV progenitors. The deletion of *Hand2* in mice results in embryonic lethality at E10.5, with a hypoplastic right ventricle and outflow tract defects, consistent with its expression pattern (15, 14). The ventricular hypoplasia observed in *Hand2*-null mice likely represents a failure of the SHF cells to expand into the RV (Fig. 3). Although a SHF progenitor population has not been found in zebrafish, knockdown of the zebrafish Hand ortholog causes a failure of ventricular precursors to expand, consistent with mouse studies (17). Hand2 is also required for proper neural crest cell (NCC) migration and formation of NCC-derived structures (discussed below).

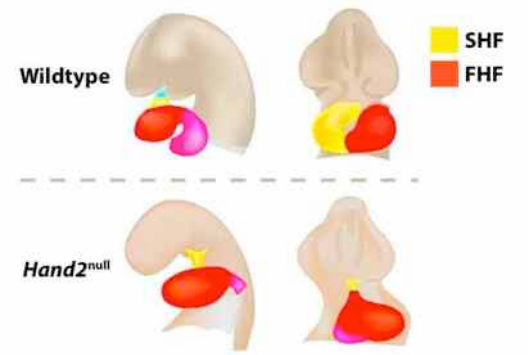

Figure 3. Schematic of *Hand2*-null mice. Lateral and frontal views of wild-type (top panel) and *Hand2*-null (bottom panel) embryos at E9.5. Null embryos have less contribution from the SHF (yellow) and have hypoplastic RV and shortened OFT formation compared to wild-type. Modified from (Srivastava, Heart Dev).

The Neural Crest Cells

NCCs are multipotent stem cells that can give rise to many tissue types, such as bone, cartilage, smooth muscle, neurons, melanocytes, and thymus. NCCs can be divided into two main populations: cranial and trunk ((18, 19). A subregion of cranial NCCs that emerge between the otic placode and third somite that contribute to outflow tract development has been dubbed the "cardiac neural crest". NCCs delaminate from the dorsal neural tube and then migrate toward and populate the head region and pharyngeal arches (Fig. 1) (20). The cranial NCCs populate the first and second pharyngeal arch (PA1 and PA2, respectively) and upon further differentiation develop into the cartilage, bone, and nerves of the face and neck. The cardiac NCCs migrate into the third, fourth, and sixth pharyngeal arches (PA3, PA4, and PA6, respectively) and contribute to the aorticopulmonary septum, conotruncal cushions, valves, and the smooth muscle of the aortic arch arteries (20, 19, 21). Additionally, the thymus, parathyroid and thyroid glands are derived from PA3 and PA4. The NCCs cooperate with the surrounding endoderm for proper molecular patterning of the transient pharyngeal arch apparatus and the formation of their subsequent structures (22).

Defects in the formation, migration, and/or differentiation of the cranial and cardiac NCCs can lead to multiple human disorders affecting face and heart formation including DiGeorge Syndrome characterized by persistent truncus arteriosus (PTA). Microablation of the cardiac NCCs in developing chick embryos results in PTA, a condition whereby the outflow tract never properly divides into the pulmonary artery and

aorta, resulting in a single artery situated predominantly over the right ventricle (23). Lack of NCCs also affects the SHF's contribution of myocardium to the OFT (24).

Hand2 is expressed in the mouse aortic sac and aortic arches at E9.5, and *Hand2*-null embryos show dilation of the aortic sac and a defect in PA1 and PA2 development (25, 14). Hand2 is a downstream effector of endothelin-1 (ET1), and mutations in ET1 signaling results in abnormal aortic arch patterning. In addition, Hand2 expression in the pharyngeal arches is dependent upon the endothelin signaling pathway (26, 27). Most likely, a member of the Distal-less family of homeodomain proteins, Dlx6, acts as an intermediary between endothelin signaling and Hand2 transcription by binding to and activating Hand2's pharyngeal arch enhancer (27). Moreover, a tissue-specific *Hand2* knockout generated by deletion of the *Hand2* pharyngeal arch enhancer–containing Dlx6 binding sites, results in perinatal mortality accompanied by craniofacial defects of the jaw and cartilage (28). Hand2 is an important regulator of neural crest development and differentiation into craniofacial and cardiovascular structures, however, downstream effectors of Hand2 that mediate neural crest-endothelial interactions for normal patterning are not known.

The Wnt signaling pathway is involved in early specification of the neural crest. Many molecules in the Wnt signaling pathway are implicated in the proliferation, migration and targeting of the cranial and cardiac NCCs. Because Wnt1 is expressed in early migrating neural crest cells and is turned off as the cells migrate away from the neural tube, and enhancer of Wnt driving Cre expression *in vivo* has been widely used to specifically knockout genes expressed in the neural crest (29). This reagent provides a useful tool to understand the function of NCC-expressed genes, such as *Hand2.*

The Outflow Tract

The mammalian cardiac OFT develops from the anterior part of the linear heart tube, forms the right-sided conotruncal region after heart looping, and is further septated resulting in formation of the aortic and pulmonary arteries. Defects in the formation of the OFT account for 20-30% of all CHD (5). The development of the OFT is complex and requires coordinated contribution from the SHF and NCCs. During early heart formation the SHF provides myocardium and endocardium to the outflow portion of the heart tube (mouse E8.5). At defined areas of the OFT, endocardial cells undergo an epithelial to mesenchymal transformation (EMT) to form endocardial cushions that will later develop into the valve leaflets (discussed in more detail below) (30). Later the SHF derivatives differentiate into smooth muscle at the base of the aorta and pulmonary artery (31). At mouse E10.5, the cardiac NCCs invade the OFT and aid in forming the aorticopulmonary septum, and in the spiral rotation of the great vessels. Additionally, the cardiac NCCs contribute to the smooth muscle of the great vessels (Fig. 1). In some cases of CHD, the aorta and pulmonary artery are misaligned with the ventricular chambers, which results in aorticopulmonary alignment defects, such as transposition of the great arteries, overriding aorta, or double-outlet right ventricle (32). When septation fails to occur, it results in a condition known as persistent truncus arteriosus (Fig. 4), which is consistent with the ablation of cardiac NCCs in chick

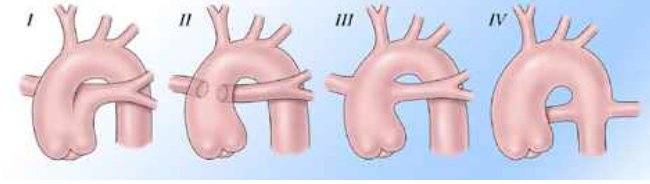

Figure 4. Four types of Truncus Arteriosus. Type I, pulmonary trunk arises from the aorta then divides into right and left branches; type II, pulmonary vessels arise indepently from the posterior part of the ascending vessel; type III, pulmonary vessels arise farther laterally from the truncus; type IV, now considered a form of pulmonary atresia with ventricular septal defect (tetralogy of Fallot with VSD). (modified from (1)).

embryos (33). However, ablation of either the cardiac NCCs or SHF results in changes of OFT length and myocardial dysfunction, suggesting that cardiac neural crest –SHF cross-talk is important for normal OFT morphogenesis (19, 31).

The neonate relies on separated pulmonary and systemic circulations for extra-uterine life, thus aorticopulmonary septation defects can be detrimental. Although surgical and pharmacological means can help correct and maintain proper postnatal circulation, the surgeries are palliative with undesirable side effects. So, understanding the mechanism by which the outflow tract develops could help elucidate potential preventative and therapeutic approaches.

In contrast to mammals, the zebrafish cardiac NCCs contribute to the myocardium of the ventricles in addition to the pharyngeal arches and OFT. Given the absence of an identified SHF component in zebrafish, it appears that the cardiac neural crest is the main contributor to OFT development (34). It may be that there is not a need for a SHF in zebrafish since the OFT does not undergo further septation and the cardiac NCCs can contribute to the ventricular myocardium (35).

The Cardiac Valves

Appropriate positioning and function of the cardiac valves is essential for chamber septation and unidirectional blood through the heart. The primordial heart valves known as cardiac cushions form as swellings of extracellular matrix between the endocardium and myocardium at the atrioventricular junction and OFT at mouse E9.0 (36). The process of endocardial cushion formation involves a distinct subset of endothelial cells in the cushions that undergo EMT, perhaps via the inductive signals from the adjacent

myocardium (37). Further remodeling allows the differentiation of the mesenchymal cells into the fibrous tissues of the valves, and involves the septation of the common atrioventricular canal into right- and left-sided orifices.

Several signaling pathways have been implicated in cardiac valve morphogenesis. Antisense RNA studies in chick showed that TGF-β signaling is essential for EMT and subsequent valve formation (37) and Notch signaling has been shown to promote EMT in mice (38). In addition, loss of endothelial neurofibromin-1 (Nf-1), which inactivates Ras, results in hyperplasia of mesenchymal cushion cells, elevated Ras signaling, and greater nuclear translocation of the transcription factor Nfatc (39).

Nfatc is expressed specifically in the valve mesenchyme precursors, and mice without Nfatc lack cardiac valve formation (40, 41). Signaling via the Ca^{2+}/calmodulin-dependent phosphatase, calcineurin, results in nuclear translocation of Nfatc. Elevated levels of intracellular Ca2+ activate calcineurin-Nfatc signaling, and calcineurin, composed of a regulatory (CnB) and a catalytic (CnA) subunit, dephosphorylates Nfatc upon this activation (42-44). The activity of calcineurin and Nfatc function can be specifically blocked by the immunosuppressive drug cyclosporine A, which binds to CnA and inhibits calcineurin's activity (45, 46). Cardiac valve morphogenesis is initiated at mouse E9 by calcineurin/Nfatc signaling in the myocardium, which acts to suppress Vegf expression in the endocardium. Vegf is a potent inhibitor of EMT and has the ability to induce endothelial proliferation and migration *in vitro* (47, 48). Calcineurin/Nfatc signaling is also necessary in the endocardium for the remodeling of the fibrous valve tissue (44). Similarly, zebrafish cardiac outflow and atrioventricular valve

morphogenesis occurs via calcineurin/Nfatc signaling, and the timing of this signaling event is crucial for proper valve formation in fish (~22-30 hpf) (44).

TRANSCRIPTIONAL REGULATION OF CARDIAC AND SMOOTH MUSCLE DEVELOPMENT

Cardiac and smooth muscle-specific transcription factors are essential for regulating the expression of genes encoding regulatory proteins or structural proteins characteristic of cardiomyocytes or SMCs, respectively. Not only are they important for normal cardiac development, but they are also essential for homeostasis of postnatal hearts. Mesodermal progenitors upregulate several highly conserved cardiac- and smooth muscle- restricted transcription factors such as Nkx2.5, Myocardin, and Hand2, upon initiation of the cardiac and smooth muscle lineages, that require the function of serum response factor (SRF). (Hand2 is discussed in the previous subsections, "The Second Heart Field" and "The Neural Crest Cells")

Nkx2.5

One of the earliest transcription factors that is specifically expressed in the cardiac precursors is the homeobox protein, Nkx2.5. The *Nkx2.5* ortholog *tinman* in *Drosophila* is essential for primitive heart formation (49, 50). In contrast, in the mouse, *Nkx2.5* is dispensable for early recruitment of cells to the cardiac cell lineage yet it is required for SHF expansion, and subsequent chamber specification and septation of the heart (51). *Nkx2.5* is expressed as early as E7.5 in mouse and continues until adulthood (52). In *Nkx2.5-null* embryos, several cardiac genes were highly downregulated, including the

basic helix-loop-helix factor, *Hand1*, and the cardiac- and smooth muscle- coactivator, *Myocardin* (*Myocd*) (51, 53-55). Indeed, Myocd has been identified as a direct downstream target of Nkx2.5 (54). The transcriptional activity of *Nkx2.5* is modulated through physical interaction with Myocd and other cardiac-enriched transcription factors such as, serum response factor (SRF) and Hand2 (56-60).

Serum Response Factor

SRF regulates transcription of numerous muscle and growth factor-inducible genes. SRF is a member of the MADS-box family of transcription factors (61). The MADs box of SRF binds to a consensus DNA sequence $CC(AT)_6GG$, called the CArG box in promoters and enhancers of muscle-specific genes that regulate differentiation, cell-cycle progression, and tissue-specific gene expression (62).

Srf-deficient embryonic stem (ES) cells fail to differentiate and form mesoderm and express myogenic genes (63). In comparison, *Srf*-null mice have a severe gastrulation defect and die before the formation of mesoderm. Cardiac- and smooth muscle specific inactivation of SRF in mice using the SM22-Cre transgenic showed disorganized cardiomyocytes and SMCs. The mutants had a marked reduction in the number of SMCs in the embryonic aorta and died by E10.5 (64). Also, the targeted deletion of SRF in the embryonic heart using the β-MHC-Cre transgenic line showed the importance of SRF in ventricular myocyte differentiation and maturation, as the mutants had a thin compact zone and defective trabeculation and died by E13.5 (65). In both cardiovascular knockouts of SRF, Myocd and Nkx2.5 were greatly reduced. Although SRF expression is largely restricted to the cardiac and muscle tissue during early

development, it is not muscle specific. It's activity becomes muscle specific by recruitment of myogenic cofactors, such as Nkx2.5 or Myocd to regulate cardiac- or smooth- muscle differentiation.

Myocardin

Smooth muscle cells switch between proliferation and differentiation programs depending on extracellular cues. SRF selectively activates genes involved in smooth muscle differentiation and proliferation by recruiting Myocd, and ternary complex factors (TCFs) of the ETS-domain family, respectively. Growth factor stimulation represses smooth muscle genes by abrogating Myocd's association with SRF and allowing Elk-1, a TCF that acts as a myogenic repressor, to bind SRF (66).

Myocd belongs to the SAP domain family of nuclear proteins and activates cardiac and smooth muscle promoters by directly binding to SRF and promoting differentiation. Myocardin is translated into a 935-amino acid (aa) or an 856-aa protein isoform, which confers its tissue-specificity to the heart and smooth muscle, respectively, and provides a mechanism to differentiate the functions of Myocd in the heart versus smooth muscle (67, 68). The SAP family of coactivators also includes the myocardin-related transcription factors, MRTF-A, and MRTF-B (69). MRTF-A and MRTF-B share a high level of sequence identity and overlapping expression patterns with Myocd. However, knockout studies of each reveal that the three are not completely redundant, and that MRTF-A and MRTF-B are important in mammary myoepithelial cells and neural crest cells, respectively (70, 71).

The genetic deletion of *Myocd* in mice leads to embryonic lethality by E10.5 due to vascular abnormalities and cardiovascular insufficiency (72). The forced expression of Myocd or the MRTFs in ES cells transactivates the endogenous SM22α promoter and induces the expression of many markers of SMC differentiation (73). Myocd can potentiate the conversion of fibroblasts into differentiated SMCs, and is a critical transcriptional coactivator in the SRF-dependent transcriptional regulatory regulating the smooth muscle phenotype (72). Although, SRF regulation is known to be important for growth-factor induced signaling and smooth muscle differentiation, the transcriptional mechanisms that confer smooth muscle phenotypic plasticity remain unclear.

SRF and its cofactor, Myocd, have been shown to also drive the expression of the recently discovered family of cardiac- and skeletal muscle-specific microRNAs, miR-1 and miR-133 (discussed below).

TRANSLATIONAL CONTROL OF CARDIOGENESIS

Protein dosage can be controlled at the mRNA transcriptional and translational level, or at the protein level. The transcriptional regulation of cardiomyocyte differentiation and cardiac morphogenesis requires precise spatiotemporal control of gene expression, and heterozygous mutations of transcription factors have frequently been implicated in human cardiac malformations (6, 74). Over the last few years, a novel mechanism involving post-transcriptional regulation by small noncoding RNAs, such as microRNAs (miRNAs), has emerged as a central regulator of many cardiogenic processes.

miRNAs are a large class of evolutionarily conserved, small, noncoding RNAs, typically 20–26 nucleotides (nt) in length, that primarily function post-transcriptionally

by interacting with the 3' untranslated region (UTR) of specific target mRNAs in a sequence-specific manner. Over 500 miRNAs are encoded in the human genome, and each is thought to target 50 to more than 100 mRNAs, resulting in mRNA degradation or translational inhibition. Interactions between miRNAs and mRNAs are thought to require sequence homology in the 5' end of the miRNA, but significant variance in the degree of complementation in the remaining sequence allows a single miRNA to target a wide range of mRNAs, often regulating multiple genes within a common pathway.

The first described animal miRNA, *lin-4,* was cloned in a forward genetic screen and characterized as a translational repressor of developmental timing in *Caenorhabditis elegans*, targeting the 3'UTR of *lin-14* mRNA (75). However, due to lack of homology of *lin-4* in other species, it was considered a genetic peculiarity specific to *C. elegans*. Years later, a second miRNA, *let-7*, was cloned. It targeted the 3'UTR of the highly conserved mRNA *lin-41,* another heterochronic gene. However, let-7 was highly conserved across species, providing the first indication that miRNAs might be widely used across species to titrate protein expression (76, 77). Through small RNA cloning efforts, it soon became clear that miRNAs were widespread in the genomes of all eukaryotes (78). Over one-third of mRNAs in the mammalian genome are thought to be regulated by one or more miRNAs (79).

Despite advances in miRNA discovery, the role of miRNAs in physiologic and pathophysiologic processes is just emerging. It has become clear that miRNAs play diverse roles in fundamental biological processes, such as cell proliferation, differentiation, apoptosis, stress response, and tumorigenesis. In many cancers, miRNAs are dysregulated and may act as tumor suppressors; in fact, the tumor suppressor gene

p53 regulates the *miR-34* family (80), and *let-7* represses a prevalent oncogene found in a variety of tumors (81). Identification of miRNAs expressed in specific cardiac cell types has led to the discovery of important regulatory roles for these small RNAs during cardiomyocyte differentiation, cell cycle, conduction, and during stages of cardiac hypertrophy in the adult, indicating that miRNAs may be as important as transcription factors in controlling cardiac gene expression.

Ultimately, knowledge of the function and regulation of specific miRNAs and their mRNA targets will further our understanding of the mechanisms that regulate gene expression and may also lead to new therapeutic targets for heart disease.

miRNA Biogenesis, Organization, and Target Recognition

miRNAs regulate gene expression at the post-transcriptional level by mRNA degradation, translation repression, or miRNA-mediated mRNA decay (Fig. 5). Mature miRNAs are formed in a multi-step biological process involving critical endonucleases. miRNAs are initially transcribed from the genome into long (several kilobases) 5' capped polyadenylated (poly(A)) primary transcripts (pri-miRNAs) by RNA polymerase II (82). Some miRNAs interspersed among repetitive DNA elements, such as Alu repeats (5' AG/CT 3'), can also be transcribed by RNA polymerase III (83). The miRNA-encoding portion of the pri-miRNA forms a hairpin structure that is recognized and cleaved in the nucleus by a microprocessor complex. This complex consists of the double-stranded RNA-specific nuclease DROSHA and its cofactor, DiGeorge syndrome critical region 8 (DGCR8) (84). The resulting ~70 nt hairpin precursor miRNA (pre-miRNA) is exported to the cytoplasm by the RAN-GTP-dependent nuclear transport receptor, exportin-5, which acts by recognizing a 2–3 basepair (bp) overhang of the pre-miRNA stem-loop

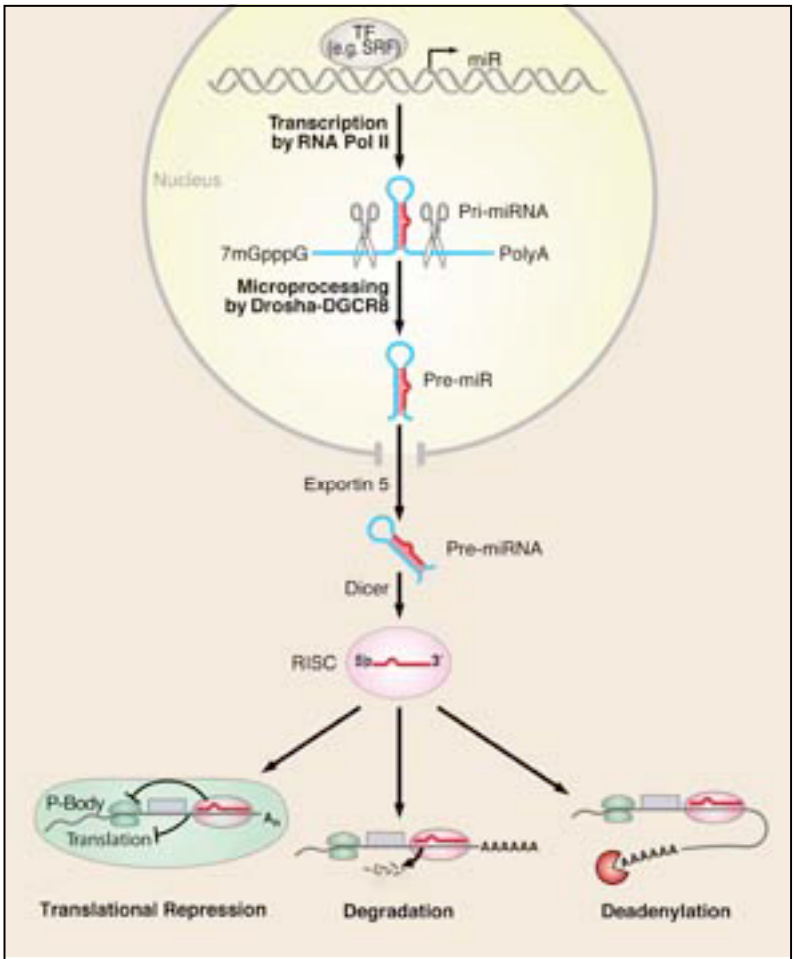

Figure 5. miRNA Biogenesis. Schematic representing initial miRNA transcription and processing inside the nucleus, to its export into the cytoplasm, cleavage by Dicer, incorporation into RISC, and the three modes of miRNA:mRNA regulation: repression, degradation or deadenylation (modified from (2)

structure (85, 86). The pre-miRNA is further processed by a complex of the RNAse III-like ribonuclease Dicer and the trans-activator RNA-binding protein, which cleaves the pre-miRNA to release the mature miRNA duplex.

An asymmetry in the relative thermodynamic stability of the 5' ends of the miRNA duplex results in preferential loading of the less stable ~22-nt strand into the RNA-induced silencing complex (RISC); the other strand is degraded, although in some cases both strands are incorporated into the RISC (87-89). The RISC helps mediate miRNA:mRNA interactions and subsequent mRNA repression or destabilization (90). miRNAs typically bind to the 3'UTRs of their mRNA targets with imprecise complementarity. Typically, the degree of Watson-Crick base-pairing between bases 2 and 7 (the “seed region”) at the 5' end of the miRNA is critical for binding mRNA targets (91, 92) and causing repression. RISC-bound miRNAs may also be

sequestered away from translational machinery in processing bodies (P-bodies) that act by recruiting poly(A) nucleases to help modulate deadenylatation of mRNA and thereby prevent translation (93-95).

miRNAs can be found in exons or introns of noncoding transcripts with independent enhancer regulation and in the introns and 3'UTRs of protein coding transcripts. They can also overlap with either an exon or an intron, depending on the alternative splicing pattern. In flies and worms, some miRNAs in intronic regions bypass Drosha processing and enter the miRNA biogenesis pathway as pre-miRNAs (96). In many cases, miRNAs are clustered near other miRNAs, suggesting they may be coregulated transcriptionally and share cooperative regulatory roles.

Among the hundreds of miRNAs identified thus far, only a limited number have been assigned target mRNAs. Several algorithmic databases have been designed for miRNA target prediction that rely, for the most part, on the following criteria: (1) conservation across species, (2) complementarity of the 5' miRNA 'seed match' to the 3'UTR (~ 7 nt) (97, 98, 92), (3) G:U wobbles in the seed (99), (4) the thermodynamic context of target mRNA binding sites (i.e., mRNA targets located in regions of high free energy and unstable secondary structure are favored) (100, 97), and (5) multiple miRNA binding sites in 3'UTR (101). These computational programs are continuously updated to integrate these criteria with knowledge from newly validated miRNA:mRNA interactions. Until more miRNA targets are validated, the precise mechanism of what makes one predicted target mRNA binding site more desirable than the next remains to be determined.

miRNA Function during Cardiogenesis

Tools similar to those used to study mRNA expression are also used to study miRNA expression, such as *in situ* hybridization, real-time PCR, and microarray profiling. The development of miRNA microarray platforms for high-throughput miRNA expression profiling has allowed identification of tissue-specific miRNAs, cancer-related miRNAs, disease-associated miRNAs, and ubiquitously expressed miRNAs. Array analyses reveal miRNAs that may be the most critical in modulating gene expression in a "tissue of interest." Ultimately, to identify the mRNA targets of miRNAs, it will be necessary to understand their biological relevance.

An approach to study the comprehensive requirements of miRNAs during vertebrate development has been to create mutations in Dicer, the enzyme required to process miRNAs into their active mature forms. *Dicer* is encoded by a single locus in vertebrates. Zebrafish lacking maternal and endogenous *Dicer* die from defects in gastrulation, brain morphogenesis, somitogenesis, and heart development (102, 103). In mice, targeted deletion of *Dicer* causes lethality at embryonic day 7.5 (E7.5), before body axis formation (104). Tissue-specific approaches to delete *Dicer* have shown that Dicer activity is essential for morphogenesis of the mouse limb, lung, brain, and heart (105-107, 97).

To create a heart-specific deletion of *Dicer*, Cre recombinase was expressed under control of the endogenous Nkx2.5 regulatory elements in the presence of a conditional *Dicer* allele. The *Nkx2.5-Cre* is active from E8.5 and onward, during heart patterning and differentiation (108). The cardiac deletion of *Dicer* results in embryonic lethality caused from cardiac dysfunction at E12.5 (97). Numerous miRNAs were affected by deletion of

Dicer and may be important in regulating aspects of cardiogenesis. It will be important to determine if *Dicer* is required for earlier stages of cardiogenesis (before E8.5), such as cardiac lineage specification, since *Dicer* is required for embryonic stem cell differentiation (109, 110). Collectively, these studies demonstrate the importance of miRNAs during development. Cardiac conditional knockouts of *Dicer*, miRNA gene targeting approaches, and conditional targeted deletions of miRNAs in different heart populations will reveal the importance of miRNAs during the different stages of heart development (e.g., cardiomyocyte commitment, chamber morphogenesis, outflow tract remodeling).

Organization and Regulation of miR-1 and miR-133

Two widely conserved miRNAs that display cardiac- and skeletal muscle–specific expression during development and in the adult are *miR-1* and *miR-133*, which are derived from a common precursor transcript (bicistronic) (100, 111). Multiple loci encode the mature *miR-1* and *miR-133* transcripts. *miR-1-1* is encoded on mouse chromosome 2 (human chromosome 20) and *miR-1-2* on mouse chromosome 18 (human chromosome 18). *miR-133a-1*, *miR-133a-2,* and *miR-133b* are on mouse chromosomes 18, 2, and 1, respectively. The mature forms of miR-1 derived from the distinct loci are identical, as are the miR-133a forms. The *miR-1* and *miR-133* paralogs are present in the human, mouse, chick, and fish genomes; a single ortholog of *miR-1* and *miR-133* exists in fly and worm (112). The *miR-1-1/miRmiR-133a-2* cluster is located in an intergenic region, whereas the *miR-1-2*/*miR-133a-1* reads in an antisense orientation between exons 12 and 13 of the *Mindbomb 1 (Mib1)* gene*,* involved in Delta-mediated Notch signaling (113).

Transcription of the *miR-1*/*miR-133* bicistronic precursors are directly regulated by the major myogenic differentiation factors, MyoD, myocyte enhancer factor-2 (Mef2), and SRF (100). MyoD functions exclusively in skeletal muscle, while Mef2 and SRF regulate gene expression in cardiac, skeletal and smooth muscle development (114, 115). In the heart, SRF binds and activates the enhancer regions of *miR-1*/*miR-133* in vitro and in vivo through a serum response element conserved from fly to human (100). Similarly, SRF regulates the cardiac expression of *miR-1* in flies, and the bHLH transcription factor Twist and Mef2 regulate somatic muscle expression (112, 116). Concordant with their common cis- and trans-regulation, both *miR-1* and *miR-133* are coexpressed in cardiac and skeletal muscle throughout mouse development and are robustly expressed in the adult (100, 111).

Function of miR-1 during Cardiogenesis

miR-1 expression directed by the enhancers described above commences at approximately E8.5 in mouse and increases throughout development. However, in *Drosophila*, miR-1 transcripts are detectable during early mesoderm formation before the onset of *mef2* expression. This may also be the case in mouse through as yet undescribed enhancers. Overexpression of *miR-1* under the control of the β-MHC promoter diminishes the pool of proliferating ventricular myocytes by causing a premature exit from the cell cycle. This negatively regulates cardiac growth, in part by inhibiting translation of *Hand2* (100), involved in ventricular myocyte expansion. In mice, *Hand2* is initially expressed throughout the linear heart tube, and then becomes restricted to the developing atrial and ventricular myocardium with highest expression in the right

ventricle. Mice that lack Hand2 die at E10.5 from right ventricular hypoplasia and decreased trabeculation in the left ventricle (25, 14, 53). In mice overexpressing *miR-1*, trabeculation is also decreased, consistent with the *Hand2* mutant phenotype, corroborating *Hand2* as a direct target of *miR-1* (100). Mice lacking miR-1 have an increase in Hand2 protein, providing further evidence of Hand2 as a direct target of miR-1.

In *Drosophila, miR-1* functions to pattern the dorsal vessel (i.e., aorta/heart tube). Moreover, the deletion of the single *miR-1* gene (*dmiR-1*), results in a muscle differentiation defect (116, 112). In a subset of *dmiR-1*-null flies, muscle progenitors are arrested in a proliferative state and accumulate ectopically. *Drosophila hand* does not seem to be a target of *miR-1*, since the fly *hand* ortholog lacks *miR-1* binding sites in its 3'UTR, suggesting that miRNA:mRNA interactions may differ somewhat between species. Instead, *dmiR-1* targets transcripts encoding the Notch ligand, *Delta*, which regulates the expansion of cardiac and muscle progenitor cells (112), suggesting that *miR-1* promotes muscle differentiation through down-regulation of the Notch signaling pathway. This is consistent with the known function of the Notch/ Delta signaling pathway during developmental cell fate decisions, including those involving cardiac specification (117).

During early cell fate decisions of mouse and human embryonic stem (ES) cells, *miR-1* and *miR-133* function in concert to promote mesoderm induction, while suppressing differentiation into the ectodermal or endodermal lineages (118). However, *miR-1* and *miR-133* have antagonistic effects on further adoption of muscle lineages: *miR-1* promotes differentiation of mouse and human ES cells toward a cardiac fate, while *miR-*

133 inhibits differentiation into cardiac muscle. *miR-1* appears to exert this effect, in part, by translationally repressing the mammalian ortholog of *delta, Delta-like-1* (*Dll-1),* similar to the repression seen in the fly (118). Thus, the bicistronic *miR-1*/*miR-133* transcript encodes distinct mature miRNAs that likely share common targets yet complement each other by balancing the differentiation and proliferation of cardiac and skeletal muscle lineages.

Surprisingly, disruption of just one of the two *miR-1* family members, *miR-1-2,* results in a range of abnormalities, including cell-cycle dysregulation, heart malformations, and postnatal electrophysiological defects. Heterozygous *miR-1-2*-null mice survive to reproduce, but 50% of *miR-1-2* homozygous null mice die between E15.5 and just after birth due to apparent ventricular septal defects (and cardiac dysfunction. These defects can occur from dysregulation of a multitude of events during cardiogenesis, and it is likely that *miR-1-2* regulates numerous genes during this process. Precise dosage of *Hand2* is crucial for normal cardiomyocyte proliferation and development, and elevated levels of *Hand2* may contribute to the ventricular septal defects and cardiac death (97).

miR-1-2-null mice that survive until birth often suffer sudden death (97). Electrophysiologic testing revealed a spectrum of cardiac arrhythmias in mutant mice, and bioinformatics combined with in-vivo approaches revealed numerous cardiac conduction genes regulated by miR-1 and miR-133, providing an example of a miRNA's role as a "master" regulator by virtue of the multiple mRNAs it can target. In addition, *miR-1-2*-null adult mice have an increase in mitotic cardiac myocytes along with cardiac hyperplasia, whereas postnatal mouse cardiomyocytes normally terminally exit the cell

cycle after the first 10 days of life. These abnormalities could reflect the effect of miR-1 on Notch signaling and the derepression of Hand2, which promotes myocyte expansion. In addition, genome-wide profiling of *miR-1-2* mutant adult hearts suggests a broad upregulation of positive regulators of the cell cycle and downregulation of tumor suppressors, indicating a shift in the "threshold" of cells to re-enter the cell cycle (97). Whether this change promotes cardiac repair after injury remains to be determined. Many targets of miR-1 may still be elucidated to further understand its function during cardiogenesis, and the deletion of both *miR-1-2* and *miR-1-1* will likely allow further insight into their roles.

Summary

miRNAs play fascinating roles in the heart, both pre- and postnatally. Through their ability to post-transcriptionally regulate mRNA levels, and thus manage protein dosage, miRNAs provide finer regulation within the complex molecular networks that regulate cardiogenesis. The importance of this fine regulation is highlighted by the recognition that most known genetic causes of heart malformations in humans result from haploinsufficiency or heterozygous point mutations. The field of miRNA biology is growing rapidly, and new tools and mechanisms are becoming available. With further characterization, elucidating the function of cardiac-enriched miRNAs may provide us with new diagnostic, prognostic, and therapeutic targets for many forms of cardiovascular disease.

References

1. Collett, R. W. & Edwards, J. E. (1949) *Surg Clin North Am* **29,** 1245-1270.
2. Hoffman, J. I. & Kaplan, S. (2002) *J Am Coll Cardiol* **39,** 1890-1900.
3. Zhao, Y. & Srivastava, D. (2007) *Trends Biochem Sci* **32,** 189-197.
4. Schoenebeck, J. J. & Yelon, D. (2007) *Semin Cell Dev Biol* **18,** 27-35.
5. Srivastava, D. (2006) *Cell* **126,** 1037-1048.
6. McFadden, D. G., Barbosa, A. C., Richardson, J. A., Schneider, M. D., Srivastava, D., & Olson, E. N. (2005) *Development* **132,** 189-201.
7. Jiang, Y., Tarzami, S., Burch, J. B., & Evans, T. (1998) *Dev Genet* **22,** 263-277.
8. Abu-Issa, R. & Kirby, M. L. (2007) *Annu Rev Cell Dev Biol* **23,** 45-68.
9. Buckingham, M., Meilhac, S., & Zaffran, S. (2005) *Nat Rev Genet* **6,** 826-835.
10. Mjaatvedt, C. H., Nakaoka, T., Moreno-Rodriguez, R., Norris, R. A., Kern, M. J., Eisenberg, C. A., Turner, D., & Markwald, R. R. (2001) *Dev Biol* **238,** 97-109.
11. Cai, C. L., Liang, X., Shi, Y., Chu, P. H., Pfaff, S. L., Chen, J., & Evans, S. (2003) *Dev Cell* **5,** 877-889.
12. Bruneau, B. G., Logan, M., Davis, N., Levi, T., Tabin, C. J., Seidman, J. G., & Seidman, C. E. (1999) *Dev Biol* **211,** 100-108.
13. Klaus, A., Saga, Y., Taketo, M. M., Tzahor, E., & Birchmeier, W. (2007) *Proc Natl Acad Sci U S A* **104,** 18531-18536.
14. Srivastava, D., Thomas, T., Lin, Q., Kirby, M. L., Brown, D., & Olson, E. N. (1997) *Nat. Genet.* **16,** 154-160.
15. Srivastava, D., Cserjesi, P., & Olson, E. N. (1995) *Science* **270,** 1995-1999.
16. Verzi, M. P., McCulley, D. J., De Val, S., Dodou, E., & Black, B. L. (2005) *Dev Biol* **287,** 134-145.
17. Yelon, D., Ticho, B., Halpern, M. E., Ruvinsky, I., Ho, R. K., Silver, L. M., & Stainier, D. Y. (2000) *Development* **127,** 2573-2582.
18. Vaglia, J. L. & Hall, B. K. (1999) *Int J Dev Biol* **43,** 95-110.
19. Hutson, M. R., Zhang, P., Stadt, H. A., Sato, A. K., Li, Y. X., Burch, J., Creazzo, T. L., & Kirby, M. L. (2006) *Dev Biol* **295,** 486-497.
20. Morriss-Kay, G., Ruberte, E., & Fukiishi, Y. (1993) *Ann Anat* **175,** 501-507.
21. Brown, C. B. & Baldwin, H. S. (2006) *Adv Exp Med Biol* **589,** 134-154.
22. Veitch, E., Begbie, J., Schilling, T. F., Smith, M. M., & Graham, A. (1999) *Curr Biol* **9,** 1481-1484.
23. Nishibatake, M., Kirby, M. L., & Van Mierop, L. H. (1987) *Circulation* **75,** 255-264.
24. Brown, C. B., Wenning, J. M., Lu, M. M., Epstein, D. J., Meyers, E. N., & Epstein, J. A. (2004) *Dev Biol* **267,** 190-202.
25. Thomas, T., Yamagishi, H., Overbeek, P. A., Olson, E. N., & Srivastava, D. (1998) *Dev. Biol.* **196,** 228-236.
26. Clouthier, D. E., Williams, S. C., Yanagisawa, H., Wieduwilt, M., Richardson, J. A., & Yanagisawa, M. (2000) *Dev Biol* **217,** 10-24.
27. Charite, J., McFadden, D. G., Merlo, G., Levi, G., Clouthier, D. E., Yanagisawa, M., Richardson, J. A., & Olson, E. N. (2001) *Genes Dev* **15,** 3039-3049.
28. Yanagisawa, H., Clouthier, D. E., Richardson, J. A., Charite, J., & Olson, E. N. (2003) *Development* **130,** 1069-1078.

29. Danielian, P. S., Echelard, Y., Vassileva, G., & McMahon, A. P. (1997) *Dev Biol* **192,** 300-309.
30. Ilagan, R., Abu-Issa, R., Brown, D., Yang, Y. P., Jiao, K., Schwartz, R. J., Klingensmith, J., & Meyers, E. N. (2006) *Development* **133,** 2435-2445.
31. Waldo, K. L., Hutson, M. R., Ward, C. C., Zdanowicz, M., Stadt, H. A., Kumiski, D., Abu-Issa, R., & Kirby, M. L. (2005) *Dev Biol* **281,** 78-90.
32. Warkany, J. (1971) *Am J Dis Child* **121,** 365-370.
33. Waldo, K. L., Hutson, M. R., Stadt, H. A., Zdanowicz, M., Zdanowicz, J., & Kirby, M. L. (2005) *Dev Biol* **281,** 66-77.
34. Sato, M. & Yost, H. J. (2003) *Dev Biol* **257,** 127-139.
35. Snider, P., Olaopa, M., Firulli, A. B., & Conway, S. J. (2007) *ScientificWorldJournal* **7,** 1090-1113.
36. Ferencz, C., Rubin, J. D., McCarter, R. J., Brenner, J. I., Neill, C. A., Perry, L. W., Hepner, S. I., & Downing, J. W. (1985) *Am J Epidemiol* **121,** 31-36.
37. Nakajima, Y., Yamagishi, T., Hokari, S., & Nakamura, H. (2000) *Anat Rec* **258,** 119-127.
38. Timmerman, L. A., Grego-Bessa, J., Raya, A., Bertran, E., Perez-Pomares, J. M., Diez, J., Aranda, S., Palomo, S., McCormick, F., Izpisua-Belmonte, J. C*., et al.* (2004) *Genes Dev* **18,** 99-115.
39. Gitler, A. D., Zhu, Y., Ismat, F. A., Lu, M. M., Yamauchi, Y., Parada, L. F., & Epstein, J. A. (2003) *Nat Genet* **33,** 75-79.
40. de la Pompa, J. L., Timmerman, L. A., Takimoto, H., Yoshida, H., Elia, A. J., Samper, E., Potter, J., Wakeham, A., Marengere, L., Langille, B. L*., et al.* (1998) *Nature* **392,** 182-186.
41. Ranger, A. M., Oukka, M., Rengarajan, J., & Glimcher, L. H. (1998) *Immunity* **9,** 627-635.
42. Beals, C. R., Clipstone, N. A., Ho, S. N., & Crabtree, G. R. (1997) *Genes Dev* **11,** 824-834.
43. Clipstone, N. A. & Crabtree, G. R. (1992) *Nature* **357,** 695-697.
44. Chang, C. P., Neilson, J. R., Bayle, J. H., Gestwicki, J. E., Kuo, A., Stankunas, K., Graef, I. A., & Crabtree, G. R. (2004) *Cell* **118,** 649-663.
45. Liu, Y. & Janeway, C. A., Jr. (1991) *Adv Exp Med Biol* **292,** 105-113.
46. Masuda, E. S., Imamura, R., Amasaki, Y., Arai, K., & Arai, N. (1998) *Cell Signal* **10,** 599-611.
47. Johnson, E. N., Lee, Y. M., Sander, T. L., Rabkin, E., Schoen, F. J., Kaushal, S., & Bischoff, J. (2003) *J Biol Chem* **278,** 1686-1692.
48. Ferrara, N. & Keyt, B. (1997) *Exs* **79,** 209-232.
49. Azpiazu, N. & Frasch, M. (1993) *Genes Dev* **7,** 1325-1340.
50. Bodmer, R. (1993) *Development* **118,** 719-729.
51. Lyons, I., Parsons, L. M., Hartley, L., Li, R., Andrews, J. E., Robb, L., & Harvey, R. P. (1995) *Genes Dev* **9,** 1654-1666.
52. Kasahara, H., Bartunkova, S., Schinke, M., Tanaka, M., & Izumo, S. (1998) *Circ Res* **82,** 936-946.
53. Yamagishi, H., Yamagishi, C., Nakagawa, O., Harvey, R. P., Olson, E. N., & Srivastava, D. (2001) *Dev. Biol.* **239,** 190-203.

54. Ueyama, T., Kasahara, H., Ishiwata, T., Nie, Q., & Izumo, S. (2003) *Mol Cell Biol* **23,** 9222-9232.
55. Biben, C. & Harvey, R. P. (1997) *Genes Dev* **11,** 1357-1369.
56. Wang, D., Chang, P. S., Wang, Z., Sutherland, L., Richardson, J. A., Small, E., Krieg, P. A., & Olson, E. N. (2001) *Cell* **105,** 851-862.
57. Durocher, D., Charron, F., Warren, R., Schwartz, R. J., & Nemer, M. (1997) *Embo J* **16,** 5687-5696.
58. Rivkees, S. A., Chen, M., Kulkarni, J., Browne, J., & Zhao, Z. (1999) *J Biol Chem* **274,** 14204-14209.
59. Chen, C. Y. & Schwartz, R. J. (1996) *Mol Cell Biol* **16,** 6372-6384.
60. Thattaliyath, B. D., Firulli, B. A., & Firulli, A. B. (2002) *J Mol Cell Cardiol* **34,** 1335-1344.
61. Norman, C. & Treisman, R. (1988) *Cold Spring Harb Symp Quant Biol* **53 Pt 2,** 719-726.
62. Catala, F., Wanner, R., Barton, P., Cohen, A., Wright, W., & Buckingham, M. (1995) *Mol. Cell. Biol.* **15,** 4585-4596.
63. Weinhold, B., Schratt, G., Arsenian, S., Berger, J., Kamino, K., Schwarz, H., Ruther, U., & Nordheim, A. (2000) *Embo J* **19,** 5835-5844.
64. Miano, J. M., Ramanan, N., Georger, M. A., de Mesy Bentley, K. L., Emerson, R. L., Balza, R. O., Jr., Xiao, Q., Weiler, H., Ginty, D. D., & Misra, R. P. (2004) *Proc Natl Acad Sci U S A* **101,** 17132-17137.
65. Parlakian, A., Tuil, D., Hamard, G., Tavernier, G., Hentzen, D., Concordet, J. P., Paulin, D., Li, Z., & Daegelen, D. (2004) *Mol Cell Biol* **24,** 5281-5289.
66. Wang, Z., Wang, D. Z., Hockemeyer, D., McAnally, J., Nordheim, A., & Olson, E. N. (2004) *Nature* **428,** 185-189.
67. Creemers, E. E., Sutherland, L. B., McAnally, J., Richardson, J. A., & Olson, E. N. (2006) *Development* **133,** 4245-4256.
68. Parmacek, M. S. (2007) *Circ Res* **100,** 633-644.
69. Wang, D. Z., Li, S., Hockemeyer, D., Sutherland, L., Wang, Z., Schratt, G., Richardson, J. A., Nordheim, A., & Olson, E. N. (2002) *Proc Natl Acad Sci U S A* **99,** 14855-14860.
70. Li, S., Chang, S., Qi, X., Richardson, J. A., & Olson, E. N. (2006) *Mol Cell Biol* **26,** 5797-5808.
71. Li, J., Zhu, X., Chen, M., Cheng, L., Zhou, D., Lu, M. M., Du, K., Epstein, J. A., & Parmacek, M. S. (2005) *Proc Natl Acad Sci U S A* **102,** 8916-8921.
72. Li, S., Wang, D. Z., Wang, Z., Richardson, J. A., & Olson, E. N. (2003) *Proc Natl Acad Sci U S A* **100,** 9366-9370.
73. Du, K. L., Ip, H. S., Li, J., Chen, M., Dandre, F., Yu, W., Lu, M. M., Owens, G. K., & Parmacek, M. S. (2003) *Mol Cell Biol* **23,** 2425-2437.
74. Pu, W. T., Ishiwata, T., Juraszek, A. L., Ma, Q., & Izumo, S. (2004) *Dev Biol* **275,** 235-244.
75. Lee, R. C., Feinbaum, R. L., & Ambros, V. (1993) *Cell* **75,** 843-854.
76. Reinhart, B. J., Slack, F. J., Basson, M., Pasquinelli, A. E., Bettinger, J. C., Rougvie, A. E., Horvitz, H. R., & Ruvkun, G. (2000) *Nature* **403,** 901-906.

77. Pasquinelli, A. E., Reinhart, B. J., Slack, F., Martindale, M. Q., Kuroda, M. I., Maller, B., Hayward, D. C., Ball, E. E., Degnan, B., Muller, P.*, et al.* (2000) *Nature* **408,** 86-89.
78. Lee, R. C. & Ambros, V. (2001) *Science* **294,** 862-864.
79. Chaudhuri, K. & Chatterjee, R. (2007) *DNA Cell Biol.* **26,** 321-337.
80. He, L., He, X., Lim, L. P., de Stanchina, E., Xuan, Z., Liang, Y., Xue, W., Zender, L., Magnus, J., Ridzon, D.*, et al.* (2007) *Nature* **447,** 1130-1134.
81. Lee, Y. S. & Dutta, A. (2007) *Genes Dev.* **21,** 1025-1030.
82. Cai, X., Hagedorn, C. H., & Cullen, B. R. (2004) *RNA* **10,** 1957-1966.
83. Borchert, G. M., Lanier, W., & Davidson, B. L. (2006) *Nat. Struct. Mol. Biol.* **13,** 1097-1101.
84. Landthaler, M., Yalcin, A., & Tuschl, T. (2004) *Curr. Biol.* **14,** 2162-2167.
85. Bohnsack, M. T., Czaplinski, K., & Gorlich, D. (2004) *RNA* **10,** 185-191.
86. Zeng, Y. & Cullen, B. R. (2004) *Nucleic Acids Res.* **32,** 4776-4785.
87. Schwarz, D. S., Hutvagner, G., Du, T., Xu, Z., Aronin, N., & Zamore, P. D. (2003) *Cell* **115,** 199-208.
88. Khvorova, A., Reynolds, A., & Jayasena, S. D. (2003) *Cell* **115,** 209-216.
89. Ro, S., Park, C., Young, D., Sanders, K. M., & Yan, W. (2007) *Nucleic Acids Res.* **35,** 5944-5953.
90. Gregory, R. I., Chendrimada, T. P., Cooch, N., & Shiekhattar, R. (2005) *Cell* **123,** 631-640.
91. Stark, A., Brennecke, J., Bushati, N., Russell, R. B., & Cohen, S. M. (2005) *Cell* **123,** 1133-1146.
92. Rajewsky, N. (2006) *Nat. Genet.* **38 Suppl,** S8-S13.
93. Liu, J., Valencia-Sanchez, M. A., Hannon, G. J., & Parker, R. (2005) *Nat. Cell Biol.* **7,** 719-723.
94. Kim, S. K., Nam, J. W., Rhee, J. K., Lee, W. J., & Zhang, B. T. (2006) *BMC Bioinformatics* **7,** 411.
95. Ezzeddine, N., Chang, T. C., Zhu, W., Yamashita, A., Chen, C. Y., Zhong, Z., Yamashita, Y., Zheng, D., & Shyu, A. B. (2007) *Mol. Cell. Biol.* **27,** 7791-7801.
96. Ruby, J. G., Jan, C. H., & Bartel, D. P. (2007) *Nature* **448,** 83-86.
97. Zhao, Y., Ransom, J. F., Li, A., Vedantham, V., von Drehle, M., Muth, A. N., Tsuchihashi, T., McManus, M. T., Schwartz, R. J., & Srivastava, D. (2007) *Cell* **129,** 303-317.
98. Lewis, B. P., Burge, C. B., & Bartel, D. P. (2005) *Cell* **120,** 15-20.
99. Brennecke, J., Stark, A., Russell, R. B., & Cohen, S. M. (2005) *PLoS Biol.* **3,** e85.
100. Zhao, Y., Samal, E., & Srivastava, D. (2005) *Nature* **436,** 214-220.
101. Doench, J. G. & Sharp, P. A. (2004) *Genes Dev.* **18,** 504-511.
102. Wienholds, E., Koudijs, M. J., van Eeden, F. J., Cuppen, E., & Plasterk, R. H. (2003) *Nat. Genet.* **35,** 217-218.
103. Giraldez, A. J., Cinalli, R. M., Glasner, M. E., Enright, A. J., Thomson, J. M., Baskerville, S., Hammond, S. M., Bartel, D. P., & Schier, A. F. (2005) *Science* **308,** 833-888.
104. Bernstein, E., Kim, S. Y., Carmell, M. A., Murchison, E. P., Alcorn, H., Li, M. Z., Mills, A. A., Elledge, S. J., Anderson, K. V., & Hannon, G. J. (2003) *Nat. Genet.* **35,** 215-217.

105. Harfe, B. D., McManus, M. T., Mansfield, J. H., Hornstein, E., & Tabin, C. J. (2005) *Proc. Natl. Acad. Sci. USA* **102,** 10898-10903.
106. Harris, K. S., Zhang, Z., McManus, M. T., Harfe, B. D., & Sun, X. (2006) *Proc. Natl. Acad. Sci. USA* **103,** 2208-2213.
107. Schaefer, A., O'Carroll, D., Tan, C. L., Hillman, D., Sugimori, M., Llinas, R., & Greengard, P. (2007) *J. Exp. Med.* **204,** 1553-1558.
108. Moses, K. A., DeMayo, F., Braun, R. M., Reecy, J. L., & Schwartz, R. J. (2001) *Genesis* **31,** 176-180.
109. Kanellopoulou, C., Muljo, S. A., Kung, A. L., Ganesan, S., Drapkin, R., Jenuwein, T., Livingston, D. M., & Rajewsky, K. (2005) *Genes Dev.* **19,** 489-501.
110. Murchison, E. P., Partridge, J. F., Tam, O. H., Cheloufi, S., & Hannon, G. J. (2005) *Proc. Natl. Acad. Sci. USA* **102,** 12135-12140.
111. Chen, J. F., Mandel, E. M., Thomson, J. M., Wu, Q., Callis, T. E., Hammond, S. M., Conlon, F. L., & Wang, D. Z. (2006) *Nat. Genet.* **38,** 228-233.
112. Kwon, C., Han, Z., Olson, E. N., & Srivastava, D. (2005) *Proc. Natl. Acad. Sci. USA* **102,** 18986-18991.
113. Itoh, M., Kim, C. H., Palardy, G., Oda, T., Jiang, Y. J., Maust, D., Yeo, S. Y., Lorick, K., Wright, G. J., Ariza-McNaughton, L*., et al.* (2003) *Dev. Cell* **4,** 67-82.
114. Edmondson, D. G., Lyons, G. E., Martin, J. F., & Olson, E. N. (1994) *Development* **120,** 1251-1263.
115. Miano, J. M. (2003) *J. Mol. Cell. Cardiol.* **35,** 577-593.
116. Sokol, N. S. & Ambros, V. (2005) *Genes Dev.* **19,** 2343-2354.
117. Artavanis-Tsakonas, S., Rand, M. D., & Lake, R. J. (1999) *Science* **284,** 770-776.
118. Ivey, K. N., Muth, A., Arnold, J., King, F. W., Yeh, R., Fish, J. E., Hsiao, E. C., Schwartz, R. J., Conklin, B. R., Bernstein, H. S*., et al.* (2008) *Cell Stem Cell***,** (in press).

CHAPTER 2

HAND2 IS REQUIRED IN THE NEURAL CREST FOR PROPER CRANIOFACIAL AND CARDIAC DEVELOPMENT

INTRODUCTION

Neural crest cells (NCCs) are a multipotent population that form in the dorsal neural tube. After neurulation, NCCs delaminate and migrate along defined pathways to differentiate into a variety of cells and tissues, such as bone, cartilage, smooth muscle cells, enteric neurons, etc (1). A subpopulation of NCCs called the cranial neural crest delaminates from the anterior neural tube, and populates the facial region and the first and second pharyngeal arch (2). Another subpopulation of NCCs called the cardiac neural crest delaminates from the dorsal neural tube between the mid-otic placode and the third somite, and migrates ventrally to enter the third, fourth, and sixth pharyngeal arches at mouse embryonic day 9.5 (E9.5). The cardiac NCCs participate in patterning the pharyngeal arch arteries and the aorticopulmonary septum (3).

The basic helix-loop-helix (bHLH) family of transcription factors plays important roles in the determination and differentiation of multiple organs during development, including craniofacial cartilage, bone, the outflow tract of the heart, cardiac cushions, and autonomic neurons (4, 5). Hand2, also known as dHAND, of the HAND subclass of the bHLH DNA-binding proteins, is expressed initially at the cardiac crescent stage and then becomes predominantly restricted to the right ventricular segment derived from the second heart field.

Neural crest-derived structures also depend upon the expression of Hand2 for normal development. Cranial and cardiac neural crest cells delaminate from the dorsal neural tube between the midotic placode and the third somite and migrate ventrally to enter the pharyngeal arches at mouse embryonic day 9.5 (E9.5). Loss of *Hand2* is embryonic lethal between E9.5-10.5, due to hypoplasia of the right ventricle (RV) and dilation of the aortic sac (4, 6). To overcome this early lethality and observe *Hand2's* specific function in the neural crest, we crossed $Hand2^{loxP/loxP}$ mice with *Wnt1-cre* transgenic mice. Previous reports found that *Hand2* expression in the neural crest is required for enteric neuronal terminal differentiation in the mouse gut, and in neurogenesis of noradrenergic sympathetic ganglion neurons (7, 8). However, the specific function of *Hand2* in the cardiac neural crest has not yet been characterized. When *Hand2* was deleted from the NCCs, the embryos die from cardiovascular defects by E12.5 and had severe craniofacial defects. Further genetic characterization of the cardiovascular abnormalities in these mice will provide further insight into the function of *Hand2*.

RESULTS

Craniofacial and Cardiovascular Phenotypes of Hand2 Conditional Mice

The inactivation of *Hand2* in neural crest cells resulted in embryonic lethality by embryonic day 12.5 (E12.5) due to severe craniofacial (Fig. 1A) and cardiovascular defects affecting the outflow tract (OFT) and ventricular septum formation. While the *Hand2*-null embryos die between E9.5-10.5 due to hypoplastic RV, the conditional mutants, had a well developed RV compared to control, suggesting that *Hand2* function

in RV expansion depends on expression in the second heart field (SHF) rather than in cardiac neural crest. It also suggests that the cardiovascular insufficiency caused by the RV defect in the *Hand2*-nulls is the reason for early embryonic lethality. At E12.5 septation of the OFT takes place, but in the mutants, they had a persistent truncus arteriosus (PTA) without septation (Fig. 1B). This could be due to either a delay in septation or an interruption in the process. Transverse sections of the hearts at E12.5 reveal a ventricular septal defect (VSD) in the mutants, which is known to associate with PTA (10).

NCC-*Hand2*-null mutants had a severe craniofacial defect. The craniofacial structures are derived from the first and second pharyngeal arches, and *Hand2* expression and precise dosage is required for proper patterning of the craniofacial structures (11, 12, 9). The mutants have a open-jaw, most likely due to short bone structures. The craniofacial defects seen in the mutants show the importance of *Hand2* in regulating proper development of the face.

DISCUSSION

This data shows that *Hand2* is required in the cardiac neural crests for proper cardiovascular development and survival. Further characterization of the cardiovascular phenotype through morphological and genetic assessment will provide further insight into *Hand2's* function in the cardiac neural crest. Morikawa et al. reported blood pooling in the major vessels and hemorrhaging in the peripheral vasculature by E12 in their neural crest-ablated *Hand2* mice. Cardiac neural crest cells contribute to the smooth muscle

cells of the aorta and pulmonary trunk, but not to the peripheral blood vessels (13), so it will be interesting to determine the genetic cause of these observations.

As mentioned, *Hand2* is also expressed in the developing RV of the heart, and has an important function in the expansion of ventricular cells in that region. Conditional deletions of *Hand2* in the second heart field progenitors will help to further elucidate *Hand2's* function in the heart during development. Together, the NCC and SHF deletions of *Hand2* will define its function in each field respectively, and will determine the similarities and differences of downstream targets between each progenitor populations.

This work is my contribution to a broader study of *Hand2* function during heart development. This work will be combined with loss-of- *Hand2* function in different domains of the heart using four different *Cre* lines - *Tbx1-Cre, Mef2c-Cre, Nkx2.5* and *Islet-1-Cre (14-17)*- which mark a defined subset of cells of the SHF domain (*Islet-1-Cre,* marks the broadest SHF domain, and *Nkx2.5-Cre* marks first heart field (FHF) progenitors as well as SHF) (in collaboration with Tsuchihashi, T, unpublished).

MATERIALS AND METHODS

Mating and genotyping mice. *Wnt1-cre* mice (18) were intercrossed with $Hand^{+/-}$ (6) mice to obtain $Hand^{+/-}$*;Wnt1-cre* mice. These were then crossed with conditional *Hand2* mice, $Hand2^{loxP/loxP}$, to obtain $Hand2^{loxP/-}$*; Wnt1-cre* mutants. To generate a conditional allele of *Hand2,* loxP sites were placed flanking intron1 and intron2, cre-recombination resulted in a deletion of both exons. Genotyping was performed by digesting DNA with BamHI and ClaI and then performing a subsequent southern analysis using a 5` ^{32}P-

radiolabeled probe as described (6), which produced a 4.5kb band representing the *Hand2*^{loxP} allele, 5.9kb band representing the null allele, and 7.5kb band representing wild-type.

Morphological analysis. Wild-type and *Dicer*$^{LoxP/-}$*; Wnt1-cre* embryos were collected at E12.5 and fixed in 10% formalin, and embedded in paraffin. Transverse sections were stained with hematoxylin and eosin. Pictures were taken on a Leica microscope.

Figure 1.

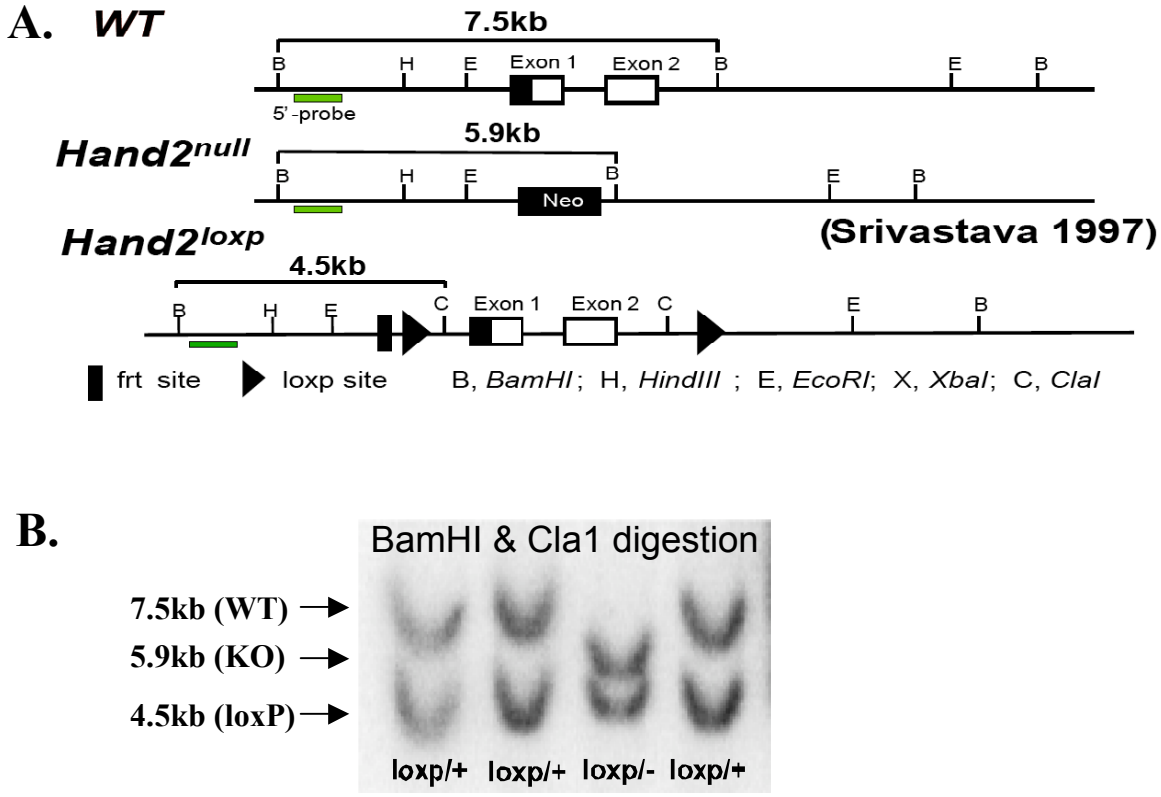

Figure 1. Targeting and genotyping strategy for *Hand2* conditional mice. (*A*) Representation of wild-type, null or loxP alleles of *Hand2*. For the *Hand* ^{loxP} allele, LoxP sites were inserted into a targeting construct to flank exon 1 and exon 2 of *Hand2*. A 5` probe described previously (6) discriminates between the alleles as shown in (*B*) Enzymatic digestion with BamHI and ClaI, and southern blot analysis depicting the genotyping results using a 5` ^{32}P-radiolabeled probe (green bar) shown in *A*.

Figure 2.

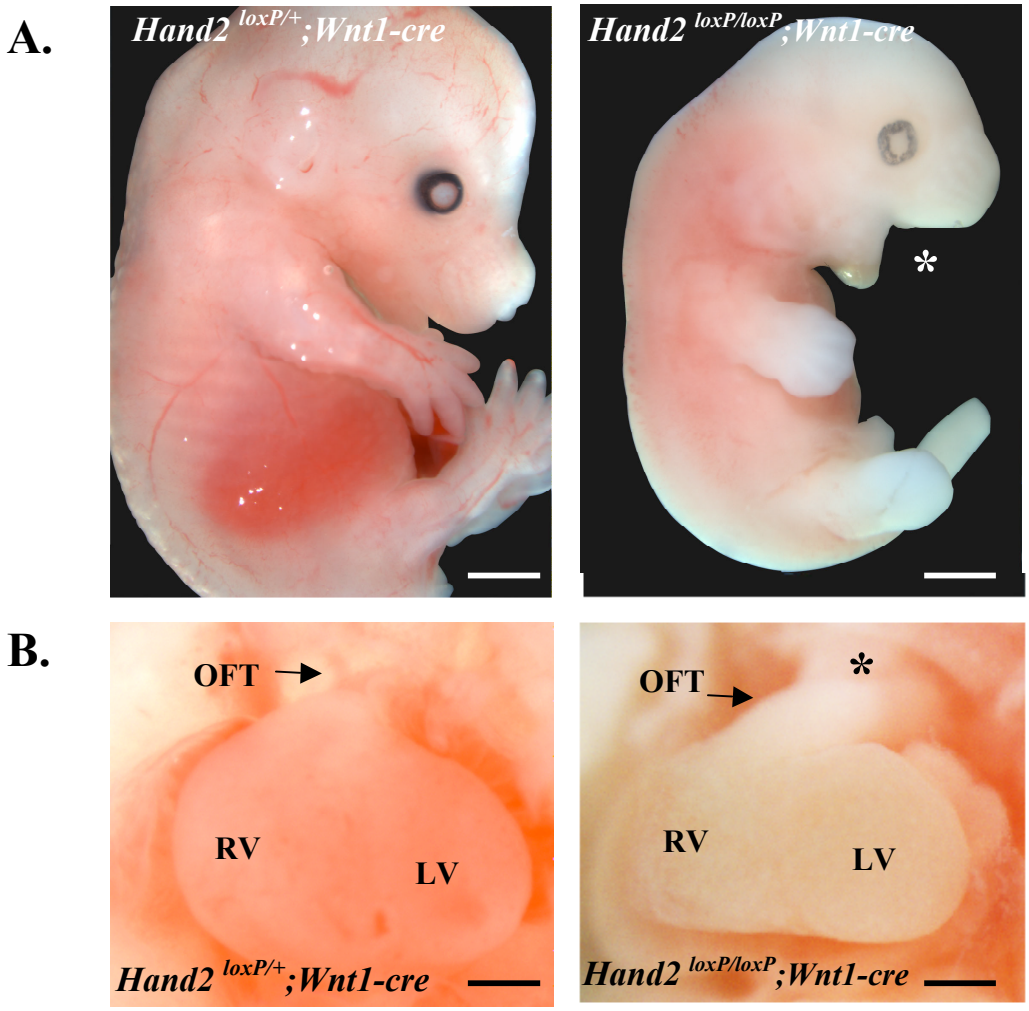

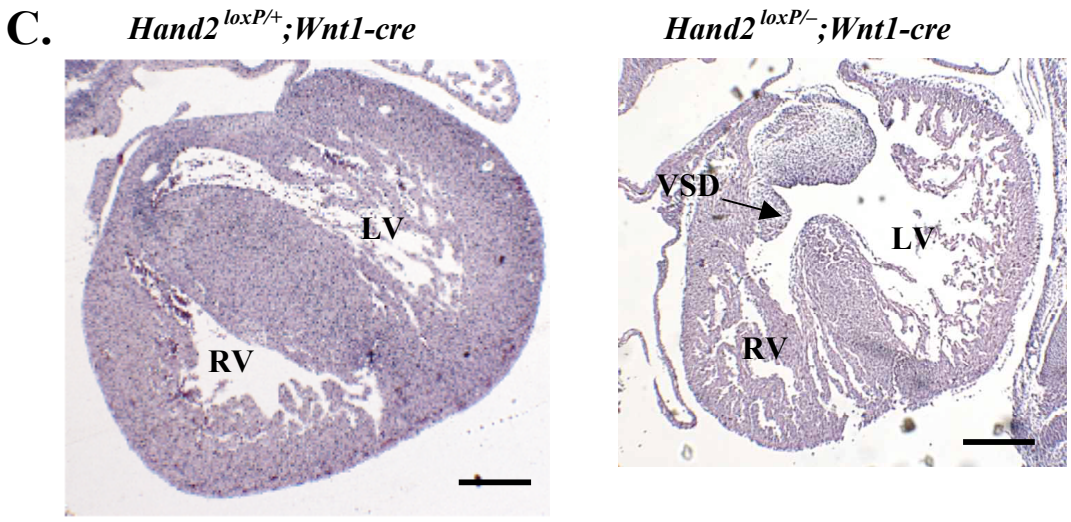

Figure 2. Morphology of *Hand2* conditional mutant hearts. (*A*) Lateral and (*B*) frontal views of wild-type and *Hand2loxP/–; Wnt1-cre* embryos at E12.5 showing the craniofacial and cardiovascular defect (*) in the mutant, (*C*) Hearts from wild-type and *Hand2loxP/–; Wnt1-cre* embryos at E12.5 were transverse sectioned and stained with Hematoxylin and Eosin. A mutant heart with a VSD is shown (arrow); OFT, outflow tract; RV, right ventricle; LV, left ventricle; VSD, ventricular septal defect.

REFERENCES

1. LaBonne, C. & Bronner-Fraser, M. (1999) *Annu Rev Cell Dev Biol* **15,** 81-112.
2. Tan, S. S. & Morriss-Kay, G. M. (1986) *J Embryol Exp Morphol* **98,** 21-58.
3. Kirby, M. L., Gale, T. F., & Stewart, D. E. (1983) *Science* **220,** 1059-1061.
4. Srivastava, D., Cserjesi, P., & Olson, E. N. (1995) *Science* **270,** 1995-1999.
5. Howard, M. J., Stanke, M., Schneider, C., Wu, X., & Rohrer, H. (2000) *Development* **127,** 4073-4081.
6. Srivastava, D. & Olson, E. N. (1997) *Trends Cell Biol* **7,** 447-453.
7. Morikawa, Y., D'Autreaux, F., Gershon, M. D., & Cserjesi, P. (2007) *Dev Biol* **307,** 114-126.
8. Hendershot, T. J., Liu, H., Clouthier, D. E., Shepherd, I. T., Coppola, E., Studer, M., Firulli, A. B., Pittman, D. L., & Howard, M. J. (2008) *Dev Biol* **319,** 179-191.
9. McFadden, D. G., Barbosa, A. C., Richardson, J. A., Schneider, M. D., Srivastava, D., & Olson, E. N. (2005) *Development* **132,** 189-201.
10. Kaartinen, V., Dudas, M., Nagy, A., Sridurongrit, S., Lu, M. M., & Epstein, J. A. (2004) *Development* **131,** 3481-3490.
11. Srivastava, D., Thomas, T., Lin, Q., Kirby, M. L., Brown, D., & Olson, E. N. (1997) *Nat Genet* **16,** 154-160.
12. Firulli, B. A., Krawchuk, D., Centonze, V. E., Vargesson, N., Virshup, D. M., Conway, S. J., Cserjesi, P., Laufer, E., & Firulli, A. B. (2005) *Nat Genet* **37,** 373-381.
13. Jiang, X., Rowitch, D. H., Soriano, P., McMahon, A. P., & Sucov, H. M. (2000) *Development* **127,** 1607-1616.
14. Yamagishi, H., Maeda, J., Hu, T., McAnally, J., Conway, S. J., Kume, T., Meyers, E. N., Yamagishi, C., & Srivastava, D. (2003) *Genes Dev* **17,** 269-281.
15. Dodou, E., Verzi, M. P., Anderson, J. P., Xu, S. M., & Black, B. L. (2004) *Development* **131,** 3931-3942.
16. McFadden, D. G., Charite, J., Richardson, J. A., Srivastava, D., Firulli, A. B., & Olson, E. N. (2000) *Development* **127,** 5331-5341.
17. Cai, S. R., He, Y. L., Huang, M. J., Peng, J. S., Wang, J. P., & Zhan, W. H. (2003) *Hepatobiliary Pancreat Dis Int* **2,** 308-312.
18. Danielian, P. S., Echelard, Y., Vassileva, G., & McMahon, A. P. (1997) *Dev Biol* **192,** 300-309.

CHAPTER 3

LOSS OF miRNA BIOGENESIS IN THE NEURAL CREST DISRUPTS CRANIOFACIAL AND CARDIOVASCULAR MORPHOGENESIS

Kimberly R. Cordes*, Neil T. Sheehy*, and Deepak Srivastava, Gladstone Institute of Cardiovascular Disease, University of California San Francisco, 1650 Owens Street, San Francisco, California 94158, USA.

* authors contributed equally

ABSTRACT

Neural crest cells (NCCs) are a subset of migratory, multipotent cells that populate many tissues during development and are important for craniofacial and cardiac morphogenesis. Disruption of the migration and differentiation of NCCs leads to a number of human diseases, including DiGeorge and Treacher-Collins Syndromes. Although microRNAs (miRNAs) have emerged as important regulators of development and disease, little is known about the role of miRNAs in neural crest development. We found that the loss of miRNA function in NCCs disrupts proper craniofacial and cardiac development in mice. In mutant mice, we showed that the expression of a known regulator of NCC development, *Dlx2*, was greatly reduced in the first pharyngeal arch. In a screen to identify the miRNA(s) responsible for regulating *Dlx2* expression, we identified nine miRNAs enriched in the neural crest. By developing a novel approach to deliver synthetic miRNAs to pharyngeal arch cultures, we found that the miRNA, miR-452, could rescue the loss of *Dlx2* expression in mutant mice. Our results demonstrate

the importance of miRNAs during NCC development and specifically show that miR-452 function is required for proper gene expression in the first pharyngeal arch.

INTRODUCTION

Neural crest cells (NCCs) are a population of multipotent cells that arise from the dorsal-neural tube during vertebrate embryogenesis (1). Cranial and cardiac NCCs migrate and populate the pharyngeal arches to form the majority of the bone, cartilage, and connective tissue of the face, and aid in outflow tract septation and smooth muscle contribution to the great vessels, respectively (2, 3). Defects in the formation, migration, and/or differentiation of the cranial and cardiac NCCs can lead to multiple human disorders including DiGeorge syndrome or Treacher Collins syndrome (3). The underlying causes of these anomalies arise from the malformation of the pharyngeal arch apparatus (4). The pharyngeal apparatus is composed of derivates of all three germ layers. The first and second pharyngeal arch, PA1 and PA2, are divided into proximal and distal regions that will contribute to defined tissues of the developing upper and lower jaw, respectively. Normal pharyngeal arch morphogenesis requires the inductive interactions between the ectomesenchymal or neural crest-derived cells, and the pharyngeal endoderm and mesoderm (5).

Normal morphogenesis of the pharyngeal arch-derived structures of the face and heart also require precise transcriptional and translational regulation. The transcriptional regulation of arch development and patterning has been studied in great detail, implicating the importance of fibroblast growth factor (Fgf), bone morphogenetic protein (Bmp), sonic hedgehog (Shh), endothelin (Edn), or distal-less homeobox protein (Dlx)

signaling within NCCs for proper arch patterning (6-10). However, translational regulation of the pharyngeal arch has not been well studied, which if known, could provide a better understanding of the disease pathogenesis and the developmental genetics of the pharyngeal apparatus.

Recently, a small class of non-coding RNA molecules, microRNAs (miRNAs), has emerged as important regulators during development and disease. They manage protein dosage by binding to the 3`untranslated regions (UTRs) of their target mRNAs and repressing gene expression. These small, roughly ~22 nucleotide (nt)-long miRNAs have been shown to provide fine regulation of translation within the complex molecular networks that regulate cardiogenesis (11, 12). The importance of this fine regulation is highlighted by the recognition that most known genetic causes of heart malformations in humans result from haploinsufficiency or heterozygous point mutations.

Multiple conditional knockouts of Dicer have revealed the importance of miRNA biogenesis during developmental processes of the brain, lung, heart and limbs (13, 14, 12, 15, 16). Given that the miRNA, miR-140, is important for craniofacial development in the zebrafish (17), we were interested in exploring the global *in vivo* function of miRNAs in the NCCs. We created a targeted deletion of *Dicer* in the neural crest cells using the *Wnt1-cre* transgenic and generated mice with severe craniofacial and cardiovascular defects. We found that the loss of miRNA function in the NCCs downregulates the expression of a known regulator of NCC development, *Dlx2*, in the first pharyngeal arch. Furthermore, we identified nine NCC-enriched miRNAs, of which we found one, miR-452, that regulates *Dlx2* expression in the first pharyngeal arch.

RESULTS

Loss of Dicer in the Neural Crest Leads to Craniofacial and Cardiovascular Defects

To evaluate the global requirement for miRNAs in the neural crest cells (NCCs), we used a previously established conditional null allele of *Dicer* to inactivate Dicer in NCCs (16) (Fig. 1A). At mouse embryonic day E9.5, cranial and cardiac neural crest cells delaminate from the dorsal neural tube and migrate ventrally to populate the pharyngeal arches PA1 and PA2, and PA3, PA4, and PA6, respectively (18). To abolish Dicer function in NCCs, we took advantage of the restricted expression of the *Wnt1-cre* allele, in which *Cre* is expressed in the NCC progenitors and progeny, and allows tracking of the NCCs throughout development. Dicer, which is essential for processing of pre-miRNAs into their mature form, was effectively deleted in NCCs of $Dicer^{loxP/loxP}$, *Wnt1-cre* mutant mouse embryos, which died at E14.5 due to severe craniofacial and cardiovascular defects (Fig. 1B-L). The mutant mice lacked any evidence of cartilaginous tissue of the maxillary and mandibular region of the face (Fig. 1B-E), and lacked a thymus. Interestingly, heterozygous mice ($Dicer^{loxP/+}$, *Wnt1-cre*) had a visible but smaller thymus than wild-type littermates at E14.5 (data not shown). Moreover, the null mutants displayed a truncus arteriosus (TA) type I, which is characterized by the origin of a partially separate main pulmonary trunk from the lateral aspect of the common trunk because of an incomplete aorticopulmonary septum (Fig. 1F-I). Accompanying the TA in the mutants is a ventricular septal defect (VSD) (Fig. 1J-L). These craniofacial and cardiac anomalies represent the result of NCC defects that are commonly seen in mouse models of neural crest-ablated genes.

Loss of Dicer Does Not Affect Neural Crest Cell Migration

The majority of craniofacial structures are derived from NCCs. The cranial NCCs migrate and populate the first and second pharyngeal arches (PA1 and PA2, respectively), and the frontonasal process, together, which are responsible for the formation of the facial bones. One potential defect in NCCs that could be contributing to the craniofacial defect of *Dicer*$^{loxP/loxP}$*, Wnt1-cre* mutant embryos is the failure of the NCCs to migrate from the neural tube to the pharyngeal arches and frontonasal process. To examine whether NCC migration was affected in the mutants, we crossed the *Dicer*$^{loxP/+}$*; Wnt1-cre* to *Dicer*$^{loxP/loxP}$; *Rosa26-EYFP* mice, and upon cre-mediated excision we were able to detect YFP-labeled NCCs in both the mutants and control littermates at E11.5. Based on YFP expression in the head skeleton, pharyngeal arches and outflow tract, we concluded that the loss of miRNA function in the NCCs had no affect on their migration (Fig 2A). This suggests that the defect is due to the maintenance of NCCs epithelial-mesenchymal interactions and/or a defect in NCC differentiation.

Loss of Dicer Affects the Proper Patterning of the First Pharyngeal Arch

Given that a combined craniofacial and cardiovascular phenotype typically arises from a defect in the development and patterning of the pharyngeal apparatus (4), we examined early stages of pharyngeal arch patterning in mouse at E10.5. The appearance of the pharyngeal arches of the mutant and control littermates were indistinguishable at E10.5, however, gene expression analysis showed downregulation of the distal-less homeobox gene, *Dlx2,* in the mandibular (distal) region of the first pharyngeal arch in mutant

embryos, while the maxillary (proximal) region and limb buds showed no significant reduction in *Dlx2* expression compared to wild-type (Fig. 2B). This downregulation of *Dlx2* implies that miRNA function is essential for epithelial-mesenchymal interactions, since *Dlx2* expression coincides with sites of epithelial-mesenchymal interactions (9, 8). Another homeobox-containing gene important for PA1-derived craniofacial development, *Msx1*, showed no change in expression between the mutant and wild-type embryo (Fig. 2C). *Dlx2*-deficient mice have severe craniofacial defects that derive from the proximal regions of the first and second pharyngeal arches, and the tissue outgrowth from the distal regions are only slightly affected (19, 20). Since *Dicer*$^{loxP/loxP}$; *Wnt1-cre* mutant mice show severe craniofacial defects that derive from both the proximal and distal portions of PA1 and PA2, this suggests that other genes are most likely affected by the loss of miRNA function.

miRNAs Enriched in the Neural Crest Cells

To determine which miRNAs were not being processed in the *Dicer*$^{loxP/loxP}$*, Wnt1-cre* mice, we crossed *Wnt1-cre* transgenic mice with *Rosa26-EYFP* to mark the *Wnt1* population with YFP. By fluorescence-activated cell sorting (FACs) at E11.5, we obtained RNA from *Wnt1+, YFP+* cells and profiled miRNA expression by microarray analysis. We identified nine miRNAs to be enriched greater than 2-fold in the NCCs (Fig. 3).

Interestingly, miR-452, one of the highest NCC-enriched miRNAs, is located within the intron of the gamma-aminobutyric acid (GABA-A) receptor, subunit epsilon, *Gabre,* which is a receptor subunit on GABAergic interneurons. The *Dlx* genes are

expressed in developing GABAergic cells, and the differentiation of immature neuronal cells into mature GABAergic interneurons requires the activity of *Dlx* genes, including *Dlx2* (21, 22). Intronic miRNAs can be regulated by their host gene and act in similar pathways (23-25).

miR-452 Rescues Dlx2 Expression

Since GABAergic differentiation requires *Dlx* activity, we tested whether the *Gabre*-embedded miR-452 could induce *Dlx2* expression in $Dicer^{loxP/loxP}$; *Wnt1-cre* mutant pharyngeal arches. The downregulation of *Dlx2* in the first pharyngeal arch provides a genetic read-out to test rescue experiments in pharyngeal arch cultures of $Dicer^{loxP/loxP}$; *Wnt1-cre* mice by introducing mature miRNA mimics. We successfully introduced a 2'O-methyl modified oligo that mimicked miR-452 into first pharyngeal arch cultures at various concentrations (Fig. 4A) and optimized our technique to achieve uniform and robust expression of our miR-452 mimic (Fig. 4B). The transfection of miR-452 mimic into $Dicer^{loxP/loxP}$; *Wnt1-cre* mutant pharyngeal arches could rescue *Dlx2* expression up to the levels of the littermate controls. However, a control mimic, miR-125b, which is not enriched in NCCs, was unable to rescue *Dlx2* expression. Since *Dlx2* is downregulated in the NCC-mutant pharyngeal arches, it is not likely a direct target of miR-452. This suggests that reintroduction of miR-452 in the NCC-mutant arches suppresses a repressor of *Dlx2*. Additionally, it suggests that *Gabre* and miR-452 may be involved in a coordinated regulatory network.

DISCUSSION

Translational regulation of gene expression by miRNAs is essential for determining the patterning of gene expression that will direct tissue outgrowth of the pharyngeal arches. The major events required for the correct development of the craniofacial structures and the cardiac outflow tract include the migration of the neural crest cells into the pharyngeal arches, stage-specific epithelial-to-mesenchymal interactions, and differentiation into chrondrogenic or smooth muscle cell types, respectively. We found that neural crest cells do not require miRNA biogenesis for migration but do require miRNA function for coordinated epithelial-mesenchymal interactions and further differentiation into defined tissues of the face and heart.

The *Dlx* family consists of six members (*Dlx1,-2,-3,-5,-6,*and *-7)*, all of which have overlapping expression pattern with *Dlx2,* especially in the distal regions of the pharyngeal arches (19). *Dlx* genes in mice and humans are linked in tandem pairs: *Dlx1* and *Dlx2*, *Dlx5* and *Dlx6, Dlx3* and *Dlx7.* *Dlx* genes are required for proper patterning of the first and second pharyngeal arches (20). Targeted deletion of single or multiple *Dlx* genes demonstrates unique and redundant functions for the *Dlx* genes in normal development and patterning of craniofacial skeletal structures (26, 19). *Dlx2*-null mice have dysmorphic or absent skeletal structures arising from the maxillary region of the first pharyngeal arch, and the mandibular structures are largely spared (19). It will be interesting to see if there are changes in expression of the other *Dlx* family members in the $Dicer^{loxP/loxP}$; *Wnt1-cre* mutants, because if so, it could suggest that a miR-452 (or multiple NCC-miRNAs) is regulating a repressive *cis*-element common to several *Dlx* genes.

We have begun to assess the mechanism by which miR-452 is regulating *Dlx2* expression in the first pharyngeal arch. To identify the direct target by which miR-452 is influencing *Dlx2* expression we can utilize bioinformatic approaches, which will provide a list of miR-452 predicted mRNA targets that can be tested *in vitro* and *in vitro.* However, we have not addressed how the miRNAs may be functioning in the other arches that give rise to the thymus (PA3) and cardiac outflow tract (PA3, -4, and -6). The thymus and cardiac outflow tract require epithelial-mesenchymal interactions for their development and maturation, thus miRNA function may be concordantly regulating this event in all neural crest tissues. *Dlx* genes are not expressed in cardiac neural crest cells, so miR-452 may not be the miRNA responsible for guiding proper aorticopulmonary septation. Overexpression and knockdown of miR-452 in the neural crest will reveal its function, if any, in cardiac neural crest cells. Interestingly, *Dlx2* is expressed in the thymus (27), and as mentioned, heterozygous $Dicer^{loxP/+}$; *Wnt1-cre* mice have a hypoplastic thymus, suggesting that haploinsufficiency of *Dicer* alters the dosage of proteins, perhaps Dlx2*,* and results in abnormal thymus development.

It will be important to determine whether miR-452 regulates its host gene, *Gabre*, or vice versa, and if miR-452 function is important for *Gabre* expression. The expression pattern of miR-452 may reveal overlap with *Gabre,* which would suggest they share common regulatory elements. The intronic miRNAs, miR-208 and miR-499, found in muscle heavy chain genes follow their host gene expression patterns, and each miRNA regulates other sarcomeric genes within a hierarchical pathway (23). Not all miRNAs contained within genes may be regulated by or with their host transcript, such as miR-21 (28), which is contained in the 3'UTR of *TMEM49* and contains regulatory elements

located in an intron of *TMEM49*. Understanding the regulation of miR-452 may help elucidate its function within the neural crest.

We have found that translational control in the neural crest is important for proper development of the face and heart, which will allow us to dissect another level of the developmental genetics of the pharyngeal apparatus, and provide a more complete understanding of the genetic cause of craniofacial and cardiovascular disorders, such as DiGeorge syndrome.

MATERIALS AND METHODS

Mating and genotyping mice. *Dicer*$^{flox/flox}$ mice (16) and *Wnt1-cre* mice (29) have been described previously and were intercrossed to generate *Dicer*$^{flox/flox}$*; Wnt1-cre* mice. Genotyping was performed by PCR using these primers: Cre1: 5'AGGTCCGTTCAC-TCATGGA3', Cre2: TCGACCAGTTTAGTTACCC, Dicer-For: 5'ATTGTTACCAGCG-CTTAGAATTCC, Dicer-Rev: 5'GTACGTCTACAATTGTCTATG3'. *R26R-YFP* mice (Jackson Labs) were bred with *Dicer*$^{flox/flox}$ mice to generate *Dicer*$^{floxP/+}$*; R26R-YFP* mice.

Histological analysis. Skeletons from embryos were stained with Alcian Blue as described by McLeod (30). Yellow latex dye (Connecticut Valley Biological Supply) was injected into the beating right ventricle of the mutant heart using a 30-1/2 gauge needle. Then hearts were dehydrated and cleared in 2:1 benzyl benzoate to visualize the yellow latex in the vasculature. Pregnant mothers were dissected to obtain E14.5 wild-type and mutant embryos were fixed in 10% formalin, and then paraffin embedded.

Transverse sections through the heart were stained with hematoxylin and eosin to analyze morphology.

Optical Projection Tomography. Embryos at E14.5 were collected, and dehydrated into 100% methanol, embedded in low-melting agarose, and cleared in 2:1 benzyl benzoate for five days. Virtual sections were taken with an optical tomography scanner as described (31).

mRNA in situ hybridization. *In-situ* hybridization of whole mount embryos was carried out with digoxigenin-labeled probes, which were synthesized with digoxigenin labeling mix (Roche) and T7 or T3 polymerase (Roche). The Msx1 and Dlx2 riboprobes were described previously (32, 8). Embryos were collected at E10.5, fixed in 4% paraformaldehyde, and dehydrated in 100% methanol. Prior to hybridization, embryos were rehydrated, treated with 10 μg/ml proteinase K (Sigma) for 15 minutes, and placed in prehybridization buffer for 4 hours at 61°C. Probes were added at 0.5 μg/ml and hybridized overnight at 61°C. After a series of washing steps, digoxigenin was detected with digoxigenin antibody conjugated with alkaline phosphatase (Roche). Color development was seen with BM Purple substrate (Roche), and pictures were taken with a Leica microscope.

Flow sorting and miRNA microarray. *Wnt1-cre* intercrossed with *Rosa26-YFP* mice were collected at E11.5, and embryos were dissected, trypsinized, spun at 2000 rpm and the pellet was resuspended in PBS and filtered through a 40 μm Millipore membrane.

Selection by FACs was based on selection of YFP expression. YFP+ and YFP– cells were collected for RNA preparation. Total RNA was isolated (Trizol, Invitrogen) from YFP+ and YFP– sorted cells and used for miRNA microarray hybridizations (Exiqon).

Pharyngeal arch culture and transfection. The pharyngeal arches from mutant and control embryos were dissected at E10.5, and incubated with dispase to dissociate the epithelial layer from the mesenchymal cells. The epithelial layer is removed with fine tungsten needles and the arches are placed on a nitrocellulose membrane supported by a wire frame. The apparatus is placed in BGJb media (Gibco) supplemented with 10% fetal bovine serum and 50 U/ml peniicillin/strptomycin antibiotics. The arches are kept at 37ºC for 48 hrs.

Pharyngeal arches are co-transfected with 2'O-methyl oligoribonucleotide mimics, miR-452 or miR-125b (Dharmacon), and the Block-iT Alexa Fluor-red fluorescent control oligo (Invitrogen) in 24-wells using Lipofectamine 2000 (Invitrogen). After 48 hours, pharyngeal arches are fixed in 4% paraformaldehyde and dehydrated in 100% MeOH or Trizol for subsequent *in situ* hybridization or qRT-PCR, respectively.

Quantitative-RT-PCR. RNA was prepared from pharyngeal arches transfected with miR-452 mimic and Block-iT Alexa Fluor-red (Invitrogen) or Block-iT alone with Trizol (Invitrogen). For miRNA qRT-PCR, cDNA was reverse transcribed from 10 ng of total RNA using the Taqman microRNA Reverse Transcription Kit (Applied Biosystems). miR-16 was used as an endogenous control.

Figure 1

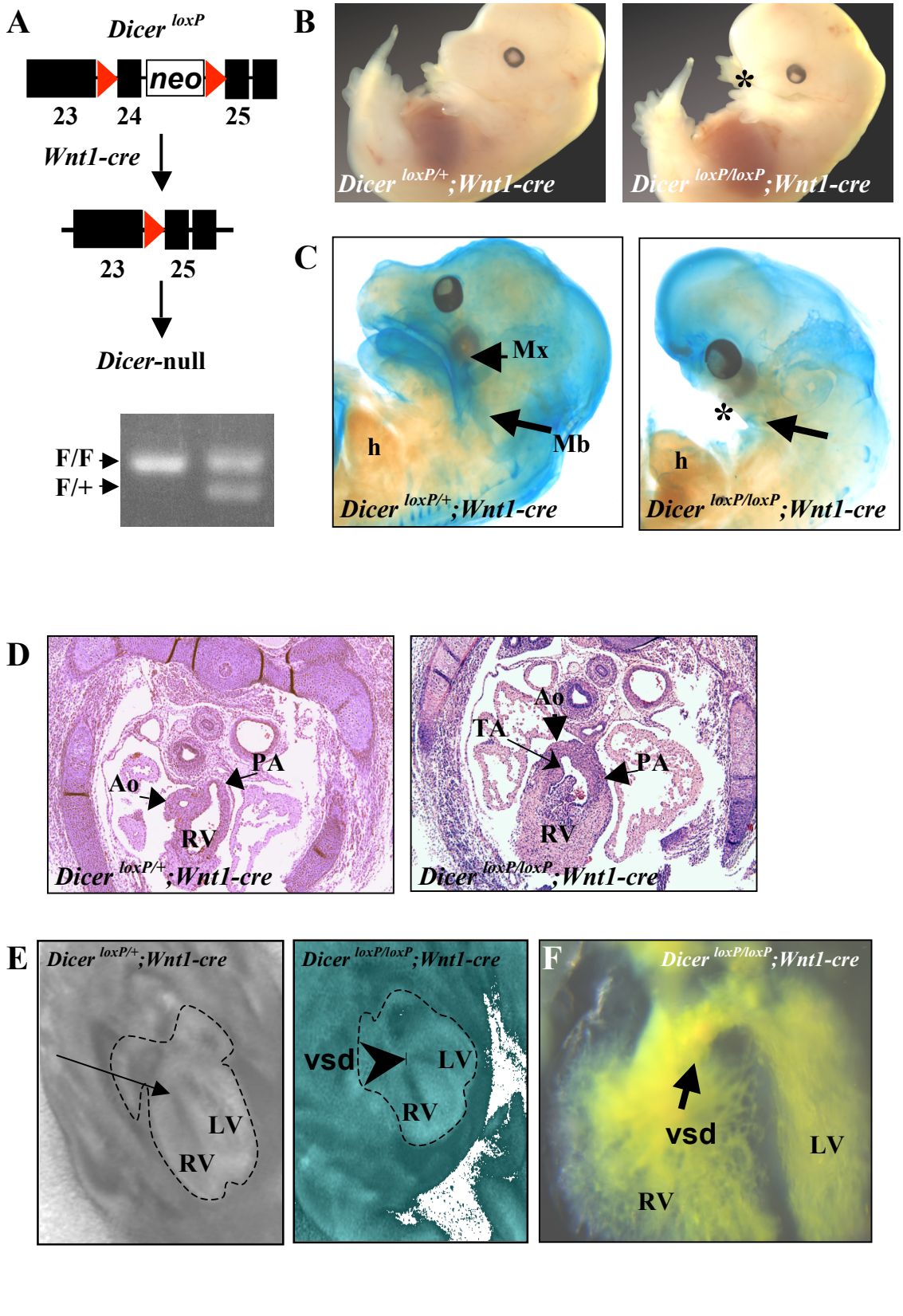
A
Dicer loxP
neo
23
24
25
Wnt1-cre
23
25
Dicer-null
F/F
F/+
B
Dicer loxP/+;Wnt1-cre
Dicer loxP/loxP;Wnt1-cre
C
Mx
Mb
h
Dicer loxP/+;Wnt1-cre
h
Dicer loxP/loxP;Wnt1-cre
D
PA
Ao
RV
Dicer loxP/+;Wnt1-cre
Ao
TA
PA
RV
Dicer loxP/loxP;Wnt1-cre
E
Dicer loxP/+;Wnt1-cre
LV
RV
Dicer loxP/loxP;Wnt1-cre
vsd
LV
RV
F
Dicer loxP/loxP;Wnt1-cre
vsd
LV
RV

Figure 1. Craniofacial and cardiac defects in *Dicer$^{loxP/loxP}$; Wnt1-cre* mutants.

(*A*) Schematic of the *DicerloxP* allele containing LoxP sites flanking exon 24, which encodes the RNAseIII domain required for Dicer's enzymatic activity. In the presence of Cre recombinase the 24th exon is removed; PCR genotyping depicting the floxed allele (F/F) and the flox and wild-type allele (F/+); (*B*) Gross morphology of *Dicer loxP/+; Wnt1-cre* compared to the mutant, *Dicer loxP/loxP;Wnt1-cre* at E14.5*,* * indicates facial defect; (*C*) Alcian blue staining of E14.5, heterozygote, showing normal maxillary (Mx) and mandibular (Mb) cartilage, mutant, * showing lack of cartilaginous jaw formation and frontal nasal process (arrow); (*D*) Transverse sections at E14.5 showing normal aorticopulmonary septation in heterozygote control, and truncus arteriosus (TA) in mutant; (*E*) Virtual OPT sections of heterozygote control, closed ventricular septum (thin arrow) and mutant, showing ventricular septal defect (VSD) (arrowhead); (*F*) Yellow latex injection into right ventricle revealing VSD (arrow); h, heart; Ao, aorta; PA, pulmonary artery; RV, right ventricle; LV, left ventricle.

Figure 2.

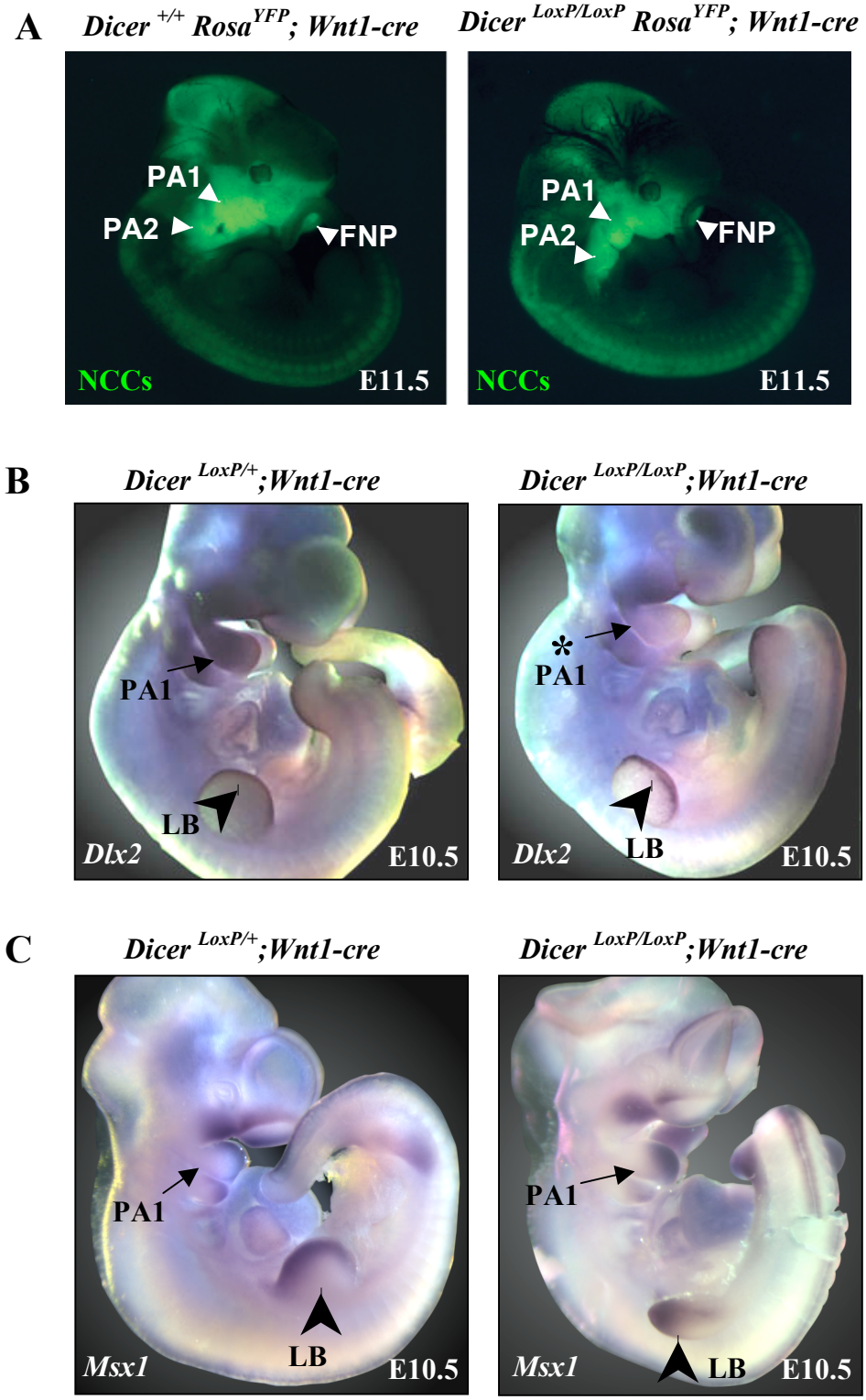
A
Dicer +/+ Rosa YFP; Wnt1-cre
Dicer LoxP/LoxP Rosa YFP; Wnt1-cre
PA1
PA2
FNP
NCCs
E11.5
PA1
PA2
FNP
NCCs
E11.5
B
Dicer LoxP/+;Wnt1-cre
Dicer LoxP/LoxP;Wnt1-cre
PA1
LB
Dlx2
E10.5
*
PA1
LB
Dlx2
E10.5
C
Dicer LoxP/+;Wnt1-cre
Dicer LoxP/LoxP;Wnt1-cre
PA1
LB
Msx1
E10.5
PA1
LB
Msx1
E10.5

Figure 2. Loss of miRNA function in the neural crest affects pharyngeal arch patterning not migration. (*A*) Lineage tracing of NCCs by *Wnt1-cre* mediated YFP expression shows normal migration of NCCs in mutants compared to control at E11.5; (*B*) Whole-mount *in situ* hybridization to detect *Dlx2* expression at E10.5; mutant shows decreased *Dlx2* (*) expression in PA1 (arrow) compared to littermate control, but shows no change of *Dlx2* in the limb bud (LB), which is a non-NCC-derived tissue; (*C*) Whole-mount *in situ* hybridization to detect *Msx1* expression at E10.5; mutant shows no significant difference compared to littermate control; NCCs, neural crest cells; PA1, first pharyngeal arch; PA2, second pharyngeal arch; FNP, frontonasal process; LB, limb bud.

Figure 3.

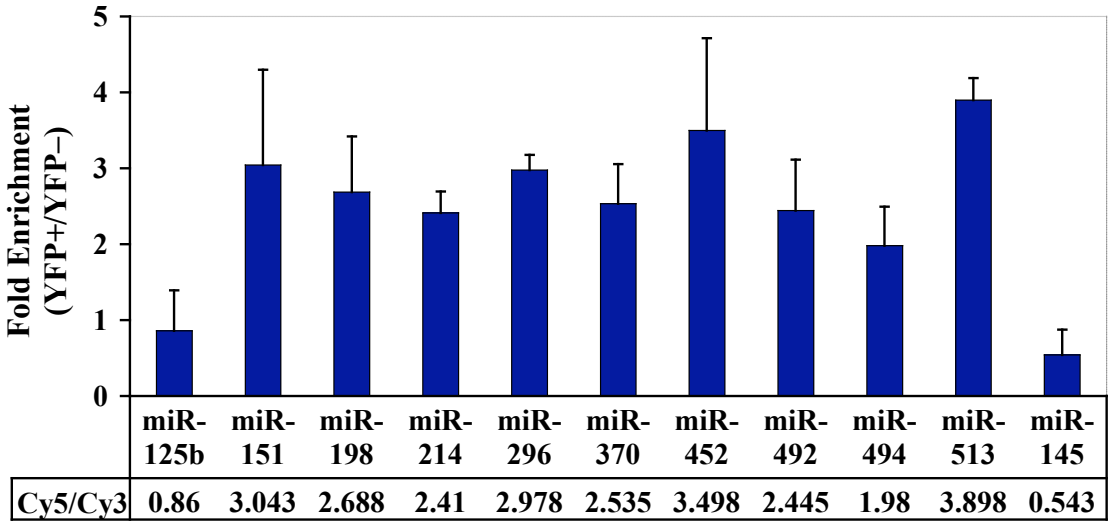

Figure 3. Neural crest-enriched miRNAs. Graph representing miRNA microarray results (Exiqon); fold enrichment calculated based on the comparison of miRNA levels in YFP-positive cells to YFP-negative cells isolated from *Rosa*^{YFP}*;Wnt1-cre* embryos at E11.5; Absolute values shown below bar-graph; Cy5/Cy3, red/green fluorescence (done in quadruplicate).

Figure 4.

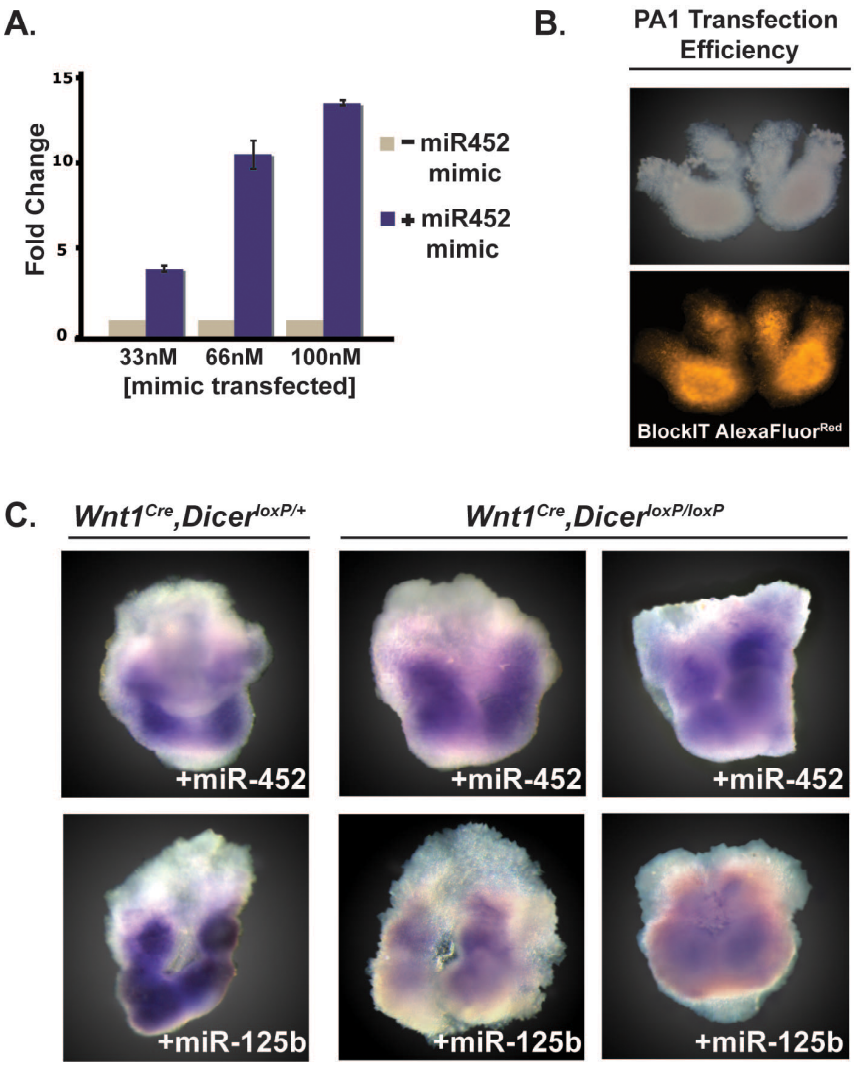

Figure 4. miR-452 rescues *Dlx2* expression in PA1. (*A*) qRT-PCR to detect miR-452 in chemically transfected pharyngeal arches; (*B*) bright-field and fluorescent images of the first pharyngeal arch post-transfection with BlockIT AlexaFluor^{Red} (Invitrogen); (*C*) Whole-mount *in situ* hybridization for *Dlx2* expression showed that the addition of miR-452 (+miR-452) could rescue *Dlx2* expression in *Wnt1*^{Cre}*, Dicer*$^{loxP/loxP}$ mutants (top right panels) back to control levels (left panel); miR-125b, control, could not rescue (bottom right panels).

REFERENCES

1. LaBonne, C. & Bronner-Fraser, M. (1999) *Annu Rev Cell Dev Biol* **15,** 81-112.
2. Kirby, M. L., Gale, T. F., & Stewart, D. E. (1983) *Science* **220,** 1059-1061.
3. Stoller, J. Z. & Epstein, J. A. (2005) *Semin Cell Dev Biol* **16,** 704-715.
4. Wurdak, H., Ittner, L. M., Lang, K. S., Leveen, P., Suter, U., Fischer, J. A., Karlsson, S., Born, W., & Sommer, L. (2005) *Genes Dev* **19,** 530-535.
5. Clouthier, D. E., Williams, S. C., Yanagisawa, H., Wieduwilt, M., Richardson, J. A., & Yanagisawa, M. (2000) *Dev Biol* **217,** 10-24.
6. Tucker, A. S., Yamada, G., Grigoriou, M., Pachnis, V., & Sharpe, P. T. (1999) *Development* **126,** 51-61.
7. Graham, A., Francis-West, P., Brickell, P., & Lumsden, A. (1994) *Nature* **372,** 684-686.
8. Yamagishi, C., Yamagishi, H., Maeda, J., Tsuchihashi, T., Ivey, K., Hu, T., & Srivastava, D. (2006) *Pediatr Res* **59,** 349-354.
9. Thomas, T., Kurihara, H., Yamagishi, H., Kurihara, Y., Yazaki, Y., Olson, E. N., & Srivastava, D. (1998) *Development* **125,** 3005-3014.
10. Bulfone, A., Kim, H. J., Puelles, L., Porteus, M. H., Grippo, J. F., & Rubenstein, J. L. (1993) *Mech Dev* **40,** 129-140.
11. Zhao, Y., Samal, E., & Srivastava, D. (2005) *Nature* **436,** 214-220.
12. Zhao, Y., Ransom, J. F., Li, A., Vedantham, V., von Drehle, M., Muth, A. N., Tsuchihashi, T., McManus, M. T., Schwartz, R. J., & Srivastava, D. (2007) *Cell* **129,** 303-317.
13. Davis, T. H., Cuellar, T. L., Koch, S. M., Barker, A. J., Harfe, B. D., McManus, M. T., & Ullian, E. M. (2008) *J Neurosci* **28,** 4322-4330.
14. Cuellar, T. L., Davis, T. H., Nelson, P. T., Loeb, G. B., Harfe, B. D., Ullian, E., & McManus, M. T. (2008) *Proc Natl Acad Sci U S A* **105,** 5614-5619.
15. Chen, J. F., Murchison, E. P., Tang, R., Callis, T. E., Tatsuguchi, M., Deng, Z., Rojas, M., Hammond, S. M., Schneider, M. D., Selzman, C. H.*, et al.* (2008) *Proc Natl Acad Sci U S A* **105,** 2111-2116.
16. Harfe, B. D., McManus, M. T., Mansfield, J. H., Hornstein, E., & Tabin, C. J. (2005) *Proc Natl Acad Sci U S A* **102,** 10898-10903.
17. Eberhart, J. K., He, X., Swartz, M. E., Yan, Y. L., Song, H., Boling, T. C., Kunerth, A. K., Walker, M. B., Kimmel, C. B., & Postlethwait, J. H. (2008) *Nat Genet* **40,** 290-298.
18. Chai, Y., Jiang, X., Ito, Y., Bringas, P., Jr., Han, J., Rowitch, D. H., Soriano, P., McMahon, A. P., & Sucov, H. M. (2000) *Development* **127,** 1671-1679.
19. Qiu, M., Bulfone, A., Ghattas, I., Meneses, J. J., Christensen, L., Sharpe, P. T., Presley, R., Pedersen, R. A., & Rubenstein, J. L. (1997) *Dev Biol* **185,** 165-184.
20. Merlo, G. R., Zerega, B., Paleari, L., Trombino, S., Mantero, S., & Levi, G. (2000) *Int J Dev Biol* **44,** 619-626.
21. Anderson, S. A., Qiu, M., Bulfone, A., Eisenstat, D. D., Meneses, J., Pedersen, R., & Rubenstein, J. L. (1997) *Neuron* **19,** 27-37.
22. Bulfone, A., Wang, F., Hevner, R., Anderson, S., Cutforth, T., Chen, S., Meneses, J., Pedersen, R., Axel, R., & Rubenstein, J. L. (1998) *Neuron* **21,** 1273-1282.
23. van Rooij, E., Liu, N., & Olson, E. N. (2008) *Trends Genet* **24,** 159-166.

24. van Rooij, E., Sutherland, L. B., Liu, N., Williams, A. H., McAnally, J., Gerard, R. D., Richardson, J. A., & Olson, E. N. (2006) *Proc Natl Acad Sci U S A* **103,** 18255-18260.
25. van Rooij, E., Sutherland, L. B., Qi, X., Richardson, J. A., Hill, J., & Olson, E. N. (2007) *Science* **316,** 575-579.
26. Depew, M. J., Lufkin, T., & Rubenstein, J. L. (2002) *Science* **298,** 381-385.
27. Woodside, K. J., Shen, H., Muntzel, C., Daller, J. A., Sommers, C. L., & Love, P. E. (2004) *Gene Expr Patterns* **4,** 315-320.
28. Fujita, S., Ito, T., Mizutani, T., Minoguchi, S., Yamamichi, N., Sakurai, K., & Iba, H. (2008) *J Mol Biol* **378,** 492-504.
29. Danielian, P. S., Echelard, Y., Vassileva, G., & McMahon, A. P. (1997) *Dev Biol* **192,** 300-309.
30. McLeod, M. J. (1980) *Teratology* **22,** 299-301.
31. Sharpe, J., Ahlgren, U., Perry, P., Hill, B., Ross, A., Hecksher-Sorensen, J., Baldock, R., & Davidson, D. (2002) *Science* **296,** 541-545.
32. Ivey, K., Tyson, B., Ukidwe, P., McFadden, D. G., Levi, G., Olson, E. N., Srivastava, D., & Wilkie, T. M. (2003) *Dev Biol* **255,** 230-237.

CHAPTER 4

miR-143 AND miR-145 REGULATE ENDOCARDIAL AND SMOOTH MUSCLE PROLIFERATION AND DIFFERENTIATION

Kimberly R. Cordes, Sarah U. Morton, Kathryn N. Ivey, Alecia N. Muth, Mark White and Deepak Srivastava, Gladstone Institute of Cardiovascular Disease, University of California San Francisco, 1650 Owens Street, San Francisco, California 94158, USA.

ABSTRACT

MicroRNAs (miRNAs) are emerging as important post-transcriptional gene regulators during development and disease. However, little is known about individual miRNAs that regulate early developmental events, in particular cardiac morphogenesis. We found that the disruption of miRNA biogenesis in a subset of cardiac progenitors known as the second heart field (SHF) results in loss of the derivatives of these progenitors in the heart. In a screen to identify enriched miRNAs, we found that the highly conserved miRNAs, miR-143 and miR-145, are expressed specifically in early cardiac progenitors and we have defined the cis- and trans-acting factors that direct expression of this miRNA in the mammalian heart. Identification of miR-143 and miR-145 targets revealed that they function in an important cardiac- and smooth muscle- specific regulatory feedback loop by targeting SRF-dependent and Calcium-dependent factors in mice and zebrafish. Together these pathways show the dynamic function this family of miRNAs can play by balancing between the proliferation and differentiation fate of cardiac and smooth muscle cells. Specifically we show that miR-143 and miR-145 promote SMC differentiation by

repressing factors that promote SMC proliferation, and provide evidence that miR-145 translationally activates the SMC-regulator, Myocardin. Finally, we found that miR-143 and miR-145 function is important for endocardial differentiation in zebrafish, and is necessary for Myocardin-dependent smooth muscle conversion of fibroblasts. Our results show that miRNA processing and function is required for development of cardiac progenitors and specifically demonstrate that miR-143 and miR-145 function is critical in this process.

INTRODUCTION

Cardiac and smooth muscle cells (SMCs) are initially formed from the mesodermal progenitors that originate in the cardiac crescent of the lateral plate mesoderm during early embryogenesis. A complex genetic differentiation program guides the progenitors into mature cardiomyocytes or SMCs (1). Although the composition of cardiac and smooth muscle cells are very different, many of the pathways that regulate their proliferation and differentiation during development overlap. Both muscle cell types are dependent on the coordinated expression and action of serum response factor (SRF), which interacts with other critical regulators of cardiac and smooth muscle-specific genes, such as the homeodomain factor Nkx2-5 and the SAP domain-containing factor Myocardin (2). SRF plays a dual role in cardiac and SMC development, influencing both proliferation and differentiation depending on the developmental stage and other signals that are present (3). A major challenge is to understand not only the basic properties of cardiac and smooth muscle progenitors but also how the balance between their proliferation and differentiation is regulated. Several recent studies have identified

microRNAs (miRNAs) as key regulators in balancing proliferation and differentiation in a variety of cancers and developmental processes, such as in B-cell lymphomas and myogenesis, respectively (4-7).

miRNAs are small ~22 nucleotide (nt), highly conserved non-coding RNAs that post-transcriptionally regulate messenger RNAs (mRNA). miRNAs are initially transcribed into a primary transcript (pri-miRNA) and then processed into ~70 nt hairpin precursor molecules (pre-miRNA) by the ribonuclease enzyme Drosha and its partner DGCR8 (8). Then the pre-miRNA is exported from the nucleus into the cytoplasm by Exportin5 where it is cleaved by Dicer into a double-stranded mature miRNA. Preferential strand separation and incorporation into the RNA-induced silencing complex (RISC) allows the mature miRNA to identify its target mRNA (8). Each individual miRNA has hundreds of predicted mRNA targets as shown by different bioinformatics algorithms, however relatively few targets have been experimentally validated. miRNAs generally inhibit mRNA translation by binding to the 3' untranslated region (3'UTR) and promoting translation repression or mRNA degradation. However, recent studies suggest that miRNAs can also activate mRNA translation by binding to the 3'UTR under certain stress conditions (9). In this study, we examined the effects of the global loss of miRNAs during early cardiogenesis and found that miR-143 and miR-145 were enriched in cardiac progenitors, and maintain expression in cardiac- and smooth muscle during development and in the adult. We demonstrate that the loss-of-function of these miRNAs in zebrafish results in cardiac malformation and dysfunction and that miR-143 and miR-145 regulates endocardial proliferation by targeting a calcium-signaling pathway. In addition, we provide evidence that this family of miRNAs functions in an important cardiac- and

smooth muscle- specific regulatory feedback loop by targeting SRF-dependent factors such as *Myocardin, Elk-1* and *Klf4* for either translational activation or repression, respectively. Furthermore, we show that miR-143 and miR-145 are necessary for Myocardin-dependent smooth muscle conversion of fibroblasts and may be important factors in vascular disease.

RESULTS

Conditional Dicer Inactivation in Cardiac Progenitors

To evaluate the global requirement of miRNAs in the cardiac progenitors, we used a previously established conditional null allele of Dicer to inactivate Dicer in the early cardiac progenitors (10) (Fig. S1). The cardiac progenitors lie in the splanchnic and lateral plate mesoderm of the cardiac crescent at embryonic day 7.5 (E7.5) in mouse and consist of two distinct cardiac progenitor populations: the first and second heart fields (FHF and SHF, respectively) (11). The FHF gives rise to the future left ventricle and atria of the heart, while the SHF contributes to the future outflow tract and right ventricle of the heart (11). To abolish Dicer function in the SHF, we took advantage of the early onset of expression of the *Islet1-cre* transgenic mice, in which *Cre* is expressed in the undifferentiated mesodermal progenitors at E7.5 that will give rise to the right ventricle and outflow tract (12). Dicer, which is essential for processing of pre-miRNAs into their mature form, was effectively deleted in the SHF progenitors, and the embryos died from heart failure by E9.5. Embryos lacking Dicer function developed a hypoplastic right ventricle and a shortened outflow tract (Fig. 1B, 1D) compared to littermate control (Fig1A, 1C). Early markers of the SHF, such as *Islet1* and *Fgf10* were expressed in their

normal domains, suggesting that the cardiac progenitors were present (Fig. S1B-C). The early lethality of Dicer mutants revealed an essential requirement for miRNA function in the cardiac progenitors, specifically in the SHF.

Identification of miRNAs Enriched in Cardiac Progenitors

We previously identified cardiac progenitor miRNAs that were enriched during differentiation of mouse ES (mES) cells into cardiomyocytes, and the most abundantly enriched miRNA was miR-143 (7). To determine if this held true *in-vivo*, we crossed *Islet1-cre* transgenic mice with *Rosa26-EYFP*, and upon cre-mediated excision we were able to mark the *Islet1* population with YFP (Fig. 1E). By fluorescence-activated cell sorting (FACs) at E9.5, we obtained RNA from Islet+, YFP+ cells (Fig. 1F) and profiled miRNA expression by microarray analysis. We identified miR-143 and miR-145 to be enriched in the SHF progenitors. Further validation by RT-PCR confirmed the expression of miR-143 and miR-145 in the *Islet1* positive cells at a level comparable to that of *Foxa2*, a meso/endodermal marker of the SHF (Fig. 1G).

miR-143 and miR-145 are two highly conserved miRNAs that lie within 1.8 kilobases (kb) (Fig. 1H) from each other on mouse chromosome 18 and have been shown to be down-regulated in various cancer cell lines, colon cancers, and B-cell malignancies (13, 14, 4). The genomic organization and proximity of *miR-143* and *miR-145* suggested that they may be contained in a bicistronic primary transcript but we were unable to amplify a common transcript. The processing of primary-miRNA transcripts (pri-miRNAs) into their active ~22 nucleotide (nt) mature form is a rapid process, so we took advantage of ES cells containing a mutation in the nuclear miRNA processing enzyme,

DGCR8, to obtain enough RNA to attempt detection of the pri-miRNA transcript. The differentiation of the DGCR8 null ES cells into embryoid bodies (EBs) allows induction of the mesodermal lineage and *miR-143* and *-145* transcription, but no further production of precursor or mature miRNAs (15). We analyzed DGCR8 null EB RNA by RT-PCR and amplified a product that encompassed both miRNAs (Fig. 1I) suggesting that they are transcribed as a bicistronic unit, and may share upstream regulatory elements to control their expression.

Expression and Regulation of miR-143 and miR-145 in Cardiac and Smooth Muscle

To identity the tissue-specific expression and regulation of the *miR-143*/ *miR-145* gene during mouse development, we searched for regulatory regions that might recapitulate *in-vivo* transcription of miR-143 and miR-145. Comparison of genomic sequences across species using ECR Browser revealed that a 4.2 kilobase (kb) genomic region upstream of miR-143 was highly conserved between human and mouse (Fig.2A). The 4.2kb miR-143/145 fragment was sufficient to direct lacZ expression in the hearts of transgenic mice starting at E7.5, with expression at the earliest stage overlapping with the cardiac progenitors present in the cardiac crescent (Fig. 2B). The expression of lacZ became more robust and uniform in the developing heart, outflow tract and surrounding pharyngeal mesoderm and endoderm, notably the second heart field, and dorsal aorta, with lack of expression in the cardinal vein and somites (Fig. 2C-E). During later cardiogenesis, lacZ expression became restricted to the myocardium and endocardium of the ventricles and atria, but was absent in the septated aortic arch arteries (Fig. 2F). Postnatally, lacZ expression became strongest in the smooth muscle of the aorta,

pulmonary artery, and coronary vessels, but was absent in the myocardium (Fig. 2G-H). The enhancer recapitulated endogenous miR-145 expression as shown by section *in situ* hybridization of the heart during adult stages (Fig. I-J).

To identify and characterize a minimal enhancer element, we made deletions of the 4.2kb miR-143/145 enhancer and found that a 0.9kb region was sufficient for miR-143/145 cardiac expression (Fig. 3A). Within this regulatory region, we observed *cis* elements highly conserved between human, mouse, and zebrafish that represented potential binding sites for the essential cardiac transcription factors SRF and Nkx2.5. The SRF site contained a classic CArG box that is highly conserved and duplicated in zebrafish. We found that SRF weakly activated the miR-143/145 enhancer placed upstream of a luciferase reporter, but addition of Myocardin (Myocd), a potent cardiac- and smooth muscle coactivator of SRF, synergistically activated luciferase when transfected into cos-1 cells (Fig. 3B). When we mutated the SRF binding site, Myocd-dependent luciferase activity decreased and showed that Myocd's activity was dependent on an intact SRF-binding site (Fig. 3B). The combination of Nkx2.5, SRF and Myocd doubled luciferase activity, suggesting that the SRF and Nkx2.5 binding sites were necessary for full transactivation of the miR-143/145 gene (Fig. 3B). In transgenic mice, mutation of the SRF binding site abolished lacZ expression in the outflow tract of the heart and disruption of the Nkx2.5 site diminished expression in the ventricles and atria (Fig. 3A). Disruption of both the SRF and Nkx2.5 binding sites abolished all activity of the enhancer within the heart (Fig. 3A). In an electromobility shift assay, SRF could specifically bind to its respective site in the miR-143/145 enhancer region (Fig. 3C). Additionally, SRF-null EBs had decreased expression of miR-143 or miR-145 by

quantitative RT-PCR compared to wild-type EBs (Fig. 3D). To verify that the decrease in miR-143 and miR-145 levels was not due to the absence of mesoderm in SRF-null EBs, we measured the levels in mesoderm-rescued SRF-null EBs (7), and continued to see a reduction of miR-143 and miR-145. This suggests that miR-143/miR-145 function in an SRF-dependent manner in the heart.

miR-143 and miR-145 Function in Zebrafish

We used zebrafish as a model to investigate the loss of miR-143 and miR-145 function in the developing heart. The zebrafish genome contains a duplication and inversion of miR-143/miR-145 and the upstream *cis*-acting sequence that contains the highly conserved SRF and Nkx2.5 binding sites. By observing a published zebrafish miRNA *in situ* hybridization database, miR-143 and miR-145 were expressed in the adult heart and outflow tract (OFT), respectively (16). We confirmed the adult expression of miR-143 and miR-145 in the zebrafish heart and OFT (4A), and further showed miR-145 expression in the atrioventricular canal and branchial arches, and miR-143 expression in the ventricle and branchial arches at earlier stages of heart development (48hpf) (Fig. 4A).

We injected 1 nanogram (ng) of morpholinos complementary to the miR-143 or miR-145 sequence in the 1-2 cell stage embryo to identify the requirement of each miRNA for heart development. By 48 hpf, both morpholino knockdowns (143^{MO} and 145^{MO}) showed decreased or absent blood flow in two of the five branchial arch arteries, as shown by using zebrafish lines fluorescent for a marker of blood, *Gata1-dsRed*, and a marker for endothelial cells, *Flk1-GFP* (Fig. 4B) (17). Additionally, confocal imaging of

zebrafish hearts at 48 hpf that contained a fluorescent nuclear myocardial marker, *H2B-GFP* revealed that both miR-143MO and miR-145MO had a dilated atria compared to controls (Fig. 4B) (17). The knockdown of miR-143 resulted in less severe defects than the knockdown of miR-145, yet the combined knockdown showed no exacerbation of the phenotype (data not shown).

We hypothesized that miR-143 and miR-145 functioned to balance between the states of proliferation and differentiation during heart development, so we performed BrdU immunostaining on whole fish and found that the loss of miR-143 or miR-145 caused an increase in proliferation (Fig. 4C). However, the increase in proliferation was not within the myocardium (Cmlc2-GFP), but within the Flk1-positive endocardial layer of the heart (Fig. 4C). Concordantly, miR-143 and miR-145 was expressed in the early endocardium of mouse (Fig. 2E).

The similar phenotype that resulted from knocking down miR-143 and miR-145 independently suggested that they may have similar targets or target members of a similar pathway. In our search for potential targets, we found that miR-143 and miR-145 targeted members of the calcium-calcineurin (Ca^{2+}–CnA) pathway. Bioinformatic approaches identified potential binding sites within the *Nfatc1* 3`UTR for miR-143 and miR-145 (Fig. 4D) and two miR-145 binding sites in the *Calcineurin A* (*CnA*) 3`UTR. To determine whether miR-143 or miR-145 directly targeted *Nfatc1* or *CnA*, we cloned the 3`UTR of each downstream of a luciferase reporter under control of the CMV promoter, and transfected it with miR-143 or miR-145 into cos-1 cells. miR-145 effectively down-regulated luciferase activity in the presence of the *Nfatc1* 3`UTR or *CnA* 3`UTR compared to a control miRNA that had no predicted binding sites within

either 3`UTR (Fig 4F). In addition, a mutation in the miR-145 binding site in each 3`UTR luciferase construct restored luciferase activity in the presence of miR-145, suggesting that both binding sites were bona fide miR-145 target sequences. However, we were unable to see a similar repression of luciferase with the addition of miR-143 in the presence of the *CnA* or *Nfatc1* 3'UTR.

Unfortunately there is not an antibody to detect zebrafish Nfat or Calcineurin A protein levels. To overcome this issue, we created stable miR-143 and miR-145 knockdown cell lines in a muscle-specific cell line, C2C12 cells that normally express Nfatc and CnA. We created a miRNA sponge construct that contains nine miR-145 imperfect binding sites in the 3'UTR of mCherry under the control of the EF-1 promoter (Fig. 4E). Recent reports showed that the imperfect binding sites mimic endogenous mRNA targets and sequester or "soak up" the miRNA away from its endogenous targets (18). By stably expressing the miR-145 sponge (miR-145^{SPO}) transgene in C2C12 cells, we were able to analyze predicted targets by western analysis in a loss-of-function model. Indeed, Nfatc1 protein levels were up-regulated in differentiated miR-145^{SPO} C2C12 cells (Fig. 4E), suggesting that the unavailability of endogenous miR-145, released suppression of its native target, *Nfatc1*. In addition, the over-expression of miR-145 in these cells was able to reduce Nfatc1 levels back to differentiated wild-type C2C12 endogenous levels (Fig. 4E). Although, we found Nfatc1 protein levels to be regulated by miR-145, we found no difference in CnA protein levels in the miR-145^{SPO} cell line (data not shown).

Activation of *Nfatc1* in mice and human pulmonary valve endothelial cells is known to increase endothelial proliferation (19). The calcineurin-Nfat signaling pathway

is conserved in zebrafish and known to regulate endothelial cell proliferation and valve morphogenesis (20). Since miR-143 and miR-145 are expressed in the endothelial cells of zebrafish, and the knockdown of either miRNA caused an increase in endocardial cell proliferation, we examined whether elevated calcineurin-Nfat signaling was the cause of the increased endocardial cell proliferation. To test this, we blocked calcineurin-Nfat signaling with the inhibitor, cyclosporine A (CsA), in control, 143^{MO}, and 145^{MO} zebrafish between 22-30 hpf, the time crucial for Nfatc signaling and heart valve formation (20) and examined the morphology and endocardial proliferation at 48 hpf. Indeed, CsA rescued the dilated atria defect and eliminated the increased proliferation in the endocardium of 48 hpf 143^{MO} or 145^{MO} (Fig 4G, H), suggesting that both miR-143 and miR-145 function to regulate the calcineurin-Nfatc pathway in zebrafish. Despite the endocardial proliferation rescue, CsA did not rescue the branchial arch and blood flow defects, most likely due to the fact that the calcineurin-Nfat pathway does not regulate branchial arch development and that both miRNAs have multiple targets during zebrafish cardiovascular development that do not affect the calcineurin-Nfatc pathway.

miR-143 and miR-145 Regulates SRF-Dependent Pathways

To study the additional functions that miR-143 and miR-145 have during cardiac and smooth muscle development, we extended our search for potential targets, and found that multiple positive and negative regulators of SRF-dependent smooth muscle development contained well-conserved binding sites for miR-143 and miR-145 in their 3'UTRs. Smooth muscle cells are known to switch between differentiated and proliferation phenotypes in response to extracellular cues (2). SRF activates genes involved in smooth

muscle differentiation and proliferation by recruiting muscle-restricted cofactors, such as Myocd, and ternary complex factors (TCFs) of the ETS-domain family, respectively. It has been shown that growth signals repress smooth muscle genes by the displacement of Myocd from SRF by Elk-1, a TCF that acts a myogenic repressor. The antagonistic influences of Myocd and Elk-1 on smooth muscle gene expression are mediated by competing for a common docking site on SRF (3). Aberrant gene expression of these antagonistic pathways can promote phenotypic modulation of vascular smooth muscle cells (VSMCs) and lead to vascular disease (2). We used a bioinformatics approach to predict mRNA targets of miR-143 and miR-145 and found multiple highly conserved binding sites within the 3'UTR of *Elk-1* or *Myocd,* respectively (Fig. 5A). We therefore cloned the 3'UTR of *Myocd* into a luciferase reporter 3'UTR, with transcription of the luciferase under the control of the constitutively active CMV promoter. Surprisingly, addition of miR-145 into cos-1 cells caused a significant activation in luciferase activity when the *Myocd* 3'UTR was present, and this activation was lost when the miR-145 binding site was mutated (Fig. 5B). On the other hand, the addition of miR-143 in the presence of the 3'UTR of *Elk-1* resulted in a repression of luciferase activity (Fig. 5C). Since Elk-1 and Myocd are important in smooth muscle regulation, we assayed mRNA and protein levels *in-vitro* in rat aortic A10 smooth muscle cells. The addition of a cholesterol-tagged antisense oligo (antagomiR; (21) or inhibitor of miR-143 (miR-$143^{inhibitor}$) to adult rat aortic A10 cells resulted in upregulation of Elk-1 protein levels (Fig. 5D). Unfortunately, a good antibody to detect endogenous Myocd levels is unavailable, which prevented us from observing Myocd protein change in response to miR-145. Yet, these results are consistent with the recent finding that miRNAs can act as

translational activators or repressors (9), and suggest that miR-143 and miR-145 are coordinately processed to help promote SRF-Myocardin dependent smooth muscle transcription with miR-143 repressing *Elk-1* and miR-145 promoting *Myocd* expression.

Interestingly, a highly conserved miR-145 binding site was also found in the 3'UTR of the *myocardin-related transcription factor- B*, *Mrtf-B* (Fig. 5F). When we expressed miR-145 in the presence of the *Mrtf-B* 3'UTR, luciferase activity was greatly reduced, indicating that miR-145 targeted *Mrtf-B* for translational repression (Fig. 5F). Mrtf-B shares comparable homology to Myocd and is required for differentiation of SMC in neural crest-derived SMC but is dispensable for SMC development in other tissues (22, 23). Although they both can bind SRF and activate SMC gene transcription, genetic deletions of each gene in mice reveal differences between their spatial expression and function in SMC differentiation (22). Correspondingly, miR-143 and miR-145 are not expressed in the cardiac neural crest (CNC)-derived smooth muscle until after birth, after Mrtf-B is required for differentiation of SMCs (data not shown). The lack of miR-143 and miR-145 expression in the CNC-derived SMC correlates with the enhancer we described that showed no activity in the embryonic aortic arches (AAs) at the time of CNCCs populating the AAs. It is interesting to speculate that miR-143 and miR-145 helps to distinguish smooth muscle identity by downregulating Mrtf-B after smooth muscle differentiation of neural crest derivatives.

Another negative regulator of SRF-myocardin dependent smooth muscle gene activation, kruppel-like factor 4 (KLF4) (24) was upregulated when we knocked down miR-145 function by transfecting a miR-145 antagomiR into A10 cells (Fig. 5D). Following vascular injury, Klf4 is rapidly induced in the proliferating smooth muscle,

whereas normal expression in smooth muscle is low (Fig. 5D; (25). Klf4 is known to abrogate Myocd's ability to promote smooth muscle gene expression (24). We identified a miR-145 binding site in the 3'UTR of *Klf4*, and confirmed that miR-145 targets it for translational repression by luciferase assay (Fig. 5H). In addition, knockdown of miR-145 in rat A10 SMCs, showed an increase in Klf4 protein levels (Fig. 5D).

miR-145 Regulates Smooth Muscle Conversion

Myocd is known to be a master regulator of smooth muscle differentiation, whereby transfection of Myocd into nonmuscle cells, such as 10T1/2 fibroblasts, converts them to smooth muscle cells (26). Introduction of miR-145 into fibroblasts was sufficient to induce many markers of smooth muscle differentiation but not all. However, miR-145 functions synergistically with Myocd to convert 10T1/2 fibroblasts into smooth muscle cells (Fig. 6A-B). We titrated the precise dosage of Myocd needed with miR-145 to induce SMC differentiation. We found that a low concentration of Myocd (50ng), which could not induce SMC differentiation alone, was sufficient to induce SMC when expressed with miR-145. However, the addition of a miR-145 antagonist abrogated Myocd's ability to convert fibroblasts to smooth muscle (Fig. 6C). The overexpression or knockdown of miR-143 had little effect on smooth muscle conversion. This suggests that miR-145 is necessary for Myocd-dependent smooth muscle conversion.

miR-143 and miR-145 Are Down-regulated during Vascular Injury

Because of the evidence for miR-143 and miR-145 to regulate the balance of smooth muscle proliferation and differentiation, we asked whether these two miRNAs were

dysregulated in vascular injury. Many of the miR-143 and miR-145 targets that we found are aberrantly expressed in response to vascular injury, such as restenosis and coronary heart disease, which results in SMCs losing their quiescent contractile state and gaining an aggressively proliferative nature (27). In a vascular-injured mouse, *in situ* hybridization of miR-143 and miR-145 revealed decreased expression of both miRNAs within the smooth muscle layer of a ligated-carotid artery, whereas the contralateral carotid artery showed normal expression of each miRNA (Fig. 7A).

Interestingly, we found that a gene recently described to be upregulated in response to vascular injury, *CamkII-delta* (*CamkII-δ;* (29)) had two conserved miR-145 binding sites within its 3`UTR (Fig. 7B). CamkII-δ is known to promote smooth muscle proliferation and vascular remodeling via a Ca^{2+}–dependent mechanism (29). We confirmed CamkII-δ as a target of miR-145 by luciferase and western analysis in A10 cells (Fig. 7C-D). This finding adds to the complexity of SMC phenotypic regulation by suggesting that miR-145 can target both SRF-dependent and independent pathways in order to sustain smooth muscle in a differentiated state.

DISCUSSION

This study identifies the expression of miR-143 and miR-145 in cardiac progenitor cells, and shows that they are expressed dynamically throughout cardiac and smooth muscle development. We provide strong evidence that both miRNAs function to regulate the balance between proliferation and differentiation in cardiac and smooth muscle cells (Fig. 7E). We revealed multiple in-vivo and in-vitro targets for miR-143 and miR-145 using loss- and gain-of function studies. In zebrafish, we showed that miR-143/145 function

by regulating endocardial proliferation through regulation of the calcineurin-Nfat pathway. Unfortunately, we could not study the smooth muscle regulation of miR-143/145 in zebrafish morpholino knockdowns because they die by 72 hpf, and smooth muscle markers have been difficult to detect during the larval stages of zebrafish development and actually do not become detectable until adult stages (>96 hpf) (30, 31). However, the lack of blood flow through two branchial arches, along with the expression of miR-143/145 in the arches, insinuates that the miRNAs are functioning in the fish vasculature prior to smooth muscle differentiation. The branchial arch defects in the 143^{MO} and 145^{MO} fish could be due, in part, by dysregulation of the same factors involved in mouse smooth muscle differentiation.

Understanding the mechanism of smooth muscle cell proliferation and differentiation will provide a foundation for elucidating the pathology of SMC-related diseases, such as atherosclerosis, restenosis, and asthma. SMC can undergo phenotypic switching- between a proliferative or differentiation state. A hallmark feature of SMC phenotypic switching during vascular injury or repair in many SMC-related disease states is downregulation of expression of SMC-specific marker genes, such as SM α-actin, SM-MHC, and SM22α (27). As such, there has been interest in identifying molecular mechanisms that induce or repress SMC marker gene expression. Here we show that miR-143 and miR-145 are also downregulated in a vascular injury mouse model, and their function is to promote and sustain differentiation of smooth muscle cells by translationally repressing multiple factors in the SRF-dependent smooth muscle proliferation pathway. This suggests the possibility that reintroducing miR-143/145 post-vascular injury will result in SMC re-differentiation for vascular repair.

One of the mechanisms that support this SMC re-differentiation is the surprising finding that miR-145 could activate in-vitro translation of *Myocd*. Recent reports have shown that miRNAs can activate mRNA translation in response to stressful conditions that affect the state of the cell cycle (9). We provide evidence that miR-145 positively regulates Myocardin-dependent smooth muscle differentiation. Interestingly, *Myocd* and the enhancer follow a similar expression profile during cardiac and smooth muscle development (32), suggesting that they positively reinforce each other throughout development. Translational activation of Myocd during vascular injury may be one way in which miR-145 could help initiate the re-differentiation of smooth muscle cells and aid in vascular repair.

Our experiments have identified multiple targets of miR-143 and miR-145 and have began to build upon existing pathways and linking new ones. We found that miR-143 and miR-145 function in regulating the smooth muscle phenotype in mice and the endocardial calcium-signaling pathway in zebrafish and mice. The mouse knockouts of miR-143 or miR-145 individually and together, will provide further insight into their function as partners to balance regulatory pathways, as well as their independent roles as major modulators during cardiac and smooth muscle development.

MATERIALS AND METHODS

Generation of Dicer Conditional Null Mice. *Dicer*$^{flox/flox}$ mice (10) and *Islet1-cre* mice (12) have been described previously and were intercrossed to generate *Islet1-cre; Dicer*$^{flox/flox}$ mice. Genotyping was performed by PCR using these primers: Cre1: 5'AGGTCCGTTCACTCATGGA3', Cre2: TCGACCAGTTTAGTTACCC, Dicer-For:

5'ATTGTTACCAGCGCTTAGAATTCC, Dicer-Rev:

5'GTACGTCTACAATTGTCTATG3'.

Transgenic Mice and Flow Cytometry. Transgenic mice were generated and Bluo-gal staining and histological analyses were performed as previously described (33). For promoter analysis, different fragments were subcloned into a pHsp68LacZ reporter vector and blastocyst injected. Islet1-cre intercrossed with Rosa26-YFP mice were collected at E9.5, and heart and surrounding tissue was dissected, trypsinized, spun at 2000 rpm and the pellet was resuspended in PBS and filtered through a 40 μm Millipore membrane. Selection by FACs was based on selection of expression YFP. YFP+ and YFP– cells were collected for RNA preparation.

miRNA Microarray and miRNA In Situ Hybridization. Total RNA was isolated (Trizol, Invitrogen) from mouse E9.5 embryonic hearts and used for miRNA microarray hybridizations (Exiqon) and quantitative real-time PCR.

miRNA *in situ* hybridization analyses were performed as described (34) with the following modifications: paraffin embedded tissue sections or cryosections were treated for15 minutes with Proteinase K, hybridized at the 59ºC for miR-145 and 42ºC for miR-143, and final color development was performed with NBT/BCIP (Roche).

Electromobility Shift Assay (EMSA). Oligoribonucleotides corresponding to the conserved SRF- and Nkx2.5-binding sites in the miR-143/145 enhancer were synthesized (Integrated DNA Technologies) as follows:

SRF binding site: GGGAGCAGCCTTGCCATATAAGGGCAGG; SRF mutant binding site: GGGAGCAGCCTTGCTACCGAAGGGCAGG.

Zebrafish lines. *wt* AB and transgenic *Tg(myl7:HRAS-mEGFP)*^{s843}, *Tg(flk1:EGFP)*^{s843}, *Tg(flk1:EGFP, gata1:RFP)*^{s843}, *Tg(H2B:GFP)* zebrafish (17) and unpublished) were raised under standard laboratory conditions at 28°C (35).

Microinjection. Embryos were injected at the 1–2-cell stage with 0.5-2 ng of dre-miR-143 MO (5´-ACUCUACUUCGUGACAUCGAG-3´, Integrated DNA Technologies (IDT)), 0.5-2 ng of dre-miR-145 MO (5´-CAGGUCUUUUGGGUCCUUAGGG-3´, IDT), 0.5-2 ng of scrambled MO (5´-CACUUGGUGGGUCAGGUCUUG-3´, IDT). The embryos were maintained at 28ºC until harvesting.

Confocal analysis. Embryos were fixed in 2% paraformaldehyde (PFA) overnight, embedded in 4% low-melt agarose, and cut into 150-μm sections with a Leica VT1000S vibratome. Images were acquired with a Zeiss LSM5 Pascal confocal microscope.

Fish in situ hybridization. Probes against miR-143 and miR-145 (Exiqon), *cmlc2* (36), *amhc* (37), and *vmhc* (36) were used. miR-143 and miR-145 *in situ* hybridization was performed according to published protocols (Exiqon, Netherlands). Probes against mRNAs were synthesized, and in situ hybridizations were performed as described (38).

miR-143 and miR-145 Target Analyses. A target prediction algorithm developed in the Srivastava laboratory was used to bioinformatically identify potential targets of miR-143 and miR-145 (39). A 250bp fragment encompassing miR-145 was ligated into pSilencer

4.1-CMV (Ambion). A 250bp fragment containing miR-143 was ligated into the pEF-Dest-51(Invitrogen). The entire 3' UTR of each mRNA containing predicted miR-143 and/or miR-145 binding sites were cloned into the pMiR-Report luciferase reporter (Applied Biosystems). Point mutations of the binding sites were generated using QuickChange II PCR (Stratagene). All assays were performed in quadruplicate in 12-well plates of Cos-1 cells and transfected with siPort XP-1 (Ambion), 350 ng miR-143 or miR-145, 150 ng of luciferase and 50 ng of renilla constructs. After 24 hours, cells were harvested and luciferase assay was measured using the Luciferase Dual-Reporter Kit (Promega). Renilla assays were performed in parallel to normalize for transfection efficiency.

Quantitative real-time-PCR. RNA was prepared from whole embryos injected with miR-143MO, or miR-145MO, or scrambled morpholinos with Trizol (Invitrogen). For miRNA qRT-PCR, cDNA was reverse transcribed from 10 ng of total RNA using the Taqman microRNA Reverse Transcription Kit (Applied Biosystems). miR-26a was used as an endogenous control. Results represent at least three experiments.

ES cells or EBs, A10 cells, and differentiated 10T1/2 fibroblasts were harvested in Trizol (Invitrogen) for total RNA isolation. For mRNA reverse transcription, 2 μg of total RNA from each sample was reversed transcribed with Superscript III (Invitrogen). Taqman primers were used to amplify genes (ABI). The primers to detect the 1.7kb miR-143/145 primary transcript were as follows: Forward: GCATCTCTGGTCAGTTGGG, Reverse: GACCTCAAGAACAGTAT. GAPDH was used as a control. DGCR8^{null} EBs (Day 8, D10 EBs) were a gift from David Blelloch. For miRNA qRT-PCR on β–MHC-GFP control, SRF^{null}, miR-1 or miR-133 -overexpressed SRF^{null} EBs, was performed as

described above, and miR-16 was used as the endogenous control. Each qRT-PCR was performed at least three times; representative results are shown as fold expression relative to undifferentiated ES cells. Error bars indicate 95% confidence intervals.

Cyclosporine A treatment. Zebrafish embryos were dechorionated between 22-30 hpf and treated with cyclosporine A (Sigma) at a final concentration of 1μg/mL as described (32). The embryos were maintained at 28ºC until harvesting at 48 hpf.

Tissue Culture. 10T1/2 fibroblasts were maintained at low density around 30% confluence in DMEM with 10% FBS and were transfected with Lipofectomine 2000 (Invitrogen) and 1-2 μg of full length or smooth muscle isoform of Myocardin (26). Pre-miR-145 was cloned into pSilencer 4.1-CMV vector (Ambion) and pre-miR-143 was cloned into the pEF-Dest-51 vector (Invitrogen). Generally, 1-2 μg of plasmid was used for each well in a 6-well plate. Two days after transfection, media was replaced with differentiation medium (DMEM, 2% horse serum). Four-five days later, further analyses, including immunocytochemistry, Western blot, and RT-PCR was performed.

A10 smooth muscle cell and Cos-1 cells were maintained in DMEM with 10% FBS (40). A10 cells were transfected with BlockIT Fluorescent oligo (Invitrogen), miR-143 or miR-145 inhibitor (Dharmacon) or antagomiR (IDT Technologies), or miR-143, 145 mimic (Dharmacon). 24-48 hours later, western blot or RT-PCR was performed.

mRNA In-situ Hybridization, Immunohistochemistry and Western Blot Analysis. mRNA *in situ* hybridization for *Islet1* and *Fgf10* was performed as described (Kwon et al., 2007). Immunostaining was performed using pre-ready mouse anti-smooth muscle

actin (1A4) antibody (Dako) and 1:400 Tritc-conjugated goat anti-mouse IgG (Jackson ImmunoResearch). Myogenic conversion assays were performed as described, and protein lysates collected (26). Rat aortic A10 cells were collected and assayed using Elk-1, Klf-4, and Nfatc1 (Cell Signaling) antibodies. Myocardin full-length cDNA and Myocardin-related transcription factor-B full length cDNA (Open Biosystems) was cloned into pEF6/V5-His (Invitrogen) and then detected by anti-V5-HRP antibody (Sigma).

Mouse Vascular Injury Model. Mice that had their left carotid ligated were sacrificed 14-days post ligation, fixed and sectioned to obtain cross-sections of the left carotid artery and the contralateral right carotid artery for control. These paraffin sections were a gift from Joseph Miano.

Figure 1.

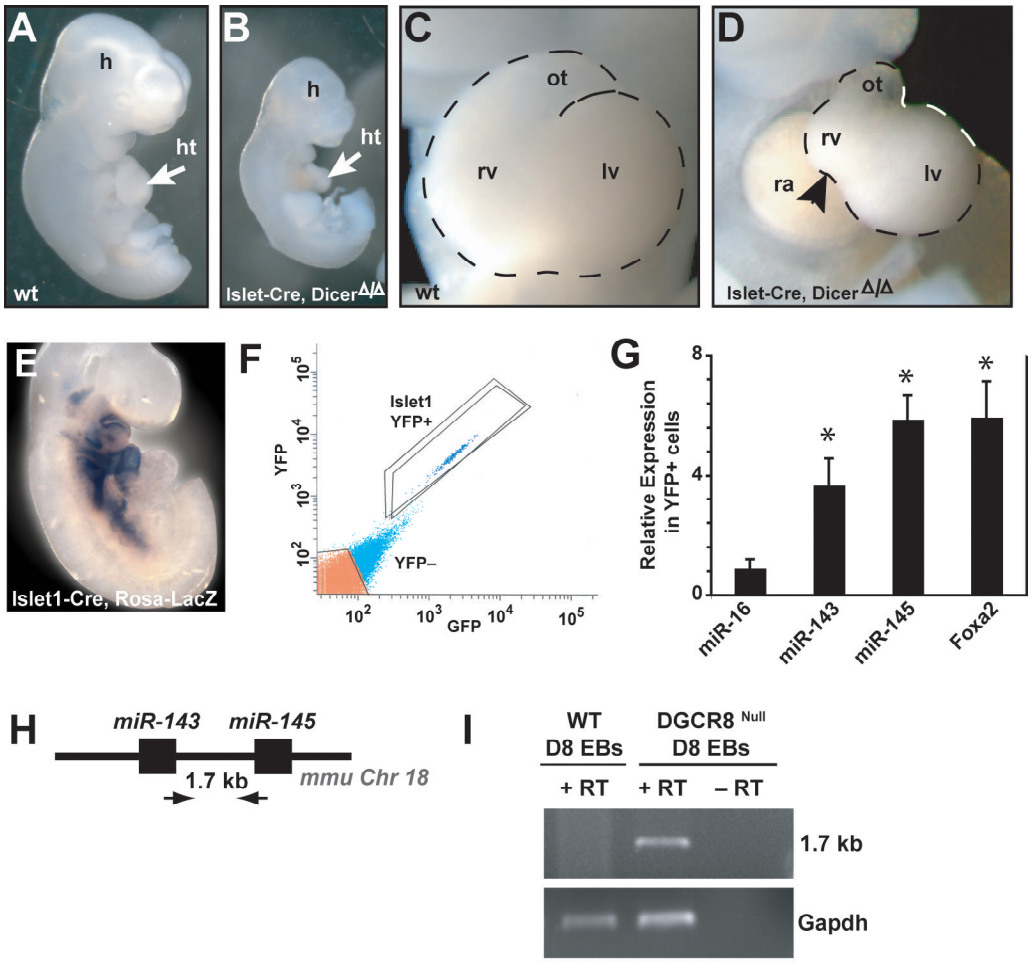

Figure 1. miRNA biogenesis is required in cardiac progenitors. (*A*) *Islet1-cre; Dicer*$^{flox/+}$(wt), (*B*) and *Islet1-cre; Dicer*$^{flox//flox}$ (mutant) embryos showed growth retardation at E9.5. (*C*) wt (*D*) and *Islet1-cre; Dicer*$^{flox//flox}$ frontal view of mutant heart showed hypoplastic RV and shortened OT **(***E***)** *Islet1-cre; R26R-LacZ* lineage tracing by X-gal staining showed expression domain at E9.5 (*F*) *Islet1-cre; R26R-YFP* fluorescent-activated cell sorting YFP+ and YFP– cells, 10,000 YFP+ cells obtained (blue/box), 60,000 YFP– cells (orange/box) **(***G***)** Quantitative RT-PCR (qRT-PCR) for relative mRNA levels of miR-143 and miR-145 in YFP+ cells; miR-16 endogenous control; Foxa2, SHF marker. (*H*) Schematic of the genomic organization of miR-143 and miR-145 on mouse Chromosome 18, arrows indicate primers designed to amplify 1.7kb

cotranscript by (*I*) reverse transcription of wt and *DGCR8*^{null} EBs, *GapdH* as control. (ht, heart; h, head; RV, right ventricle; LV, left ventricle; RA, right atrium; OT, outflow tract; EB, embryoid body); *, $p<0.05$.

Figure 2.

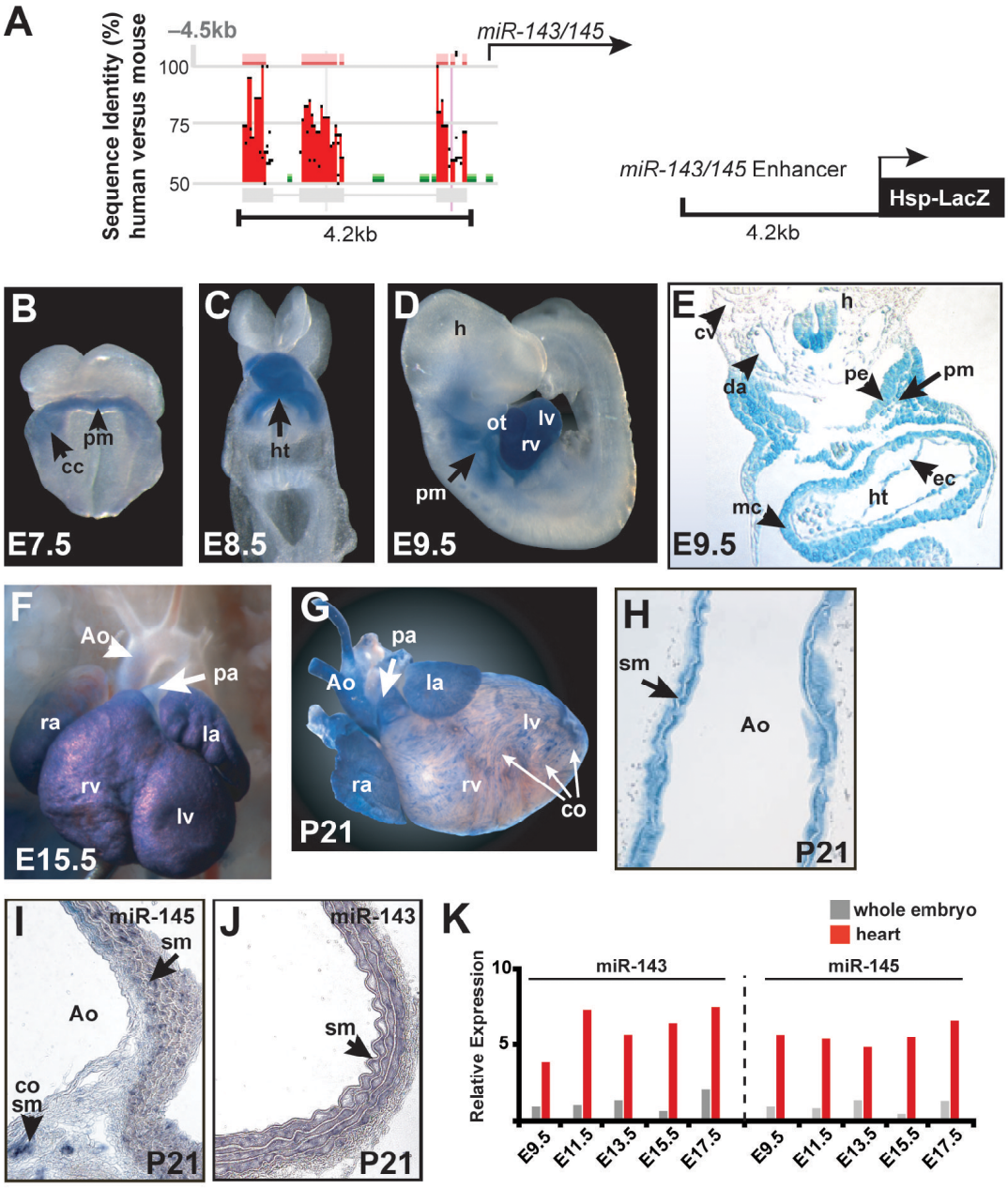

Figure 2. miR-143/145 are highly conserved and are cardiac- and smooth-muscle-specific. (*A*) Comparison of the miR-143/145 promoter regions between mouse and human. Percent conservation of a 4.2kb genomic region upstream of miR-143/145 is shown; that region is cloned into a HSP-LacZ cassette. **(***B-H***)** Whole mounts and sections showing β-gal activity driven by the genomic fragment shown in (A), (B) E7.5 X-gal expression in the cardiac crescent and PM, **(***C***)** E8.5, expression in linear heart tube, **(***D***)** E10, expression in PM and heart, **(***E***)** E10, transverse section of (*D*) showing X-gal expression in PM, PE, DA, and heart, **(***F***)** E15.5, expression in the myocardium of the heart, absent in the aortic arch arteries, **(***G***)** P21, β-gal activity in the epicardium of the atria, smooth muscle of the aorta, pulmonary artery, and coronary vessels, (*H***)** P21, transverse section of (*G*) showing smooth muscle expression in the aorta, (*I-J*) miR-145 (*I*) and miR-143 (*J*) section *in situ* hybridization showing smooth muscle and coronary vessel expression. (*K),* qRT-PCR showing miR-143 and miR-145 expression through out embryonic stages in the heart compared to the whole embryo. (pm, pharyngeal mesoderm; cc, cardiac crescent; ht, heart; h, head; ot, outflow tract; rv, right ventricle; lv, left ventricle; cv, cardinal vein; da, dorsal aorta; pe, pharyngeal endoderm; ec, endocardium; mc, myocardium; Ao, aorta; ra, right atrium; la, left atrium; pa, pulmonary artery; co, coronary vessels; sm, smooth muscle; co sm, coronary smooth muscle).

Figure 3.

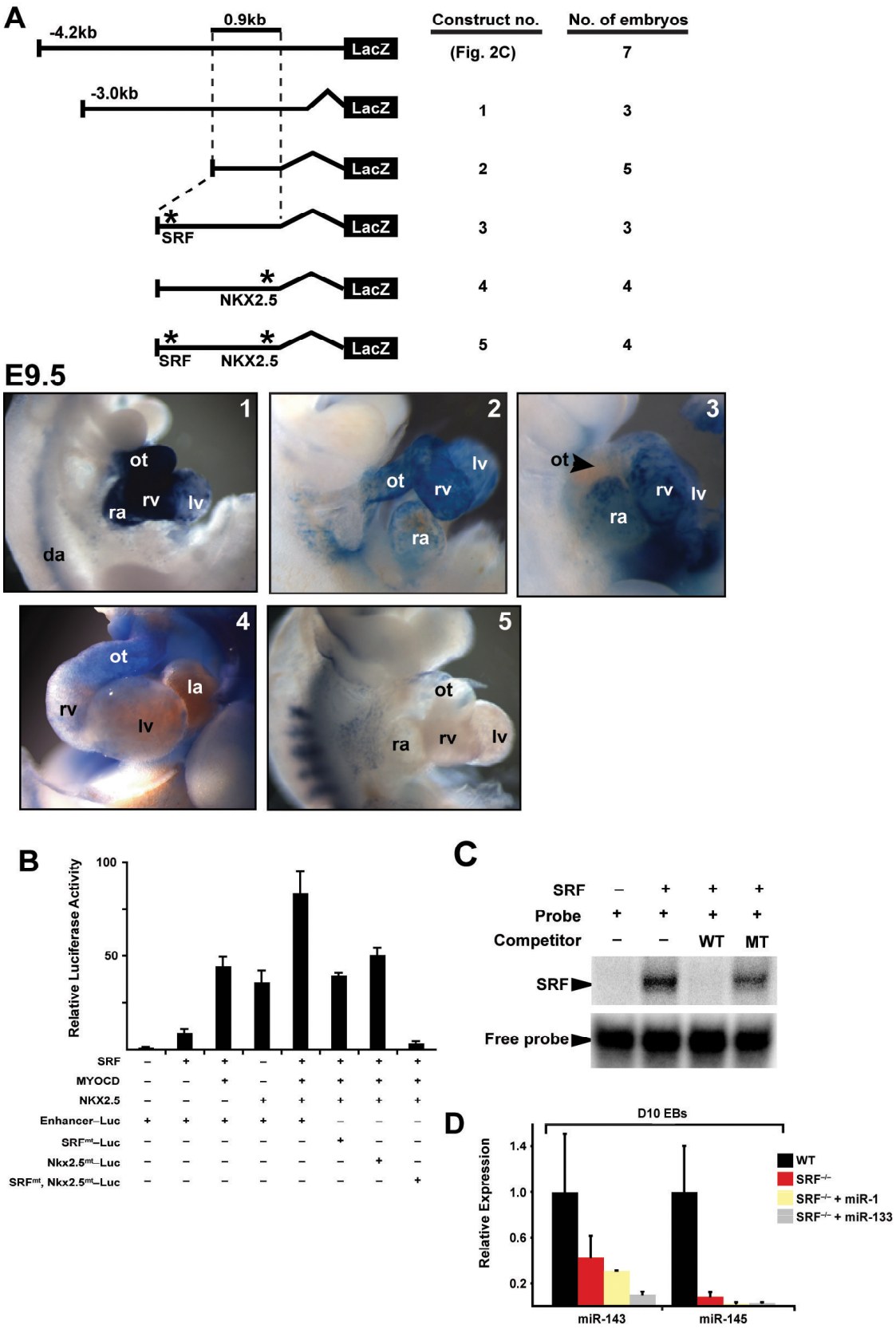
A
-4.2kb
0.9kb
LacZ
-3.0kb
SRF
NKX2.5
Construct no.
No. of embryos
(Fig. 2C)
7
1
3
2
5
3
3
4
4
5
4
E9.5
ot
rv
lv
ra
da
la
B
Relative Luciferase Activity
100
50
SRF
MYOCD
NKX2.5
Enhancer–Luc
SRFmt–Luc
Nkx2.5mt–Luc
SRFmt, Nkx2.5mt–Luc
C
SRF
Probe
Competitor
WT
MT
Free probe
D
D10 EBs
Relative Expression
1.4
1.0
0.6
0.2
WT
SRF−/−
SRF−/− + miR-1
SRF−/− + miR-133
miR-143
miR-145

Figure 3. SRF and Nkx2.5 directly regulate cardiac expression of miR-143 and miR-145. (*A*) A summary of the deletion and mutation analyses of upstream enhancer region of miR-143/145, asterisks (*) indicate mutations in the SRF or Nkx2.5 binding sites, construct number matches corresponding image of β-gal activity, heart shown. **(***B***)** Fold activation of luciferase downstream of miR-143/145 enhancer in Cos-1 cells by SRF, Myocardin, or Nkx2.5 with or with out point mutation. (*C*), Electrophoretic mobility-shift assay using radiolabeled probes (wild type, wt, or mutant, mt) for SRF binding site. (*D*) miR-143 and miR-145 levels checked by qRT-PCR in SRF^{null} EBs compared to β-MHC wild-type EBs, miR-1 and miR-133 overexpression in the SRF^{null} EB background showed an even greater reduction in miR-143 and miR-145 levels. Results shown are the average of three experiments in (*B***)*** and (*D*)*. (ot, outflow tract; ra, right atrium; lv, left ventricle; rv, right ventricle; la, left atrium; *, $p<0.05$)

Figure 4.

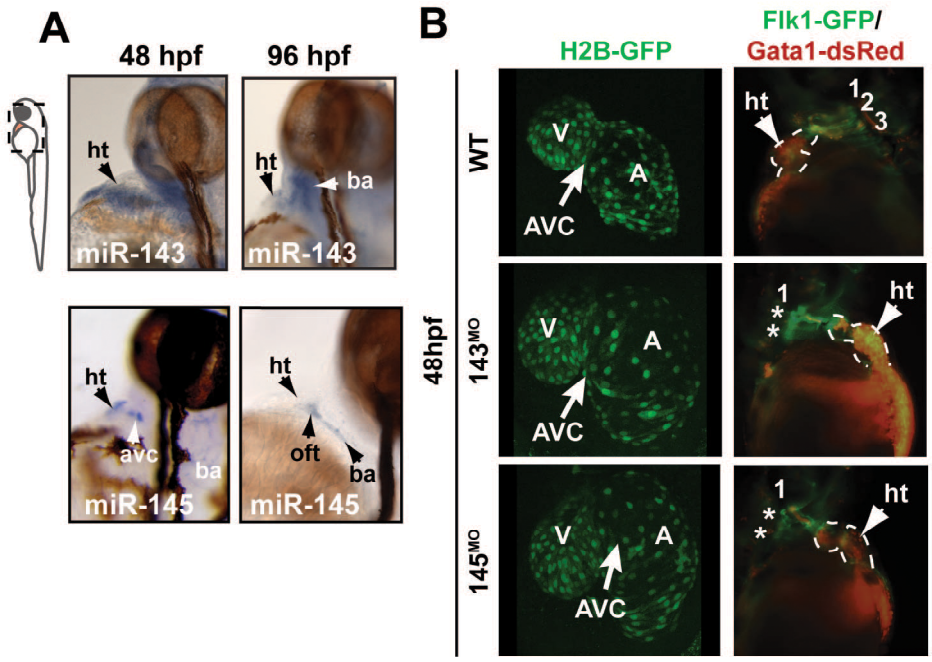

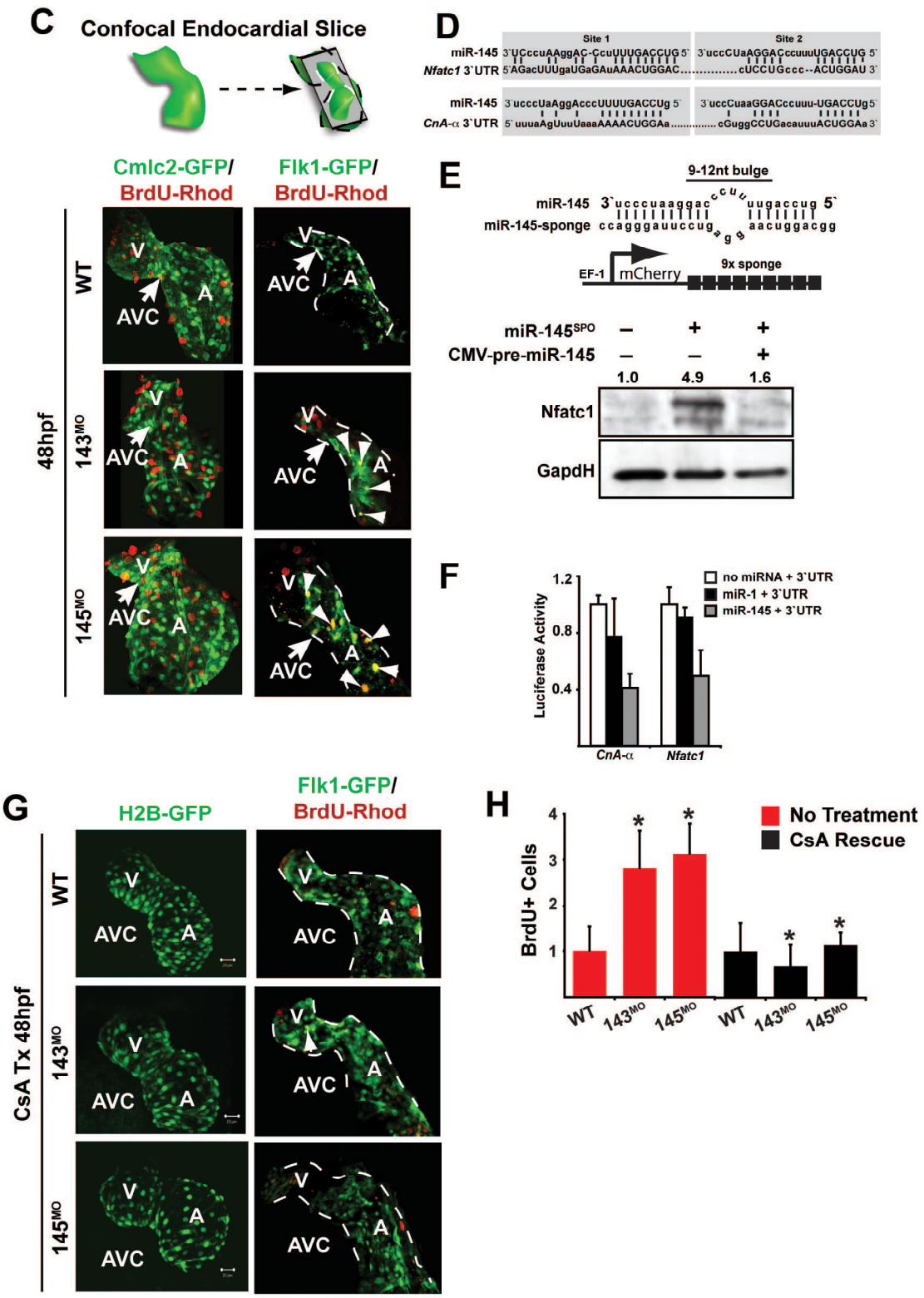
C
Confocal Endocardial Slice
Cmlc2-GFP/
BrdU-Rhod
Flk1-GFP/
BrdU-Rhod
48hpf
WT
143MO
145MO
V
A
AVC
D
Site 1
Site 2
miR-145 3`UCccuAAggAC-CcuUUUGACCUG 5`
Nfatc1 3`UTR 5`AGacUUUgaUGaGAuAAACUGGAC
miR-145 3`ucccUaAggAcccUUUUGACCUg 5`
CnA-α 3`UTR 5`uuuaAgUuuUaaaAAAACUGGAa
E
9-12nt bulge
miR-145 3`ucccuaaggac uugaccug 5`
miR-145-sponge ccagggauuccug aacuggacgg
EF-1
mCherry
9x sponge
miR-145SPO – + +
CMV-pre-miR-145 – – +
1.0 4.9 1.6
Nfatc1
GapdH
F
Luciferase Activity
1.2
0.8
0.4
no miRNA + 3`UTR
miR-1 + 3`UTR
miR-145 + 3`UTR
CnA-α
Nfatc1
G
H2B-GFP
Flk1-GFP/
BrdU-Rhod
CsA Tx 48hpf
WT
143MO
145MO
H
BrdU+ Cells
No Treatment
CsA Rescue
WT
143MO
145MO

Figure 4. miR-143 and miR-145 are required for cardiac development in zebrafish and function by regulating endocardium differentiation. (*A*) Lateral views of miR-143 and miR-145 whole-mount *in situ* hybridization showed expression of both in the heart at 48 hpf, with specific expression of miR-145 in the atrioventricular canal (avc) and in the heart, outflow tract (ot) and branchial arches (ba) at 96 hpf. **(***B***)** Confocal microscopy images of *H2B-GFP* miR-143MO and miR-145MO fish revealed dilated atria by 48 hpf, and decreased blood flow (*Gata1-dsRed*) in two branchial arches (*Flk1-GFP*) shown with an asterisk (*). **(***C***)** Confocal images of *cmlc2-GFP* fish immunostained with BrdU showed increased BrdU staining in miR-143MO and miR-145MO fish, and confocal image slices (see schematic) of *Flk1-GFP* fish immunostained with BrdU showed the endothelial cells overlap with BrdU positive cells (arrowheads), BrdU-positive cells quantified on right. **(***D***)** Schematic of the predicted miR-145 binding sites in the 3`untranslated region (UTR) of *Nfatc1* and *Calcineurin A;* (*E*) Schematic of the miR-145 sponge construct containing a 9-12 nt bulge, binding to miR-145 sequence; sponge construct was cloned in the 3`UTR of mCherry driven by the EF1 promoter and transduced into C2C12 cells to make a stable line that showed an increase in Nfatc1 protein levels **(***E***)** and that increase was reduced by the overexpression of miR-145 in the miR-145 sponge line. **(***F***)** Luciferase activity in Cos-1 cells upon introduction of *Nfatc1* or *Calcineurin A* 3`UTR sequences downstream of a CMV-driven luciferase reporter with no miRNA (negative control) or miR-1 (negative control) or miR-145 shown. **(***G***)** Confocal images of cyclosporine (CsA) treated *H2B-GFP* miR-143MO and miR-145MO fish, and confocal image slices of *Flk1-GFP* miR-143MO and miR-145MO fish stained with BrdU (arrowhead); BrdU quantification of CsA-treated fish on the right**.** Results shown represent at least three experiments in (*C*)*, (*F*)* and (*H*)*. Error bars indicate 95% confidence intervals. **(**ht, heart; oft, outflow tract; avc, atrioventricular canal; a, atrium; v, ventricle; *, $p<0.05$.)

Figure 5.

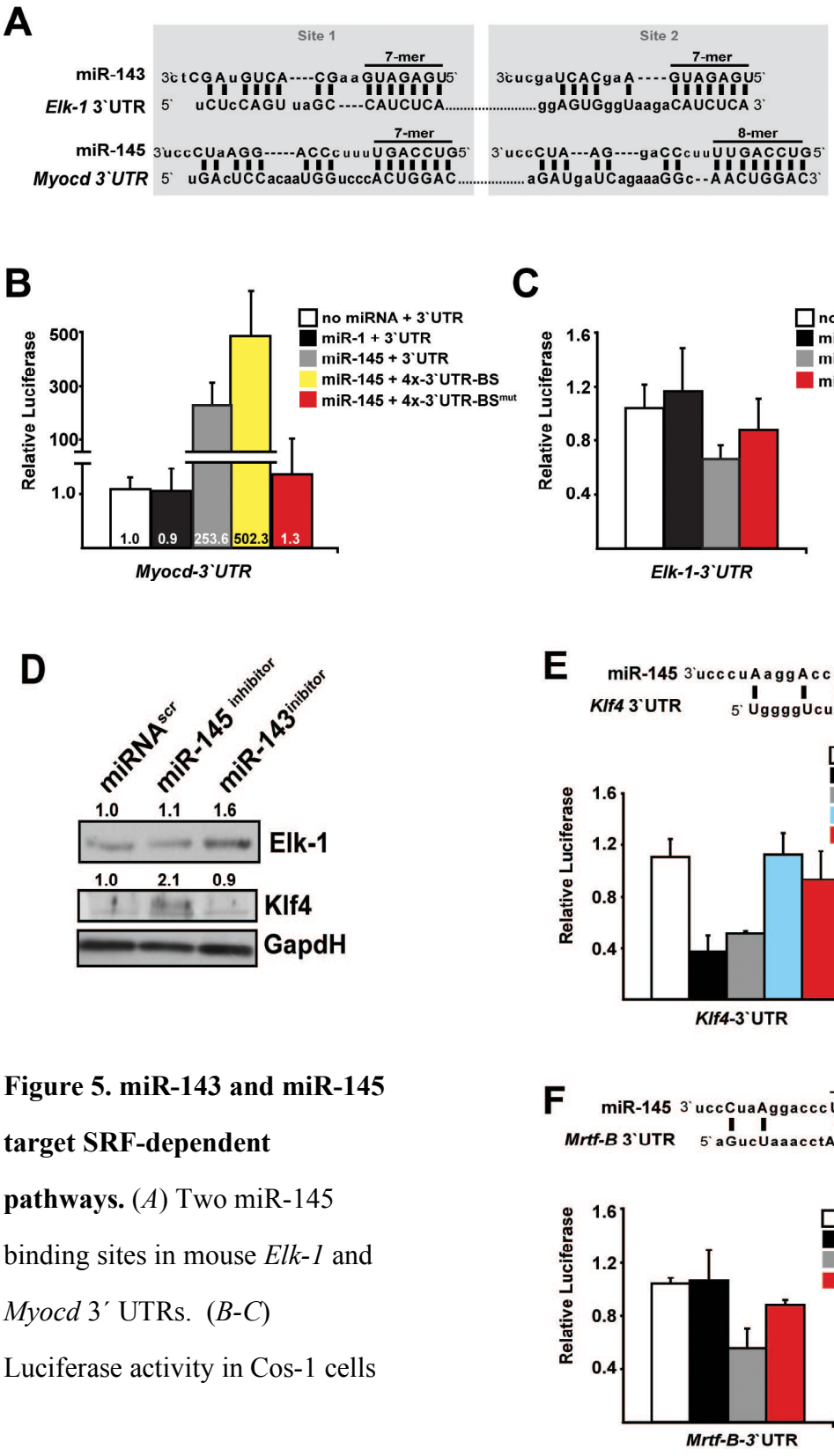

Figure 5. miR-143 and miR-145 target SRF-dependent pathways. (*A*) Two miR-145 binding sites in mouse *Elk-1* and *Myocd* 3′ UTRs. (*B-C*) Luciferase activity in Cos-1 cells

upon introduction of wild type (wt) or mutated *Myocd* (*B*) or *Elk-1* (*C*) 3´ UTR sequences downstream of a CMV-driven luciferase reporter with no miRNA (negative control), miR-1 (control miRNA) or miR-145 or miR-143, respectively, is shown; a 4x-multimer of one miR-145 binding site in Myocd 3`UTR is shown in (*B,* yellow bar); **(***D***)** Analysis of cell lysates from A10 smooth muscle cells that were transfected with a scrambled miRNA, or an antisense oligo to miR-143 or miR-145 ($miRNA^{scr}$, $miR\text{-}145^{inhibitor}$, $miR\text{-}143^{inhibitor}$, respectively) for Elk-1 and Klf4 protein levels assessed by western blot showed that Elk-1 protein level was up by 1.6-fold when miR-143 was knocked down, and Klf4 protein was increased by 2.1-fold when miR-145 was inhibited. **(***E***)** Measure luciferase activity of wt or mutated *Klf4*-3`UTR upon introduction of no miRNA (negative control), miR-1 (control miRNA), miR-145 or miR-452 (control miRNA). The decrease of luciferase in the presence of miR-1 is presumably due to miR-1 binding site within the *Klf4*-3`UTR. (*F*) Measured luciferase for wt or mutated *Mrtf-B* (*Mkl2)*-3`UTR upon addition of no miRNA (negative control), miR-1 (control miRNA), or miR-145. Results shown in (*B*)*, (*C*)*, (*E*)*, and (*F*)* represent at least four experiments with error bars indicating 95% confidence intervals. (densitometry calculations performed by Image J; *, $p<0.05$).

Figure 6.

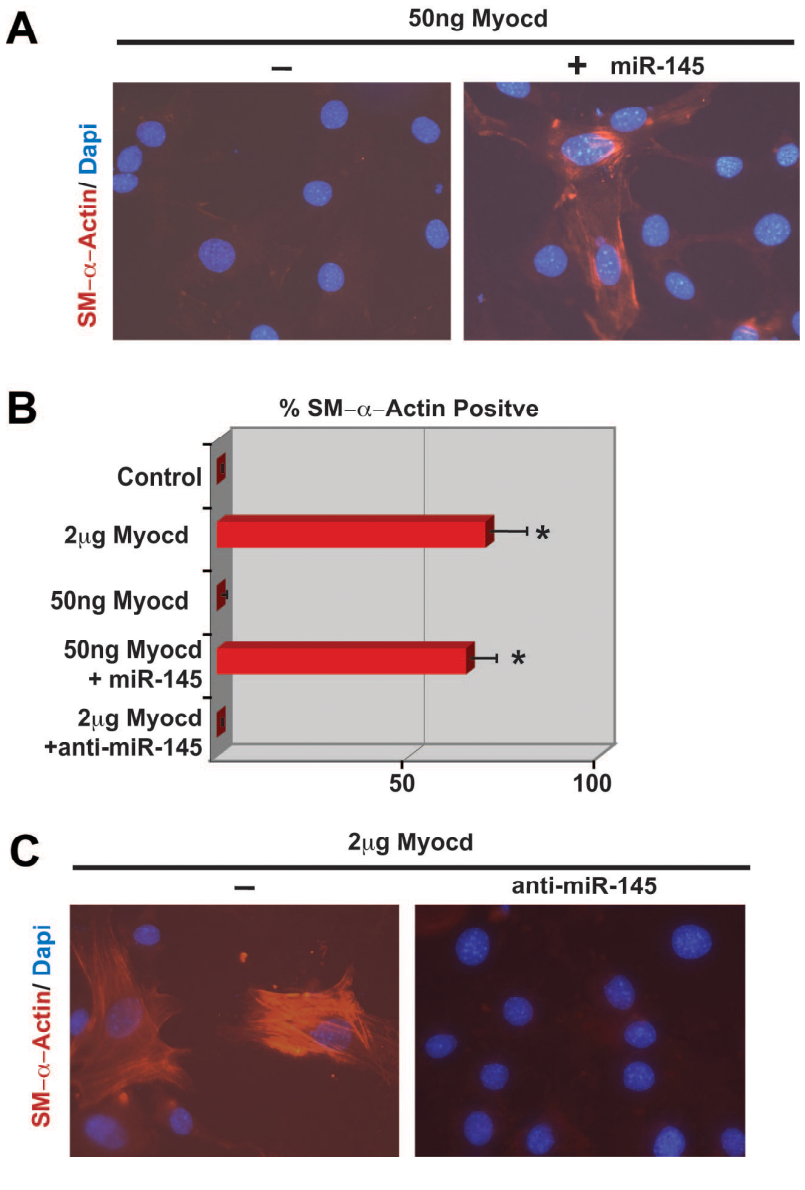

Figure 6. miR-145 is necessary for Myocardin-dependent smooth muscle conversion and smooth muscle gene expression. (*A*) Immunofluorescence showing smooth muscle alpha-actin (SMA, red) staining of 10T1/2 fibroblasts converted into smooth muscle by miR-145 overexpression with a minimum of 50ng of Myocd, 50ng of Myocd is not sufficient for smooth muscle conversion; nuclear stain, Dapi (blue). (*B*) Quantification of smooth muscle alpha-actin positive cells upon Myocd and miR-145-induced conversion. (*C*) Immunofluorescence of 10T1/2 cells undergoing smooth muscle conversion with 2 μg Myocd is blocked by an inhibitor of miR-145 (anti-miR-145). Results shown in (*B*), represent at least five experiments with error bars indicating 95% confidence intervals. (*, $p<0.05$).

Figure 7.

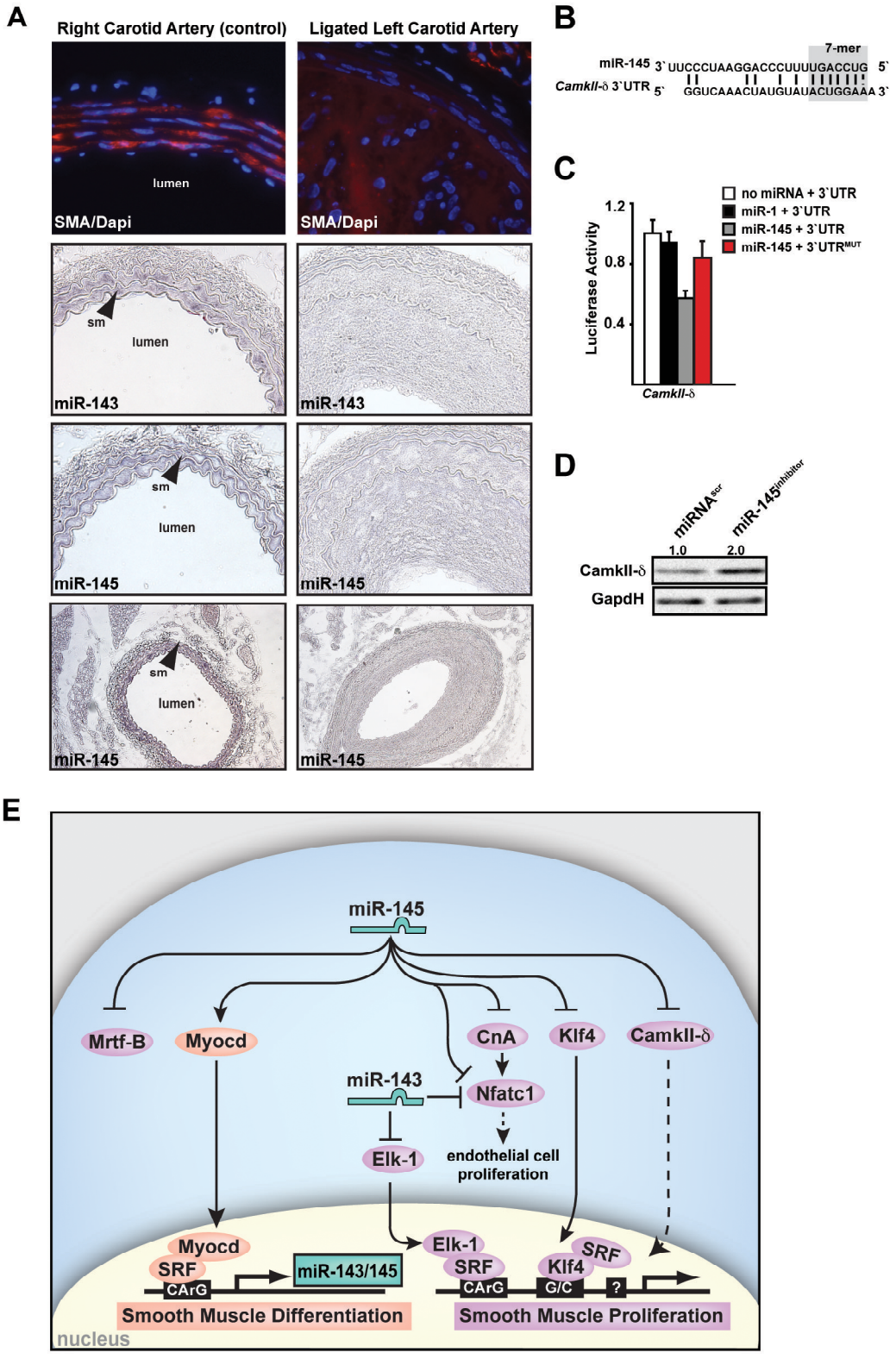
A
Right Carotid Artery (control)
Ligated Left Carotid Artery
lumen
SMA/Dapi
SMA/Dapi
sm
lumen
miR-143
miR-143
sm
lumen
miR-145
miR-145
sm
lumen
miR-145
miR-145
B
7-mer
miR-145 3`UUCCCUAAGGACCCUUUUGACCUG 5`
Camkll-δ 3`UTR 5` GGUCAAACUAUGUAUACUGGAAA 3`
C
Luciferase Activity
1.2
0.8
0.4
no miRNA + 3`UTR
miR-1 + 3`UTR
miR-145 + 3`UTR
miR-145 + 3`UTRMUT
Camkll-δ
D
miRNAscr
miR-145inhibitor
1.0
2.0
Camkll-δ
GapdH
E
miR-145
Mrtf-B
Myocd
CnA
Klf4
Camkll-δ
miR-143
Nfatc1
Elk-1
endothelial cell proliferation
Myocd
SRF
CArG
miR-143/145
Elk-1
SRF
CArG
Klf4
SRF
G/C
?
Smooth Muscle Differentiation
Smooth Muscle Proliferation
nucleus

Figure 7. miR-143 and miR-145 are downregulated in vascular injury and miR-145 targets the Ca^{2+}-dependent subunit *CamkII-delta*. (*A*) Cross-sections from mice 14-days post-ligation of the left carotid artery and no ligation of the contralateral right carotid (internal control) showed normal smooth muscle alpha-actin antibody (SMA, red; Dapi, blue), miR-143, and miR-145 expression (DIG-AP staining, dark purple) in the non-ligated artery, but reduced smooth muscle, miR-143, and miR-145 expression in the ligated artery. **(***B***)** Depiction of the one miR-145 binding site in the *CamkII-delta* 3`UTR. **(***C***)** Measured luciferase activity of wt and mutated *CamkII-δ* 3`UTR with no miRNA (negative control), miR-1 (control miRNA), and miR-145 shown. (*D*) And corresponding western analysis for CamkII-δ analyzed from A10 smooth muscle cells transfected with an inhibitor of miR-145 ($miR\text{-}145^{inhibitor}$) showed 2-fold increase in protein levels when miR-145 was knocked down. (*E*) Model representing miR-143 and miR-145's function to repress the cardiac and smooth muscle proliferation (purple) programs and thereby promote the differentiation (pink) pathway in an SRF-dependent or –independent mechanism. Results shown in (*C*) represent at least five experiments with error bars indicating 95% confidence intervals. (densitometry calculation performed by Image J; *, $p<0.05$).

Supplementary Figure 1.

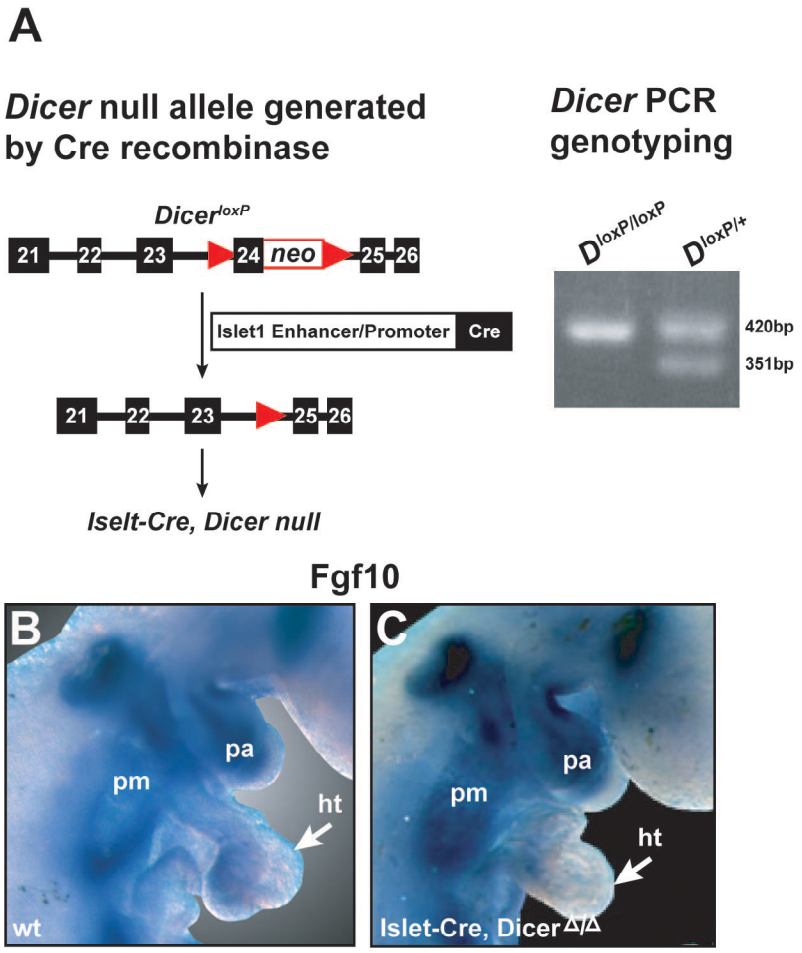

Supplementary Figure 1. Schematic and genotyping strategy for conditional *Dicer* mutants. (*A*) Schematic representing loxp sites flanking the 24th exon of *Dicer*, which encodes the RNAseIII enzymatic domain, and a neomyocin cassette is inserted for initial selection; the *Islet1* promoter driving cre results in recombination and removal of exon 24, creating a second heart field deletion of *Dicer*; genotyping results of embryos; $D^{loxp/loxp}$, $Dicer^{loxp/loxp}$; $D^{loxp/+}$, $Dicer^{loxP/+}$, (*B, C*) whole mount *in situ* hybridization showing normal expression of *Fgf10* in the wild-type (*B*) and mutant (*C*) embyro at E9.5.

REFERENCES

1. **Kattman, S. J., Adler, E. D., & Keller, G. M. (2007)** ***Trends Cardiovasc Med*** **17, 240-246.**
2. **Miano, J. M. (2003)** ***J Mol Cell Cardiol*** **35, 577-593.**
3. **Wang, Z., Wang, D. Z., Hockemeyer, D., McAnally, J., Nordheim, A., & Olson, E. N. (2004)** ***Nature*** **428, 185-189.**
4. **Akao, Y., Nakagawa, Y., & Naoe, T. (2007)** ***DNA Cell Biol*** **26, 311-320.**
5. **Ventura, A. C. & Merajver, S. D. (2008)** ***Annu Rev Med*** **59, 199-212.**
6. **Chen, J. F., Mandel, E. M., Thomson, J. M., Wu, Q., Callis, T. E., Hammond, S. M., Conlon, F. L., & Wang, D. Z. (2006)** ***Nat Genet*** **38, 228-233.**
7. **Ivey, K. N., Muth, A., Arnold, J., King, F. W., Yeh, R. F., Fish, J. E., Hsiao, E. C., Schwartz, R. J., Conklin, B. R., Bernstein, H. S.,** ***et al.*** **(2008)** ***Cell Stem Cell*** **2, 219-229.**
8. **Zhao, Y. & Srivastava, D. (2007)** ***Trends Biochem Sci*** **32, 189-197.**
9. **Vasudevan, S., Tong, Y., & Steitz, J. A. (2007)** ***Science*** **318, 1931-1934.**
10. **Harfe, B. D., McManus, M. T., Mansfield, J. H., Hornstein, E., & Tabin, C. J. (2005)** ***Proc Natl Acad Sci U S A*** **102, 10898-10903.**
11. **Buckingham, M., Meilhac, S., & Zaffran, S. (2005)** ***Nat Rev Genet*** **6, 826-835.**
12. **Cai, C. L., Liang, X., Shi, Y., Chu, P. H., Pfaff, S. L., Chen, J., & Evans, S. (2003)** ***Dev Cell*** **5, 877-889.**
13. **Akao, Y., Nakagawa, Y., & Naoe, T. (2006)** ***Biol Pharm Bull*** **29, 903-906.**
14. **Michael, M. Z., SM, O. C., van Holst Pellekaan, N. G., Young, G. P., & James, R. J. (2003)** ***Mol Cancer Res*** **1, 882-891.**
15. **Wang, Y., Medvid, R., Melton, C., Jaenisch, R., & Blelloch, R. (2007)** ***Nat Genet*** **39, 380-385.**
16. **Wienholds, E., Kloosterman, W. P., Miska, E., Alvarez-Saavedra, E., Berezikov, E., de Bruijn, E., Horvitz, H. R., Kauppinen, S., & Plasterk, R. H. (2005)** ***Science*** **309, 310-311.**
17. **D'Amico, L., Scott, I. C., Jungblut, B., & Stainier, D. Y. (2007)** ***Curr Biol*** **17, 252-259.**
18. **Ebert, M. S., Neilson, J. R., & Sharp, P. A. (2007)** ***Nat Methods*** **4, 721-726.**
19. **Johnson, E. N., Lee, Y. M., Sander, T. L., Rabkin, E., Schoen, F. J., Kaushal, S., & Bischoff, J. (2003)** ***J Biol Chem*** **278, 1686-1692.**
20. **Chang, C. P., Neilson, J. R., Bayle, J. H., Gestwicki, J. E., Kuo, A., Stankunas, K., Graef, I. A., & Crabtree, G. R. (2004)** ***Cell*** **118, 649-663.**
21. **Krutzfeldt, J., Rajewsky, N., Braich, R., Rajeev, K. G., Tuschl, T., Manoharan, M., & Stoffel, M. (2005)** ***Nature*** **438, 685-689.**
22. **Parmacek, M. S. (2007)** ***Circ Res*** **100, 633-644.**
23. **Oh, J., Richardson, J. A., & Olson, E. N. (2005)** ***Proc Natl Acad Sci U S A*** **102, 15122-15127.**
24. **Liu, Y., Sinha, S., McDonald, O. G., Shang, Y., Hoofnagle, M. H., & Owens, G. K. (2005)** ***J Biol Chem*** **280, 9719-9727.**
25. **Yoshida, T., Kaestner, K. H., & Owens, G. K. (2008)** ***Circ Res*** **102, 1548-1557.**
26. **Wang, Z., Wang, D. Z., Pipes, G. C., & Olson, E. N. (2003)** ***Proc Natl Acad Sci U S A*** **100, 7129-7134.**

27. **Owens, G. K. (2007) *Novartis Found Symp* 283, 174-191; discussion 191-173, 238-141.**
28. **Ji, R., Cheng, Y., Yue, J., Yang, J., Liu, X., Chen, H., Dean, D. B., & Zhang, C. (2007) *Circ Res* 100, 1579-1588.**
29. **House, S. J. & Singer, H. A. (2008) *Arterioscler Thromb Vasc Biol* 28, 441-447.**
30. **Miano, J. M. (2006) *Circ Res* 98, 723-726.**
31. **Davis, J. L., Long, X., Georger, M. A., Scott, I. C., Rich, A., & Miano, J. M. (2008) *Int J Dev Biol* 52, 389-396.**
32. **Li, S., Wang, D. Z., Wang, Z., Richardson, J. A., & Olson, E. N. (2003) *Proc Natl Acad Sci U S A* 100, 9366-9370.**
33. **Zhao, Y., Samal, E., & Srivastava, D. (2005) *Nature* 436, 214-220.**
34. **Obernosterer, G., Martinez, J., & Alenius, M. (2007) *Nat Protoc* 2, 1508-1514.**
35. **Westerfield, M. (2000) *University of Oregan Press, Eugene* 4th Ed.**
36. **Yelon, D., Horne, S. A., & Stainier, D. Y. (1999) *Dev Biol* 214, 23-37.**
37. **Berdougo, E., Coleman, H., Lee, D. H., Stainier, D. Y., & Yelon, D. (2003) *Development* 130, 6121-6129.**
38. **Aanstad, P. & Whitaker, M. (1999) *Mech Dev* 88, 33-41.**
39. **Zhao, Y., Ransom, J. F., Li, A., Vedantham, V., von Drehle, M., Muth, A. N., Tsuchihashi, T., McManus, M. T., Schwartz, R. J., & Srivastava, D. (2007) *Cell* 129, 303-317.**
40. **Kimes, B. W. & Brandt, B. L. (1976) *Exp Cell Res* 98, 349-366.**

CHAPTER 5

DISCUSSION AND FUTURE DIRECTIONS

Summary

Overall, the studies described in this thesis demonstrate the importance of transcriptional and translational regulation in the cardiac progenitors for proper heart development. First, we found that the deletion of *Hand2* in the NCCs had severe craniofacial and cardiovascular defects, including persistent truncus arteriosus, and died at mouse E12.5. This reveals an essential role for *Hand2* function within the NCCs for proper face and outflow tract development. Next, I found that miRNA biogenesis was required in the cardiac progenitor populations, specifically the SHF and NCCs, by creating conditional deletions of *Dicer* in each progenitor background using the *Islet1-cre* or *Wnt1-cre* transgenics, respectively. miRNA function in the NCCs was found to be critical for formation of the craniofacial structures of the jaw, thymus, and proper outflow tract septation. We specifically found that the distal-less homeobox gene, *Dlx2,* was downregulated in the first pharyngeal arch (PA1) suggesting that abnormal patterning of the PA1 led, in part, to the lack of maxillary and mandibular structures in the $Dicer^{loxp/loxp}$*; Wnt1-cre* mutant mice. We further identified NCC-enriched miRNAs, and found that one in particular, miR-452, could rescue *Dlx2* expression in the PA1. The deletion of *Dicer* in the SHF showed the importance of miRNA function for proper formation of the SHF-derived RV and OFT. The $Dicer^{loxp/loxp}$*; Islet-1-cre* mutant mice had a hypoplastic RV and shortened OFT and died early at E10.5. We identified a bicistronic transcript containing miR-143 and miR-145, to be enriched in the SHF

progenitors. Furthermore, we found that SRF and Nkx2.5 regulate their cardiac and smooth muscle expression. Loss-of-function studies in zebrafish revealed similar roles for miR-143 and miR-145 in regulating endocardial proliferation in the heart. In addition, miR-143 and miR-145 promoted differentiation of SMC by repressing factors that would promote SMC proliferation. Concordantly, we found that miR-145 could translationally activate Myocardin, and thus potentiate SMC differentiation. Both miR-143 and miR-145 were downregulated in a mouse vascular injury model, suggesting that these two miRNAs may be important for SMC differentiation and maintenance of the SMC quiescent and contractile phenotype. Collectively, this thesis work has added to the understanding of transcriptional and translational networks that regulate the cardiovascular system.

Unveiling the Function of Hand2 in the Cardiac Neural Crest

Questions still remain regarding the function of *Hand2* in the neural crest. As mentioned, others have published the conditional deletion of *Hand2* in the neural crest using the *Wnt1-cre* neural crest-specific transgenic mouse(1-4). Although their focus was on neurogenesis in the autonomic or enteric systems, they all reported embryonic lethality due to cardiovascular defects, such as blood pooling, hemorrhages and outflow tract abnormalities. They suggest that hemorrhaging is due to neural crest patterning defects in smooth contribution to the great vessels, which lead to poor blood flow and secondary defects in the peripheral vascular system (5). *Hand2* is expressed in diverse cell-types such as the noradrenergic neurons of the autonomic nervous system, and *Hand2* function in noradrenergic neurons is to maintain the proliferative abilities of the neural precursor

pools (2). It will be interesting to examine whether proliferation is a key function of *Hand2* in the cardiac neural crest cells, too.

Interestingly, we find the craniofacial defect is more severe in our neural crest conditional knockout of Hand2, compared to published studies of *Hand2;Wnt1-cre* mice (1-4), which is most likely due to the differences in design of the conditional allele of *Hand2*. Our conditional *Hand2* construct contained *loxp* sites flanking both exons, whereas others designed their *Hand2* targeting construct with *loxp* sites flanking only the first exon (3). This supports previous data that the precise dosage of Hand2 is critical for proper craniofacial and cardiac development (6), and *Hand2* is very sensitive to changes in its protein levels.

The regulation of protein dosage has steered my thinking in a new direction and my focus has transitioned towards translational regulation of cardiac development. Our future goals with the *Hand2* studies will involve performing miRNA microarrays to determine whether the loss of *Hand2* disrupts expression of neural crest-enriched miRNAs, and in conjunction, perform mRNA microarrays to observe gene expression changes that may cause the cardiovascular phenotype. We have knowledge of miRNAs enriched in the neural crest, and that their function is critical for neural crest contribution to the craniofacial and cardiac outflow tract.

In addition, *Hand2* is expressed in the second heart field (SHF), which contributes cells to the developing myocardium of the OFT and RV, so it will be informative to compare the function of *Hand2* in the NCCs and the SHF, and determine if the function is the similar between the two cardiac progenitor cell-types.

miRNA Function in the Craniofacial and Cardiac Neural Crest

Out of our screen for neural crest enriched miRNAs, we can begin to decipher the mechanism of action these miRNAs by looking at their predicted targets, and performing overexpression and knockdown studies to elucidate their function in the neural crest. Many of the same tools to study transcription factors have been applied to study miRNA expression and function *in vivo* and *in vitro*. One such tool, miRNA *in situ* hybridization, will be extremely informative to show the spatiotemporal expression of the NCC-enriched miRNAs that we have described, and may shed light onto particular miRNA function.

The evidence I provided that miR-452 rescues of *Dlx2* expression, sets up the next task of searching for miR-452 targets that may directly or indirectly repress *Dlx2* expression. Bioinformatic prediction programs allow us to identify potential targets, and then we can clone their 3`UTRs into a luciferase reporter construct to test putative miRNA binding sites. This *in vitro* screen allows us to assess potential targets, which can further be validated *in vivo* by analyzing the protein levels in miR-452 knockdown or overexpression cell lines or in the *Dicer*$^{loxP/loxP}$*;Wnt-cre* mice. We have found interesting predicted targets that may be responsible for *Dlx2* regulation, and are being tested. Of interest are factors involved in the *Sonic hedgehog (Shh)* pathway, since we know that Shh is essential for pharyngeal arch development and targeted disruption of *Shh* in mice leads to a lack of craniofacial skeleton (7, 8).

Cardiac NCCs are the primary precursor cells that form the vascular smooth muscle cells (VSMCs) of the outflow tract and great vessels, specifically to the ascending aorta and pulmonary trunk. The mechanism remains unclear how SMCs develop from

these precursors, or if miRNAs are involved in the process. It is known that TGF-β signaling induces NCC-SMC differentiation, in part by upregulating the *response gene to complement-32, RGC-32,* which is expressed in the great vessels, and mediates cell proliferation (9, 10). Based on miRNA binding prediction algorithms, *RGC-32* has a miR-452 binding site within its 3`UTR that contains a 9-nt seed match ('seed match', discussed on pg. 16). Further testing of this site using *in vitro* luciferase reporter assays will reveal whether the binding site is responsive to miR-452 One way to address the function of miRNAs in cardiac NCCs is to use the Monc-1 or JoMa1.3 NCC lines, which can be differentiated into SMCs (11, 12). In these cell lines, we can knockdown the nine NCC-enriched miRNAs we found, including miR-452, and determine if their function is required for NCC-SMC differentiation. Although, this cell culture setting negates the understanding of aorticopulmonary septation, it may provide clues of the miRNAs and their targets that are important during this process.

Implications of miR-143/145 in Vascular Disease

Our finding that miR-143 and miR-145 are downregulated in a mouse model of vascular injury, similar to smooth muscle differentiation markers such as smooth muscle 22-alpha (SM22α), suggests a potential role for regulating SMC differentiation and proliferation programs. miRNAs have recently been described to act as translational activators as well as translational repressors, depending on the state of the cell cycle or cellular stress (13, 14). The surprising finding that miR-145 could translationally stabilize protein expression through the 3`UTR of *Myocardin* suggests that miR-145 may have the potential to increase *Myocardin's* protein expression and activate smooth muscle

differentiation, when the cell becomes stressed, as in the case of vascular injury. One way to study miR-145's effect in vascular injury is to overexpress it via the SM22 promoter, which drives expression in the vascular smooth muscle (15, 16), and then injure the carotid artery and see if miR-145-overexpresion has protective effects. This would be predicted based on the targets that I have identified that are known to inhibit or compete with Myocardin for SRF binding and promote proliferation of smooth muscle cells, Klf4 and Elk-1, respectively (17, 18).

As we identify and validate more targets of miR-143 and miR-145, it will be interesting to understand the mechanism by which these miRNAs seem to target multiple factors in the same pathway. Does a tissue-specific cofactor associate with the miRNA to confer its tissue-specificity? And what is the sequence recognition between the miRNA and cofactor? To help elucidate the mechanism of action for each miRNA, genetic deletions of miR-143 and miR-145 separately and together will provide insight to their function.

Conclusion

The study of cardiac development is a complex process that requires the spatiotemporal cooperation of three cardiac progenitor populations: FHF, SHF, and cardiac NCCs. Transcriptional regulation has been extensively studied in the heart, so by using the cardiac transcriptional network as my template, my work has focused on overlaying it with a translational network mediated by miRNAs. From my studies, I have discovered many miRNAs enriched in cardiac progenitors, and have began to understand the function of two important cardiovascular progenitor miRNAs, miR-143 and miR-145,

that are essential for cardiac development in the zebrafish, and smooth muscle development in mice. Their enrichment in cardiac progenitors and the developing heart in mice and zebrafish suggest they function early in cardiac development, and future knockout studies of each miRNA or in combination will provide more insight into their function.

References

1. D'Autreaux, F., Morikawa, Y., Cserjesi, P., & Gershon, M. D. (2007) *Development* **134,** 2237-2249.
2. Hendershot, T. J., Liu, H., Clouthier, D. E., Shepherd, I. T., Coppola, E., Studer, M., Firulli, A. B., Pittman, D. L., & Howard, M. J. (2008) *Dev Biol* **319,** 179-191.
3. Hendershot, T. J., Liu, H., Sarkar, A. A., Giovannucci, D. R., Clouthier, D. E., Abe, M., & Howard, M. J. (2007) *Dev Dyn* **236,** 93-105.
4. Morikawa, Y., D'Autreaux, F., Gershon, M. D., & Cserjesi, P. (2007) *Dev Biol* **307,** 114-126.
5. Jiang, X., Rowitch, D. H., Soriano, P., McMahon, A. P., & Sucov, H. M. (2000) *Development* **127,** 1607-1616.
6. McFadden, D. G., Barbosa, A. C., Richardson, J. A., Schneider, M. D., Srivastava, D., & Olson, E. N. (2005) *Development* **132,** 189-201.
7. Chiang, C., Litingtung, Y., Lee, E., Young, K. E., Corden, J. L., Westphal, H., & Beachy, P. A. (1996) *Nature* **383,** 407-413.
8. Yamagishi, C., Yamagishi, H., Maeda, J., Tsuchihashi, T., Ivey, K., Hu, T., & Srivastava, D. (2006) *Pediatr Res* **59,** 349-354.
9. Li, F., Luo, Z., Huang, W., Lu, Q., Wilcox, C. S., Jose, P. A., & Chen, S. (2007) *J Biol Chem* **282,** 10133-10137.
10. Badea, T., Niculescu, F., Soane, L., Fosbrink, M., Sorana, H., Rus, V., Shin, M. L., & Rus, H. (2002) *J Biol Chem* **277,** 502-508.
11. Rao, M. S. & Anderson, D. J. (1997) *J Neurobiol* **32,** 722-746.
12. Maurer, J., Fuchs, S., Jager, R., Kurz, B., Sommer, L., & Schorle, H. (2007) *Differentiation* **75,** 580-591.
13. Vasudevan, S., Tong, Y., & Steitz, J. A. (2007) *Science* **318,** 1931-1934.
14. Vasudevan, S., Tong, Y., & Steitz, J. A. (2008) *Cell Cycle* **7,** 1545-1549.
15. Holtwick, R., Gotthardt, M., Skryabin, B., Steinmetz, M., Potthast, R., Zetsche, B., Hammer, R. E., Herz, J., & Kuhn, M. (2002) *Proc Natl Acad Sci U S A* **99,** 7142-7147.
16. Li, L., Miano, J. M., Mercer, B., & Olson, E. N. (1996) *J Cell Biol* **132,** 849-859.
17. Liu, Y., Sinha, S., McDonald, O. G., Shang, Y., Hoofnagle, M. H., & Owens, G. K. (2005) *J Biol Chem* **280,** 9719-9727.
18. Wang, Z., Wang, D. Z., Hockemeyer, D., McAnally, J., Nordheim, A., & Olson, E. N. (2004) *Nature* **428,** 185-189.